Role of Microtubule Motor Proteins in Adenoviral Infections

Julian Scherer

Submitted in partial fulfillment of the
requirements for the degree of
Doctor of Philosophy
in the Graduate School of Arts and Sciences

COLUMBIA UNIVERSITY

2013

ABSTRACT

Role of Microtubule Motor Proteins in Adenoviral Infections

Julian Scherer

Viruses have been described as a piece of nucleic acid surrounded by bad news. These bad news determine host specificity, pathogenicity, and virulence. In the case of adenovirus, a non-enveloped double-stranded DNA virus that causes self-limiting disease in healthy individuals but can cause severe and even fatal infection in immunocompromised patients, the bad news can be reduced to the viral capsid. The adenoviral capsid mainly consists of three proteins (fiber, penton base, hexon), which form a rigid shell to protect the viral genome outside of host cells. However, they are able to orchestrate a precise disassembly program initiated once the next susceptible cell is reached, leading to step-wise virus entry, controlled capsid disintegration, efficient DNA delivery, and production of progeny virus. Understanding adenovirus entry is not only beneficial for pathogenic but also therapeutic reasons since adenoviruses have become an increasingly popular vaccine and gene transfer vector due to their ability to infect a large array of dividing and post-mitotic cells, their large DNA capacity, and easy amplification. Attachment to cell surface receptors leads to cellular signaling events, some of which regulate receptor-mediated uptake into clathrin-coated pits. Conditions inside the endosome trigger escape of the virions from the organelle through membrane disruption 5-15 min post-infection and most capsids gain access to the nucleus about 30-45 min thereafter. Interestingly, adenovirus relies on the

microtubule (MT) network, MT-dependent motor proteins, and virus-stimulated cAMP-activated kinase (protein kinase A, PKA) activity to traverse the cytoplasm during the critical intracellular transport phase between endosomal escape and nuclear pore complex attachment. The main virus transporter is the MT minus-end directed motor protein complex cytoplasmic dynein, which functions in organelle positioning, cell migration, cell division, and cell differentiation in uninfected cells. Cytoplasmic dynein subunits known to interact with physiological cargo also bind directly to the adenovirus capsid protein hexon, which remains with the viral genome until its delivery through the nuclear pore complex. Strikingly, for strong binding to cytoplasmic dynein, hexon requires an acidification step, indicating an additional functional role of the passage through the acidic endosomal lumen during entry, priming of hexon for cytoplasmic dynein binding.

Here, we continue previous research of the hexon – dynein interaction and describe the determinants of dynein-mediated capsid transport in further detail. We show that the requirement for stimulated PKA activity on MT minus-end directed motility involves a PKA phosphorylation site in the dynein light intermediate chain 1 (LIC1). PKA phosphorylation or a phosphomimetic mutation increase hexon binding of LIC1 in vitro and RNAi rescue experiments confirm a clear role of PKA phosphorylation in adenovirus redistribution to the nucleus. To our surprise, the same phosphorylation site also plays a role in positioning of lysosomes/late endosomes (lyso/LE) a class of organelles shown to be under PKA control in other systems. However, in contrast to dynein-mediated viral cargo transport which is stimulated upon phosphorylation, dynein-mediated lyso/LE motility is strongly reduced

leading to lyso/LE dispersal into the periphery. Hence, during adenoviral infections, stimulation of PKA activity mediates two distinct functions, lyso/LE dispersal and efficient capsid transport.

Remarkably, adenovirus transport is not only mediated by cytoplasmic dynein towards the cell center but also by opposite polarity motors towards the cell periphery leading to bidirectional capsid motility along MTs, similar to endogenous cargo. The motility pattern implies the involvement of members of the kinesin family, which are MT plus end directed motor proteins regulating MT dynamics, cell division, and organelle transport in uninfected cells. We provide evidence for a direct capsid interaction with kinesin-1, which shows striking differences from the interaction between the capsid and cytoplasmic dynein. Kinesin binding appears to occur independent of low pH treatment of the virion and independent of hexon, but is very likely mediated through the capsid protein penton base.

In addition, we also explored the pH dependent change in hexon affinity for cytoplasmic dynein by testing the viral capsid protein for structural changes at acidic pH conditions. In its native form inside the capsid or as soluble antigen, hexon is present as a tightly associated trimer, which is resistant to elevated temperature, high ionic strength, detergent treatment, and low pH. However, we now show that low pH treatment strongly increases the sensitivity of the trimeric structure to SDS, leading to hexon monomerization. These data indicate a subtle structural change in the hexon polypeptide upon low pH treatment, increasing dynein affinity and SDS-sensitivity.

Taken together, the here presented work contributes to our understanding of adenovirus entry, especially during the cytoplasmic transport phase, and reveals mechanisms of finely orchestrated host-pathogen interactions at the evolutionary interface of viral attack and cellular host defense.

TABLE OF CONTENTS

LIST OF TABLES AND FIGURES

Chapter 3: Adenovirus Penton Base Interaction with Kinesin-1

Chapter 4: Structural Change of Adenovirus Hexon Dependent on pH

ACKNOWLEDGEMENTS

First and foremost, I want to express my very special gratitude toward my PhD advisor Professor Richard Vallee. He is an extraordinary teacher and as a researcher, a rare example of tremendous scientific curiosity and drive. He remains highly interested in every single bit of data generated in his lab and elsewhere and he always gave me the impression that repeated scientific discourse with members of the same or of different areas of research is the essence of individual and also general scientific progress.

I am deeply thankful that he gave me the opportunity to complete this work in his laboratory and to follow my ideas under his extremely helpful and supportive supervision. The many "5mins" of discussion time in his office, through which I learned more and more about him as a person and as a researcher, shaped me into the scientist I am now.

Furthermore, I want to thank the members of my PhD committee, Professors Chloë Bulinski, Yinghui Mao, and Vincent Racaniello for their suggestions and support from my qualifying exam up until my defense date. Many of the ideas that we developed and discussed in my committee meetings found their way into this work and improved it tremendously. With their guidance and accessibility, they greatly facilitated my career as a graduate student. I also want to thank Professor Lynn Enquist for immediately agreeing to serve as additional examiner on my thesis committee.

I want to thank the Department of Biological Sciences at Columbia University for admitting me to the PhD program and setting a great environment through the core curriculum and biannual retreats for young scientists. A special thank to Sarah Kim Fein for being such a wonderful presence in the student office and an immense help while guiding me through the bureaucracy of graduate student life.

Obviously, no PhD work can be completed alone and besides guidance from established researchers, help from others facing the same challenges (and broken equipment) is elementary. I want to thank the early crew of the Vallee lab, who left before me: Helen Bremner for teaching me everything about adenoviruses and awakening my curiosity for this project, Serena Tan for introducing me to organelle motility and LICs, Garrett Seale for explaining to me every cell fixation method (twice), Stephanie Stehman and Tanja Najak for being supportive bay mates, Wei-Nan Liang and Jin-Wu Tsai for showing me what it means to work "around the clock", Silvia Cappello, Pascale Monzo, and Dileep Varma for showing me what it means to work hard and party hard, and Peter Höök. A special thanks goes to the first all-scientist couple I have ever had the pleasure to meet, Kassandra Ori-McKenney and Richard McKenney. They introduced me to the dynein-centric view of science, were and remain to be extremely dedicated researchers and became great friends, also as co-founders of Journal Club and Wendy's Wednesday. Their absence is truly felt.

In addition, I want to thank those who are working in the laboratory today: Julie Yi for being of tremendous help when the “virus project” boiled down to the two of us, when lysosome motility moved more into the focus of this work, and for making the “black box” of automated data analysis a little lighter, Shahrnaz Kemal for being the social nucleus of the laboratory and always a great address to inquire about protocols, reagents, hippocampal neurons, and gossip, Sarah Weil for sharing all the ups and downs of being a Biology PhD with me. They’ve all become much more than just colleagues.

I also want to thank the new generation of Vallee lab members: Caitlin Lazar for keeping the lab running, for helping me out whenever possible and becoming a good friend, Dan Hu for help with the microscopes, for getting my old frame to go running semi-regularly, and for being a mainstay on Wednesdays at 11:45am, Jie Zhou for her support in the kinesin related work and for ensuring the survival of the “virus project”, Alexandre Baffet for being a great colleague and friend, Dave Dubin and Tiago Dantas for fun lab conversations.

In addition, I want to thank members of all laboratories organized in the Cell Biology Research Group for stimulating talks and discussions, especially, Gant Luxton, Guilherme Nader, Nagendran Ramalingam and Francesca Bartolini from the Gundersen laboratory.

I want to thank my family in Mannheim-Feudenheim for their unconditioned love and support. I am extremely grateful for the possibilities they have handed to me. (Mama, Papa, Laura – Ohne Euch hätt's nie geklappt!) I want to thank my extended family in Baden-Württemberg, Syracuse, Washington DC, San Francisco, and Singapore for their great help whenever needed. I want to thank all my friends on both sides of the big pond, especially Alex, Juli, Tobias, Verena, Christoph, Max, Geoff, the Kims, and the Mathews.

Above all that, I want to say a heartfelt "Thank you so much!" to my beloved wife Vivian. For her kindness and understanding when things did not work out as planned but also for joyfully sharing with me all the small and great achievements inside and outside the laboratory. I feel deeply blessed we found each other and that the little one found us.

I love you with all my heart.

For Vivian

Chapter 1: Introduction to Microtubule Motor Proteins and Adenovirus Entry and Transport

1.1. MT Motors

All transport processes inside eukaryotic cells are mediated by molecular motor proteins of the myosin, kinesin, and dynein families. Whereas myosins translocate along actin filaments, kinesins and dyneins use microtubules (MT) for transport towards MT plus or minus ends, respectively. The MT network is centered at the MT organizing center (MTOC), which in most cells is located close to the nucleus and bundles the slow growing minus ends of the MT. The fast-growing MT plus ends radiate into the cell periphery and hence set a polarity for MT based transport with cytoplasmic dynein moving towards the cell center (in the retrograde direction) and kinesins towards the plasma membrane (anterograde). As the founding member of the kinesin class of motor proteins, kinesin-1 was first described about 30 years ago (Allen et al., 1982; Brady et al., 1982; Vale et al., 1985) and shares structural homology with myosin, especially in their motor domains. Subsequently, more than 50 different kinesins have been characterized, grouped in 15 families based on sequence, structure and their function in MT minus or plus end directed translocation and MT depolymerization (Hirokawa et al., 2009; Lawrence et al., 2004). Cytoplasmic dynein 1 was identified as a high-molecular weight (HMW) MT associated protein, previously named MAP1C (Paschal et al., 1987; Paschal and Vallee, 1987). Besides cytoplasmic dynein 1 (described below), there also exist

cytoplasmic dynein 2 and axonemal dyneins. Cytoplasmic dynein 2 is, together with kinesin-2, responsible for intraflagellar transport and the concerted activity of axonemal dyneins provide the mechanical force to generate the flagellar waveform (Gibbons and Rowe, 1965).

1.1.1. Cytoplasmic Dynein 1

1.1.1.1. Structure and Force Production

Cytoplasmic dynein 1 (herein referred to as "dynein" unless noted otherwise) represents a 1.5MDa protein complex that consists of dimers of the heavy chain (DHC), one of two different intermediate chains (IC1 and IC2), light intermediate chains (LIC1 and LIC2), and up to three classes of light chains (LC8, TcTex, and LC7/Roadbock) (Paschal and Vallee, 1987; Pfister et al., 2005) and can be structurally divided in a motor and tail domain (Figure 1-1). The motor domain consists of the C-terminal part of the DHC organized in a ring shaped arrangement of six **A**TPase **A**ssociated with several cellular **A**ctivities (AAA) domains, which have structural, regulatory, and force generating function. AAA+ proteins are known to contain P-loop sequences required for ATP hydrolysis and function by connecting ATP-mediated conformational changes to chemo-mechanical motions that are propagated to a target macromolecule (Erzberger and Berger, 2006). Nucleotide binding and hydrolysis defines at least two distinct conformational states and therefore these proteins act as molecular switches. The ability to switch between conformations in a coordinated and tunable fashion results in efficient and processive molecular motors like dynein.

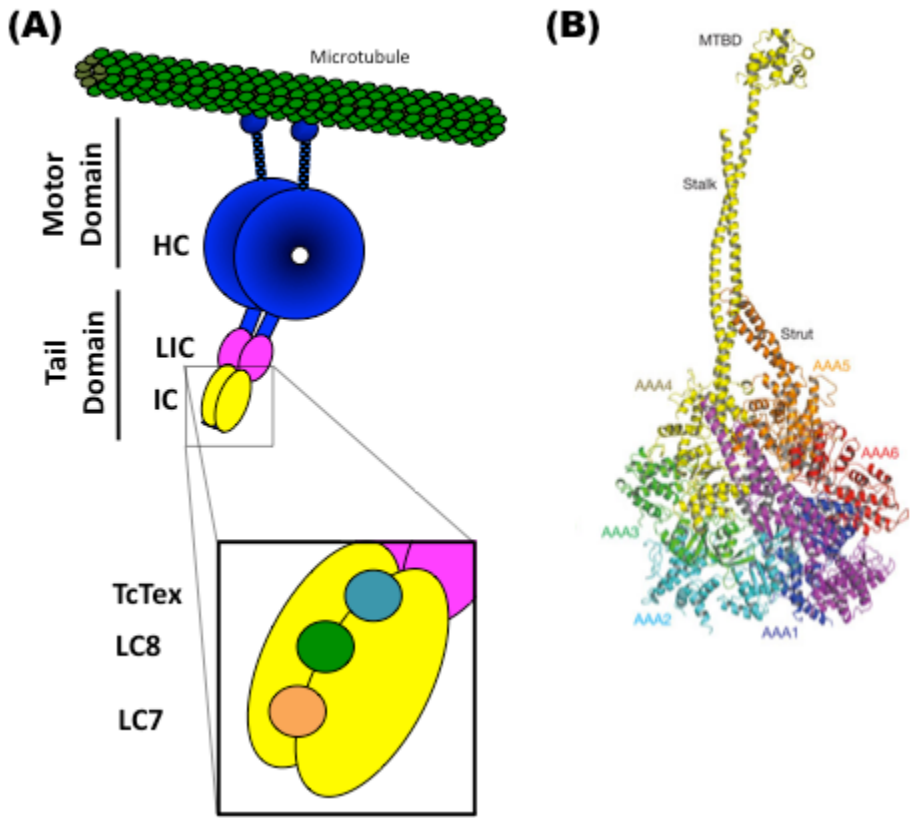

Figure 1-1: Dynein Structure.

(A) Model diagram of cytoplasmic dynein complex translocating along a microtubule (MT). The motor complex can be divided into a tail domain and force generating motor domain. The N-terminal tail of the dynein heavy chain (blue) interacts with light intermediate (pink) and intermediate chains (yellow), which in turn binds to the dynein light chains LC7 (orange), LC8 (green), and TcTex (light blue). Cargo interactions are usually mediated through the accessory subunits (adapted from (Scherer and Vallee, 2011)).
(B) Motor domain of cytoplasmic dynein at atomic detail (X-ray structure from (Kon et al., 2012)) illustrates the required length of signal propagation from AAA1 to the MT-binding domain.

In dynein, only AAA1-4 are known to bind ATP, and only AAA1 shows hydrolysis at a reasonable rate (Gibbons et al., 1987; Mocz and Gibbons, 2001). Binding of ATP to AAA2-4 may have regulatory function and AAA5-6 are thought to be of structural importance since they lack P-loops sequences. From the AAA ring, within AAA4, the stalk emerges, a 15nm coiled-coil loop structure with the MT binding domain (MTBD) at its tip. High-resolution x-ray crystallographic data (Kon et al., 2012; Schmidt et al., 2012) reviewed in (Hook and Vallee, 2012) is beginning to illustrate the structural changes occurring during the cross-bridge cycle of the dynein motor and how the effect of ATP hydrolysis is propagated through the AAA ring and stalk to the MTBD (Burgess et al., 2003). Dynein motility is powered by the cross-bridge cycle of the motor domains (Figure 1-2). Dynein binds tightly to MTs in the apo-state when no nucleotide is bound to AAA1. ATP binding and hydrolysis induces the power stroke, which leads to release of the MT, stepping of the motor molecule and rebinding to the MT. MT rebinding promotes a concerted conformational change in the AAA ring, thereby activating release of ADP and phosphate from AAA1 (Burgess et al., 2003) and preparing the motor for the subsequent cycle. Elegant structural work on the stalk has elucidated that during the cross-bridge cycle the register of the coiled-coil changes slightly resulting in a half-heptad shift in coiled-coil registry (Carter et al., 2008). The shift is further propagated into the MTBD affecting MT affinity, but obviously MT binding at the MTBD is also communicated back to the AAA ring in a reverse fashion affecting ATP turnover (Carter et al., 2008).

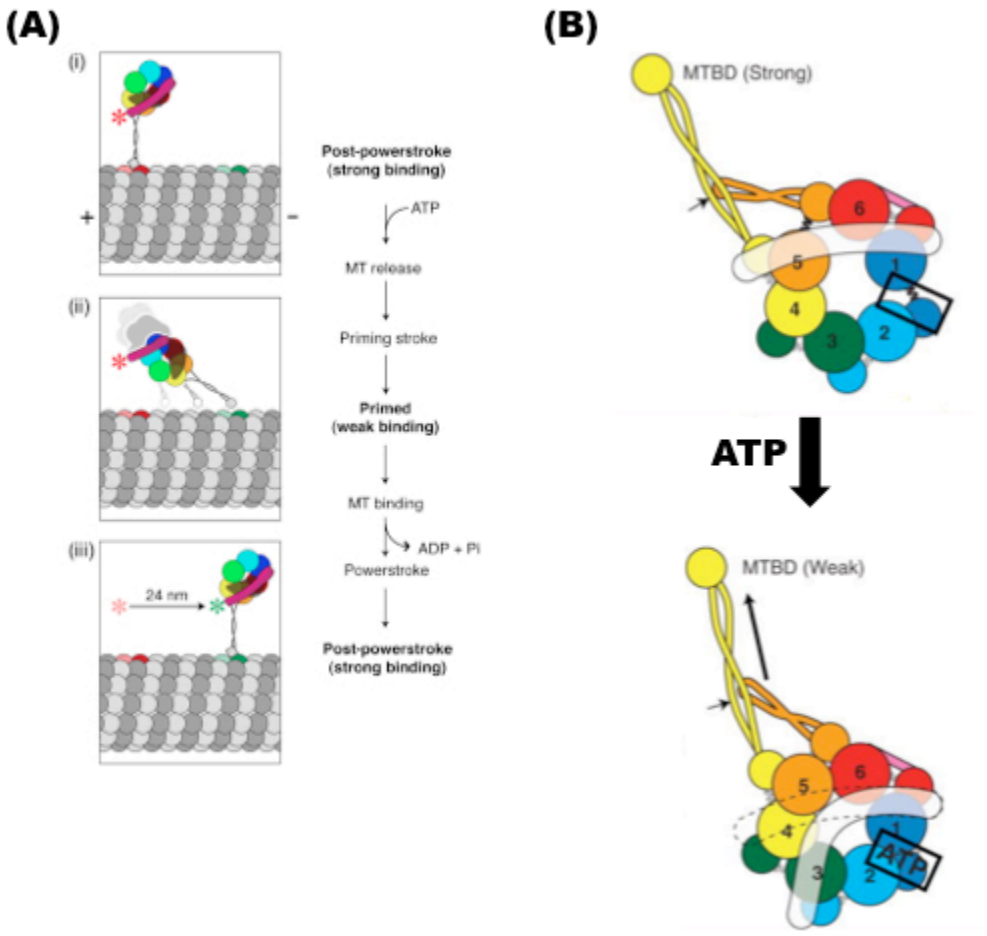

Figure 1-2: Dynein Cross-Bridge Cycle.

(A) Model illustration of possible movements of dynein heavy chain linker sequence and stalk relative to the AAA ring to generate movement along the MT during the cross-bridge cycle. (i) Post-power stroke dynein binds tightly to the MT. (ii) ATP binding induces MT release and primes the motor domain for the power stroke. Rebinding to the next tubulin dimer leads to ADP and phosphate release and the actual power stroke causing linker displacement. (iii) Dynein reaches the post-power stroke state indicated by high MT affinity (illustration from (Roberts et al., 2009)). (B) Representation of the dynein motor domain in non-ATP and ATP-bound states. ATP binding alone induces structural rearrangements leading to linker (white) and stalk (yellow) movements, which affect orientation of the two heads relative to each other and MT affinity in the MT binding domain (MTBD), respectively (illustration from (Carter et al., 2011)).

Furthermore, ATP hydrolysis in AAA1 is not only propagated through a flexible movement of ring to the stalk but also to the linker, another flexible part of the DHC between motor domain and N-terminus (Burgess et al., 2003; Roberts et al., 2012; Schmidt et al., 2012). The linker swing together with tight DHC-DHC binding in the homo-dimerization domain (Tynan et al., 2000a) allows for movement of the two motor heads relative to one another, exerting a maximal stall force of up to 1.1pN (Mallik et al., 2004). Advances in microscopy are allowing for more detailed descriptions of the dynein stepping behavior. The step-size of dynein does not seem to be restricted to the tubulin dimer length of 8nm. It has been shown that dynein steps-sizes vary as multiples of 8nm up to 32nm, depending on the opposing load (Mallik et al., 2004), indicating flexibility and force-sensing within the motor complex. Furthermore, dynein has been shown to side-step off the MT main axis, using multiple MT filaments during one run (Ori-McKenney et al., 2010; Qiu et al., 2012). For processive movement along the MT lattice, the two motor domains are taking repetitive steps in a stochastic and coordinated fashion, which leads to an inchworm-like motility pattern (DeWitt et al., 2012; Qiu et al., 2012).

Besides the dimerization domain, the N-terminus of the DHC also contains the binding regions for LICs and ICs (Tynan et al., 2000a). Based on treatment of the dynein complex with the chaotropic salt potassium iodide, LICs seem to be associated more tightly with the DHC than the ICs which in turn form a subcomplex with the dynein LCs (King et al., 2002; Kini and Collins, 2001). Further evidence from knock-out experiments in the filamentous fungus *A. nidulans* indicates that LICs might be crucial for the core assembly of the dynein complex (Zhang et al.,

2009). All three classes of accessory subunits have been implicated in cargo recruitment (Table 1-1). Interestingly, the dynein ICs also bind to the dynein regulators dynactin and NudE/EL (Karki and Holzbaur, 1995; Stehman et al., 2007; Vaughan and Vallee, 1995) and might represent the major interaction hub of the motor complex (see below). In addition, dynactin-p150^{Glued} and NudE bind to and compete for the same N-terminal region of the IC (McKenney et al., 2011) which is facing towards the dynein motor domain (Watanabe et al., 2011) and presumably can bring the regulators in close proximity to the motor domain, in addition to mediating possible allosteric effects.

Table 1-1: Dynein Subunits and Interacting Proteins.

Non-dynein Binding Partners of Dynein Subunits. Y2H, yeast two hybrid; coIP, co-immunoprecipitation; (1) binding partners that show an interaction only in the absence of IC are omitted; (2) for a complete list, please refer to (Rapali et al., 2011).

Subunit	binding partner	Assay	binding region	Reference
DHC	Lis1	Y2H, coIP pull-down, cofractionation x-ray strucure	AAA1, 649-907, AAA1 n/a AAA4	(Sasaki et al., 2000) (Tai et al., 2002) (McKenney et al., 2010) (Huang et al., 2012)
	NudE/EL	Y2H		(Sasaki et al., 2000)
IC	NudE/EL	pull-down, NMR	1-70	(McKenney et al., 2011; Nyarko et al., 2012; Stehman et al., 2007)
	dynactin p150^{Glued}	coIP, cofractionation, pull-down, NMR	1-70	(Karki and Holzbaur, 1995; McKenney et al., 2011; Morgan et al., 2011; Vaughan and Vallee, 1995)
	snapin	coIP, pull-down	108-268	(Cai et al., 2010)
	paxillin	coIP	reg by S84 PKC site	(Rosse et al., 2012)
	ZW10	coIP	reg by T89 PLK1 site	(Whyte et al., 2008)
IC	huntingtin	Y2H, pull-down	1-283	(Caviston et al., 2007)

	kinesin light chains	Y2H, coIP, pull-down, cofractionation	1-283	(Ligon et al., 2004)
	Herpes Virus UL34	pull-down	1-228	(Ye et al., 2000)
	beta-catenin	coIP, pull-down		(Ligon et al., 2001)
	hexon	coIP, pull-down	150-250	(Bremner et al., 2009); this work
LIC	Zyg12	Y2H	C-terminus	(Malone et al., 2003)
	JIP3/unc-16	Y2H, coIP		(Arimoto et al., 2011)
LIC1	pericentrin	coIP, pull-down	140-236	(Purohit et al., 1999; Tynan et al., 2000b)
	Rab4a	Y2H	181-302	(Bielli et al., 2001)
	Mad2	coIP (indirect by dynein complex in LIC1 RNAi cells)		(Sivaram et al., 2009)
	Kinesin light chain 2	coIP		(Arimoto et al., 2011)
	hexon	coIP, competition with dynein complex	174-348	(Bremner et al., 2009); this work
LIC2	Par3	coIP		(Schmoranzer et al., 2009)
	Rab11-Fib3	Blot Overlay		(Horgan et al., 2010a; Horgan et al., 2010b)
LC8 (1) (2)	Bassoon	Y2H, coIP, pull-down, Biosensor		(Fejtova et al., 2009)
	swallow	Y2H, pull-down		(Schnorrer et al., 2000)
	NOS1	Y2H, coIP		(Jaffrey and Snyder, 1996)
	IκBα	Y2H, pull-down, coIP		(Crepieux et al., 1997)
	Ebola VP35	Y2H		(Kubota et al., 2009)
	Human Foamy Virus gag	coIP		(Petit et al., 2003)
	Rabies Virus Phospho-Protein	Y2H, coIP		(Jacob et al., 2000; Raux et al., 2000)
	African Swine Fever Virus p54	Y2H, coIP		(Alonso et al., 2001)
TcTex-1 (1)	Lfc	Y2H, coIP		(Conde et al., 2010)
	VDAC1	Y2H, coIP		(Fang et al., 2011; Schwarzer et al., 2002)
	OX1R	Y2H, coIP		(Duguay et al., 2011)
	Rab3D	Y2H, coIP		(Pavlos et al., 2011),
	rhodopsin	pull-down, MT pelleting with dynein		(Tai et al., 1999; Yeh et al., 2006)
	PTHR	Y2H, pull-down		(Sugai et al., 2003),
	Doc2	Y2H, pull-down, coIP		(Nagano et al., 1998)
	Trk neurotrophin receptor	coIP		(Yano et al., 2001)
TcTex-1 (1)	FIP-1	Y2H		(Lukashok et al., 2000)

	p59 fyn kinase	Y2H, pull-down		(Campbell et al., 1998; Mou et al., 1998)
	Human Papilloma Virus 16 L2	Y2H, coIP, pull-down		(Schneider et al., 2011)
	Polio receptor CD155	Y2H, pull-down, co-IP		(Mueller et al., 2002), (Ohka et al., 2004)
	Herpes Virus VP26	Y2H, pull-down		(Douglas et al., 2004)
	Mason-Pfizer monkey virus Gag protein	coIP, pull-down		(Vlach et al., 2008),
RP3 (1)	OX1R	Y2H, coIP		(Duguay et al., 2011)
	Herpes Virus VP26	Y2H, pull-down		(Douglas et al., 2004)
	Human Papilloma Virus 16 L2	Y2H, coIP, pull-down		(Schneider et al., 2011)
LC7/Road block (1)	Rab6	Y2H, coIP, pull-down		(Wanschers et al., 2008)

1.1.1.2. Cellular Functions and Regulation

In contrast to the kinesin family, which has diversified to cover a wide range of cellular functions, there is only one dynein gene product that solely regulates a large number of cellular processes, including organelle transport, mitotic spindle organization and orientation, chromosome movement, cell migration, neuronal outgrowth, and nuclear movement (Vallee et al., 2012). Diversity of dynein subunits might contribute to some specificity, but it is widely accepted that additional dynein regulators and recruitment factors are the main reason how individual dynein motor protein complexes can perform different functions.

Two well-studied dynein associated regulatory complexes are dynactin and Lis1, the latter in association with NudE and NudEL (Efimov and Morris, 2000; Gill et al.,

1991; Holzbaur et al., 1991; Minke et al., 1999). In a physiological context, these complexes can have multiple functions ensuring proper motor attachment to the cargo (Burkhardt et al., 1997; Stehman et al., 2007) and affecting the biophysical properties of cytoplasmic dynein (King and Schroer, 2000; McKenney et al., 2010). Dynactin is a 1.5MDa regulatory complex of dynein, but its role in dynein force production and processivity remains controversial. Dynactin interacts with the first 70 residues of the dynein IC through the N-terminal coiled-coil domain (CC1) of p150^{Glued} (Karki and Holzbaur, 1995; McKenney et al., 2011; Morgan et al., 2011; Vaughan and Vallee, 1995). The additional role of p150^{Glued} MT binding is still being investigated (Culver-Hanlon et al., 2006; Kardon et al., 2009; Kim et al., 2007; King and Schroer, 2000). Evidence exist that both dynactin and NudE-LIS1 modulate dynein processivity and force production via allosteric effects. Furthermore, the mechanism with which the binding event to a dynein tail subunit is propagated to the MD remains unknown. However, the dynein regulator Lis1 has been show to directly interact with the dynein MD at AAA3/4 (Huang et al., 2012), acting as a molecular "clutch", possibly uncoupling ATP hydrolysis from changes in the MTBD at the end of the stalk (Huang et al., 2012; McKenney et al., 2010). Lis1 increases dynein persistence against an opposing force, which is essential under high-load, low-speed conditions (Faulkner et al., 2000; McKenney et al., 2010; Tsai et al., 2007; Yi et al., 2011). In addition, Lis1 interacts with NudE/EL, which by itself binds to the dynein IC, has inhibitory effects on dynein force production, and, given its long coiled-coil structure, might bridge the distance from the dynein tail to the MD providing Lis1 transiently to its site of action (McKenney et al., 2010). Interestingly,

individual dynein complexes are presumably controlled by dynactin or NudE/EL, but not both, in view of mutually exclusive interaction of the two regulatory complexes to the dynein IC binding site (McKenney et al., 2011; Nyarko et al., 2012).

During **interphase**, dynein is involved in cell migration (Dujardin et al., 2003), centrosome positioning (Palazzo et al., 2001), and also mediates growth of the growth cone and axon extension in neurons (Vallee et al., 2009). Furthermore, it is responsible for the positioning of membranous organelles such as mitochondria (Thomas Schwarz, personal communication), the nucleus (Splinter et al., 2010; Tsai et al., 2007), endosomes, lysosomes, and components of the Golgi apparatus (Burkhardt et al., 1997).

Distinct classes of organelles seem to require specific dynein components for their motility, an issue of particular interest for the endo-lysosomal pathway (Caviston et al., 2011; Deacon et al., 2003; Horgan et al., 2010b; Palmer et al., 2009; Tan et al., 2011). Dynein localizes to lysosomes in a Ca2+ and serum-dependent manner (Lin and Collins, 1992; Lin and Collins, 1993). Starved fibroblasts or fibroblasts grown in Ca2+ depleted medium lose lysosomal dynein staining while kinesin staining persists resulting in lysosome dispersal (see also chapter 1.1.2.2.). The role of an okadaic acid sensitive DHC phosphorylation has been reported in this process (Lin et al., 1994). In addition to possible indirect recruitment pathways through Rab7, RILP and dynactin (Bucci et al., 2000; Cantalupo et al., 2001; Jordens et al., 2001), dynein recruitment to lysosomes might be mediated directly through IC binding to the membrane-associated scaffolding protein huntingtin (Caviston et al., 2007;

Caviston et al., 2011) or through LICs (Tan et al., 2011). Using RILP truncation mutants impaired in dynactin binding leads to dispersed lysosomes remaining LIC1-positive, indicative of at least one dynactin-independent dynein recruitment pathway. Interestingly, LIC1 or LIC2 RNAi specifically affected the distribution of lysosomes and late endosomes (lyso/LE), with no effects on early endosomes and the Golgi apparatus (Tan et al., 2011), disputing results, suggesting no LIC RNAi effects on lyso/LEs (Palmer et al., 2009).

The **mitotic functions** of dynein include spindle positioning, aster formation, MT-kinetochore attachment and movement (Bader and Vaughan, 2010; Kim and Yu, 2011). Of note, dynein localizes to the kinetochore and mitotic spindle (Steuer et al., 1990) and most of its regulators and recruitment factors during interphase are also detectable at those sites (Echeverri et al., 1996; Stehman et al., 2007; Whyte et al., 2008). Hence, additional cues must regulate mitotic priming of the dynein complex. Interestingly, LIC show a cell-cycle specific phosphorylation pattern (Pascale Monzo, personal communication; (Niclas et al., 1996) and four Cdk1 sites have been described in LIC1 (Addinall et al., 2001; Dell et al., 2000). *In vitro* Cdk1 phosphorylation work with recombinant LIC1 and purified dynein showed that Cdk1 phosphorylation inhibits dynein interaction with membranes (Addinall et al., 2001). This result is in accordance with drastically decreased organelle motility during mitosis.

Another phosphorylation-dependent switch between mitotic and interphase dynein involves T89 of the dynein IC, which can be phosphorylated by Polo-like kinase1

increasing dynein localization to kinetochores via a direct ZW10 interaction (Bader et al., 2011). T89 dephosphorylation by PP1-γ decreases ZW10 but increases dynactin affinity responsible for dynein-mediated streaming of kinetochore-associated proteins towards the spindle poles by anaphase onset (Bader and Vaughan, 2010).

Besides these physiological functions, dynein has been implicated in the transport and infectious cycle of various **pathogens**, especially viruses (see chapter 1.3.1. and (Dodding and Way, 2011; Enquist, 2012; Greber and Way, 2006; Scherer and Vallee, 2011).

1.1.1. Kinesin-1 (KIF5)

1.1.2.1. Structure and Cross-bridge Cycle

Kinesin-1 (herein referred to as "kinesin" unless noted otherwise) is the founding member of the kinesin family of motor proteins (Brady, 1985; Vale et al., 1985) and functions in conventional cargo transport in non-neuronal cells but also in axonal and dendritic transport in neurons. With three gene-duplication induced subtypes - KIF5A, KIF5B, and KIF5C – kinesin represents the dominant MT plus end-directed motor in interphase cells (Hirokawa et al., 2009). Interestingly, KIF5A and KIF5C are expressed almost exclusively in neurons, while KIF5B shows a ubiquitous expression profile (Kanai et al., 2000). Kinesins consists of two heavy chains (KHCs) of approximately 120kDa (Pfister et al., 1989) with an N-terminal motor domain, a

long central coiled-coil dimerization domain, and a C-terminal tail for light chain (KLC) and cargo binding (described below).

The kinesin motor domain propelles the molecule along the MT lattice spanning one MT dimer at a time in strictly 8nm steps (Svoboda et al., 1993) and generats about 5-7pN of force (Svoboda and Block, 1994). In contrast to dynein, kinesin shows very little side-stepping off the MT main axis, higher processivity (Toprak et al., 2009), and the cross-bridge cycle of the two MT motors differs as well. For kinesin, MT association is strengthened in the presence of ATP. Hence, the lagging head binds ATP and MTs simultaneously, while the ADP bound leading head is connecting to the next tubulin dimer. Once the leading heads interacts with the MT, ATP hydrolysis and phosphate release in the lagging head drives forward displacement via a shift of the neck linker from a rearward- to a forward-pointing conformation (Rice et al., 1999). Indeed, it could be shown that length of the neck-linker directly influences kinesin stepping behavior (Yildiz et al., 2008). During that motion, the former leading head exchanges ADP for ATP and binds tightly to the MT, locking the motor to the track and allowing processive runs along the MT.

1.1.2.2. Cargo Recruitment

The kinesin tail domain can interact with cargo directly or through one of four ~60kDa classes of kinesin light chains (KLC1-4). Approximately half of the kinesin molecules in brain extracts are present as heterotetramers containing KLCs (Hirokawa et al., 2009). KLCs bind cargo through their tetratricopeptide repeat (TPR) domains (D'Andrea and Regan, 2003; Zhu et al., 2012). Of note, a tryptophan-

containing motif in KLC-binding proteins has recently been described (Morgan et al., 2010), expanding the possible pool of kinesin cargos and cargo proteins (Dodding et al., 2011).

For a number of organelles, the kinesin recruitment mechanism has been explored in greater detail.

Mitochondria react to local energy deficiencies by repositioning along MTs, which can be illustrated in differentiated neuronal cells where mitochondria are dynamically distributed along the axon. About 30-40% of mitochondria move bidirectionally along the axon, according to the need for ATP. Besides kinesin recruitment through the adaptor proteins syntabulin, syntaphilin, and Ran-binding protein 2 (RanBP2) (Cai et al., 2005; Chen et al., 2009; Cho et al., 2007), a different mechanisms of motor attachment and transport regulation has been identified. Mitochondria have been reported to recruit kinesin through their associated proteins milton and miro. The miro/milton complex binds O-glucose-transferase in the mitochondria membrane and can also sense Ca^{2+}-concentration through EF hand domains in miro. Milton/miro complex is constitutively associated with the KHC tail and miro can additionally compete with the MT for the KHC motor domain in response to Ca^{2+} levels. Low ATP concentration is indicated by high Ca^{2+} levels which leads to a high affinity confirmation of miro for the kinesin motor domain and therefore reduced kinesin motility along the MT (Wang and Schwarz, 2009) (Figure 1-3).

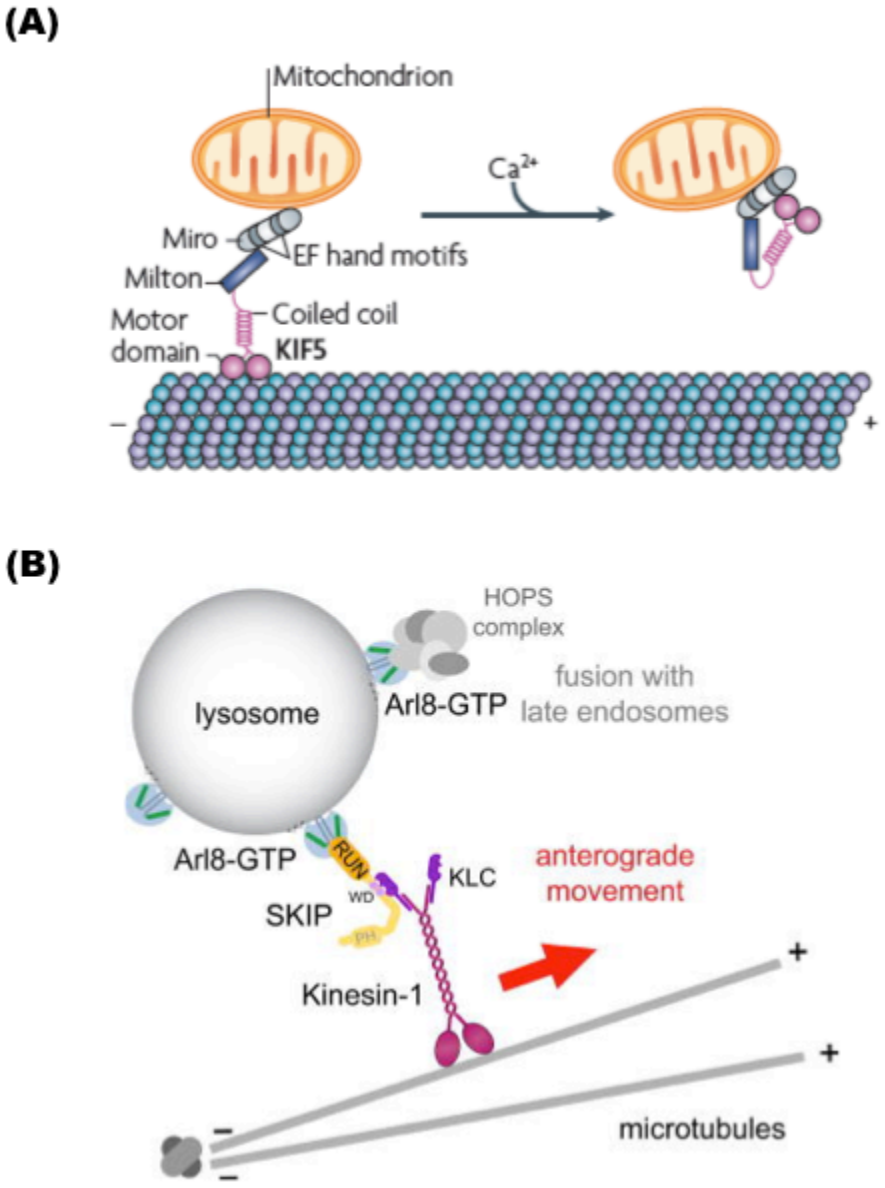

Figure 1-3: Kinesin Recruitment Mechanisms.

(A) Kinesin is recruited to mitochondria by the miro/milton protein complex. Miro is associated with the mitochondrial membrane, and milton acts as direct motor recruitment factor. Calcium-binding to miro increases its affinity for the kinesin motor domain, which detaches from the MT and inhibits MT plus-end directed mitochondria motility (illustration from (Hirokawa et al., 2009). (B) Recruitment of kinesin to lysosomes involves the adaptor protein SKIP and the lysosome-associated GTPase Arl8 (illustration from (Rosa-Ferreira and Munro, 2011)).

Furthermore, p150^{Glued}-CC2 has been shown to interact with milton/miro and this interaction likely recruits the dynein/dynactin complex to mitochondria as well (Cox and Spradling, 2009).

Lysosomes in steady-state move bidirectionally along MT in fibroblasts with net MT minus-end directed motility leading to a perinuclear localization but disperse towards the cell periphery in response to cytoplasmic acidification, trypanosome infection (see also chapter 1.1.3.), starvation, or dynein inhibition (Heuser, 1989; Lin and Collins, 1993; Burkhardt et al., 1997; Tardieux et al., 1992; Yi et al., 2011). Lysosome dispersal upon direct dynein inhibition is even better visible in axons of hippocampal neurons (Yi et al., 2011). Acidity-induced lysosome dispersal is inhibited in KIF5B knock-out and knock-down cells (Cardoso et al., 2009; Tanaka et al., 1998), and microinjection of a function-blocking kinesin antibody abolishes trypanosome-induced dispersal (Rodriguez et al., 1996), indicating the direct involvement of KIF5B in centrifugal lysosome motility. One of the recruitment mechanisms connecting KIF5B to lysosomes involves Arl8-SKIP (Rosa-Ferreira and Munro, 2011). Arl8 is a lysosome-associated GTPase that also binds to a member of the HOPS complex, which is involved in endo-lysosomal fusion (Bagshaw et al., 2006; Garg et al., 2011; Hofmann and Munro, 2006). SKIP has been reported to interact with Arl8 and KLC and therefore acts as a recruitment factor of the kinesin motor to Arl8-positive lysosomes (Dumont et al., 2010; Rosa-Ferreira and Munro, 2011) (Figure 1-3). Another possible kinesin recruitment mechanism via kinectin (Ong et al., 2000) has been disputed, in view of observatins that kinectin-deficient

mice show no abnormalities in the trafficking of lysosomes, phagosomes, and mitochondria (Plitz and Pfeffer, 2001).

If KLC binding to axonal vesicles positive for **amyloid precursor protein** (APP vesicle) (Kamal et al., 2001; Kamal et al., 2000) represents a physiological interaction is under debate now, since the interaction seems to be unspecific and motility of postulated APP vesicle cargos remained motile in APP-deficient mice (Lazarov et al., 2005).

1.1.3. PKA Regulation of Motility

The canonical pathway leading to PKA (protein kinase A, cAMP dependent kinase) activation involves ligand binding to G-protein coupled receptors. The liberated G-alpha subunit activates adenylate cyclase, catalyzing the reaction from ATP to cAMP (Tang and Gilman, 1992). PKA is a heterotetramer of two catalytic subunits along with two regulatory subunits, of which several isoforms have been identified. Binding of cAMP to the regulatory subunits dissociates the tetramer, and the free catalytic subunits phosphorylate protein substrates containing the RRXS/T, KRXS/T or RXXS/T consensus motifs (Dell'Acqua and Scott, 1997). An additional PKA activating pathway through cell surface integrins and TRPM7 has been postulated (Howe, 2011). Phosphodiesterases down-regulates intracellular cAMP levels, allowing an excess of regulatory subunits to rebind and inactivate free catalytic subunits (Amieux et al., 1997). In addition, the ubiquitous inhibitor, PKI, may serve as a fail-safe device, which sequesters free catalytic subunit and mediates export of

the kinase from the nucleus, which is devoid of regulatory subunits (Wen et al., 1995).

The PKA pathway is susceptible to a large array of pharmacological stimulators and inhibitors. Forskolin activates cAMP production by stimulating adenylate cyclase; caffeine, bucladesine (dibutyryl cAMP) and 3-isobutyl-1-methylxanthine (IBMX) inhibit phosphodiesterase; whereas H-89 and exogenous PKI inhibit PKA directly and MDL-12,330A indirectly through irreversible inhibition of adenylate cyclase.

Some MT-dependent transport processes are regulated by PKA.

Lysosomes show PKA- and Ca2+-dependent anterograde movement in rat fibroblasts (Rodriguez et al., 1997) in response to *Trypanosoma cruzi* infection (Chagas disease; Chagas, 1909). Host cells exhibit increased cAMP levels, and peripheralization of lysosomes, which fuse with the parasitophorous vacuole and enable *T. cruzi* to escape from the vacuole and establish infection (Andrews, 1995). Levels of intracellular cAMP levels determine the ability of *T. cruzi* to establish successful infections and lysosome exocytosis. MDL-12,330A treatment decreases lysosome exocytosis about two-fold, whereas IBMX and forskolin can increase levels up to two-fold (Rodriguez et al., 1999).

Melanosomes, the melanin-containing granules share several characteristics with conventional lysosomes, in spite of the existence of unique biogenetic steps (Marks and Seabra, 2001; Raposo et al., 2001; Schiaffino, 2010). Studies using amphibian melanin-pigmented cells have shown that melanosomes respond reliably and quickly to environmental cues (Reilein et al., 1998; Tuma and Gelfand, 1999). The

canonical pathway for melanosome aggregation towards the MTOC involves binding of noradrenaline, melatonin, or melatonin-concentrating hormone to cell surface receptors, which leads to inhibition of adenylate cyclase, lower cAMP levels and a reduction of PKA activity. Dynein activity is responsible for this process (Nilsson and Wallin, 1997). Melanosome dispersal is stimulated by high cAMP concentration, leading to kinesin 2-driven plus-end motility and myosin and actin-dependent scattering (Gross et al., 2002). The specific effect of PKA on kinesins and dynein during aggregation and dispersal are unknown (Figure 1-4).

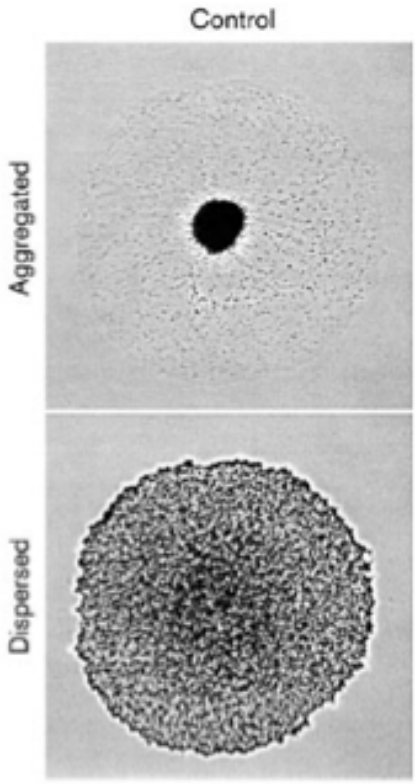

Figure 1-4: PKA-regulated Organelle Movement in Melanosomes.

Melanosome movement in fish pigment cells can be regulated by changing cAMP levels and PKA activity. Stimulation of PKA for 5min leads to aggregated pigment vesicles, whereas PKA inhibition disperses them within 15 min. (picture from (Rodionov et al., 1998)).

Kinesin binding to **synaptic vesicles** has been reported to be decreased after PKA-phosphorylation in vitro, in neuronal cells (Hirokawa et al., 1991; Sato-Yoshitake et al., 1992). Whether kinesin phosphorylation contributes to the observed phenotypes remains to be elucidated (Nakata and Hirokawa, 1995; Rodriguez et al., 1996).

Finally, adenovirus infection has been reported to stimulate PKA activity and affect MT minus end-directed transport of the capsid (Suomalainen et al., 2001).

1.2. Adenovirus

1.2.1. Structure

Adenoviruses represent one of the best-characterized families of non-enveloped double-stranded DNA viruses. They cause mild, self-limiting infections in healthy individuals but can be fatal in immunocompromised patients. Since their first isolation from adenoid tissue in 1953 (Rowe et al., 1953) more than 55 serotypes have been identified, which can be divided into seven subgroups (A-G). The serotypes share a common structure (Figure 1-5), which has been solved at near atomic resolution for the prototypical subgroup C adenovirus 5 (Ad5) by cryo-electronmicroscopy (cryo-EM) and by x-ray crystallography for an Ad5/35 chimera (Liu et al., 2010; Reddy et al., 2010). These studies reveal an apparent evolutionary relationship to the bacteriophage PRD1 (Benson et al., 1999). The adenovirus capsid has a diameter of about 90nm and consists of three major and four minor

capsid proteins (Stewart et al., 1993). The major capsid proteins fiber and penton base form the penton complex, which is located at each of the vertices of the icosahedral.

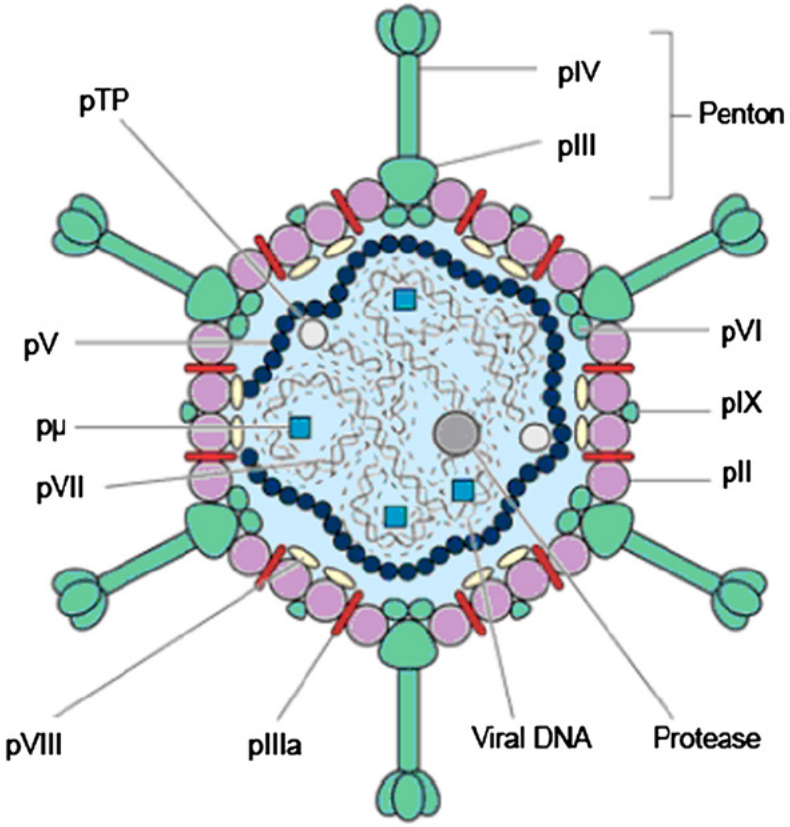

Figure 1-5: Adenovirus Structure.

Three major (pII (hexon), pIII (penton base), pIV (fiber) and four minor capsid proteins (pIIIa, pVI, pVIII, pIX) form the icosahedra protecting the viral genome from the environment and mediating cell attachment and entry. Inner capsid proteins (pV, pVII, pμ, pTP) are responsible for DNA stability. The viral protease functions during capsid maturation and cell entry (illustration from Lind et al., Virology, 2012).

The spike-like timeric fiber proteins protrude away from the capsid and bind the coxsackie-and-adenovirus receptor (CAR). Pentameric penton base also plays a direct role in cell surface binding, interacting directly with integrins (Wickham et al., 1993). The third major capsid protein, hexon, is the most abundant one with 240 hexon trimers in each virus, twelve of which form one facet of the virion. The extreme resistance of adenovirus to environmental influences such as pH, temperature, and ionic strength (Rexroad et al., 2003) is likely due to the tight quarternary structure of hexon (Rux et al., 2003) and the contributionsn of additional minor capsid components pIIIa, pVI, pVIII, and pIX, which act as "cement proteins", bridging gaps between the major components (Figure 1-6). Protein IIIa links penton base and peripentonal hexons, while hexon trimers are connected by protein VIII at their base and protein IX on the surface of the capsid. Because of its prominent location on the outer surface of the virus, protein IX has been used as a platform to artificially introduce tags and fluorescent proteins into the capsid without significant loss of infectivity (Dmitriev et al., 2002; Meulenbroek et al., 2004). Another minor capsid subunit, protein VI, resides on the inside surface, binding to a cavity on the underside of the hexons (for more detailed review (Vellinga et al., 2005)). Its role at this site is incompletely understood. Protein V, which interacrts with penton base and proteins IIIa and VI, is associates directly with the viral DNA, therefore connecting the protein shell with the viral core. The core contains the viral protease adenain, the 36kb virus genome, and the DNA-associated proteins V, VII, μ, and terminal protein.

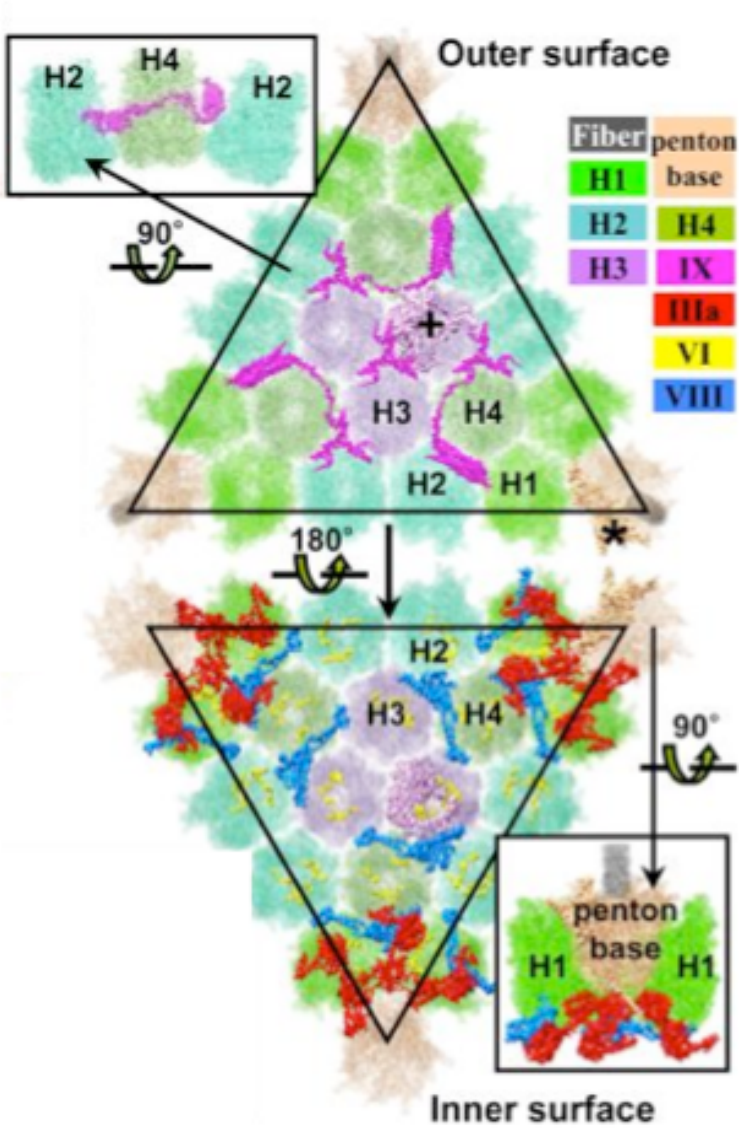

Figure 1-6: Minor Capsid Proteins in Facets of Adenovirus.

Atomic structure of one capsid facet viewed from the outside (outer surface, upper panel) and the inside (inner surface, lower panel). Four hexon localizations can be distinguished filling the face of the facet, while the penton complexes are present only at the vertices. Localization of minor capsid proteins pIIIa (red), pVI (yellow), and pVIII (blue) on the inside, whereas pIX (pink) is visible in the outside view (illustration from (Liu et al., 2010)).

1.2.2. Infectious Cycle

1.2.2.1. Cell Entry

The distinct shape of the viral capsid and abundance of anti-viral antibodies facilitated early negative stain EM and immunocytochemical studies of the entry pathway of adenoviruses. To gain access to the nucleus where the viral genome is replicated and transcribed, the virus has to overcome two cellular hurdles: The plasma membrane, which is impermeable to macromolecules and the cytoplasm which restricts the 150MDa adenovirus capsid to sub-diffusional behavior (Seksek et al., 1997). Hence, virus entry into host cells is a step-wise process that requires the concerted interaction of virus ligands with their host cell receptors (Greber et al., 1993) (Figure 1-7).

For most adenovirus serotypes, uptake into the cell is initiated by the fiber knob – CAR binding (Bergelson et al., 1997) and strengthened by the interaction of the RGD motif in penton base with α5 integrins (Wickham et al., 1993). Fiber and penton base proteins undergo a structural rearrangement during receptor binding (Lindert et al., 2009), which may facilitate endocytosis of the capsid into clathrin coated pits (Chardonnet and Dales, 1970; Patterson and Russell, 1983). Integrin binding stimulates activity of various cellular kinases. The lipid kinase, phosphatidylinositol-3-OH kinase (PI3K) has been implied in endosomal uptake of viral capsids through the local activation of its p85 subunit and seems to be crucial for infection (Li et al., 1998b).

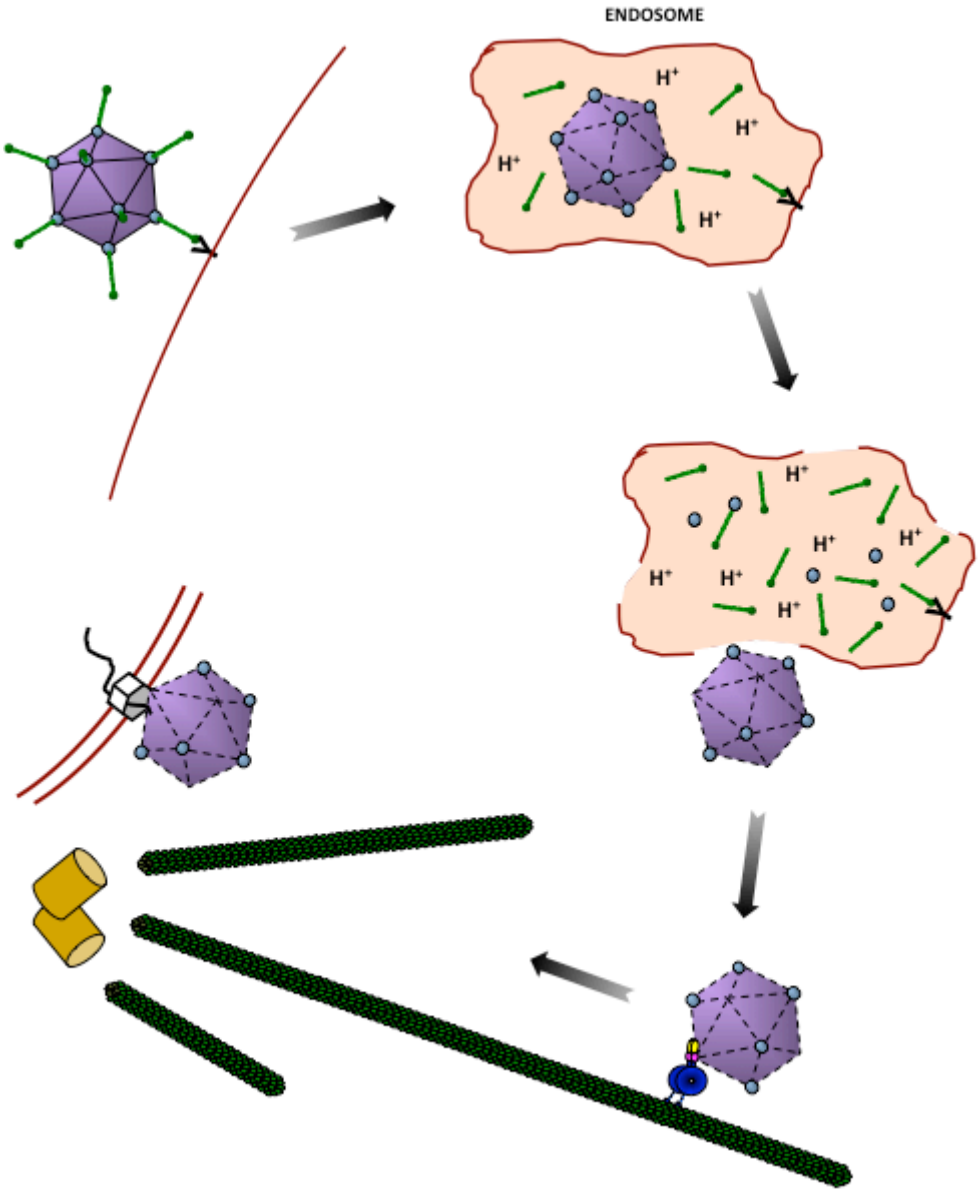

Figure 1-7: Adenovirus Entry.

Entry Pathway of Adenovirus into Host Cells. After binding to the cell membrane through the Coxsackie and Adenovirus receptor, adenovirus is taken up by the cell into endosomes. . Further loss of capsid proteins in the acidic endosomal lumen facilitates rupture of the membrane and endosomal escape of the virus. Following endosomalysis, adenovirus moves bidirectionally along MTs, using dynein for transport towards MT minus ends, which are typically focused at the centrosome and the vicinity of the nucleus. Finally, adenovirus binds to the nuclear pore complex through which it injects its genome for viral reproduction (illustration from (Scherer and Vallee, 2011)).

Besides PI3K effects on cell cycle progression, it could be demonstrated that the PI3K linked signaling cascade through the Rho family GTPases, Rac1, CDC42, and RhoA promote reorganization of the actin cytoskeleton for capsid endocytosis (Li et al., 1998a). Hence, actin depolymerization with cytochalasin D inhibits Ad uptake into cells, but a role of the actin cytoskeleton in viral endocytosis remains to be determined in greater detail (Nemerow and Stewart, 1999).

Inside the endosome, the acidification is thought to change the hydrophobicity of the major capsid proteins (Seth et al., 1985), leading to the shedding of fiber proteins from the capsid (Nakano et al., 2000) and the release of protein VI into the endosomal lumen (Wiethoff et al., 2005). The amino-terminal end of protein VI has an amphipathic helix that ruptures the endosomal membrane by inducing positive curvature (Maier et al., 2010), thus allowing the capsid to escape into the cytoplasm. About 15min post-infection (p.i.), adenovirus subgroups A, C, D, E, and G escape the early endosome (Gastaldelli et al., 2008), while subgroup B and F adenoviruses stay in the endosomal/lysosomal pathway for up to 8 hours (Albinsson and Kidd, 1999; Miyazawa et al., 2001). Interestingly, endosomal acidification seems to be accelerated in adenovirus infected cells with pH values measured in the range of pH 4.6-6.0 (Martin-Fernandez et al., 2004) at 15min p.i., somewhat lower than the range reported for early endosomes of uninfected cells, at pH5.0 to pH6.2, (Saftig and Klumperman, 2009).

After endosomal escape, the virus capsid is transported towards the nucleus within 30-45min in a microtubule (MT) dependent fashion (Mabit et al., 2002) (see chapter 1.3.2.), where hexon interacts tightly with the nuclear pore complex (NPC)

component Nup214/CAN (Trotman et al., 2001). Furthermore, histone H1 is postulated to interact with the hypervariable region 1 of adenovirus hexon and H1 import factors are responsible, in a Ca^{2+}-dependent fashion, to shuttle H1, hexon, and the viral DNA into the nucleus (Trotman et al., 2001). In addition to the histone import machinery, kinesin-1C has also been reported to contribute to capsid disassembly at the NPC (Figure 1-8). Besides the hexon–Nup214 interaction, adenovirus pIX has been reported to bind to kinesin light chains of kinesin-1C which in turn interacts with the NPC component RanBP2 (Nup358) and exerts a force on capsid and NPC, possibly enhancing viral DNA injection from a disrupted capsid through a structurally compromised NPC into the nucleus (Strunze et al., 2011).

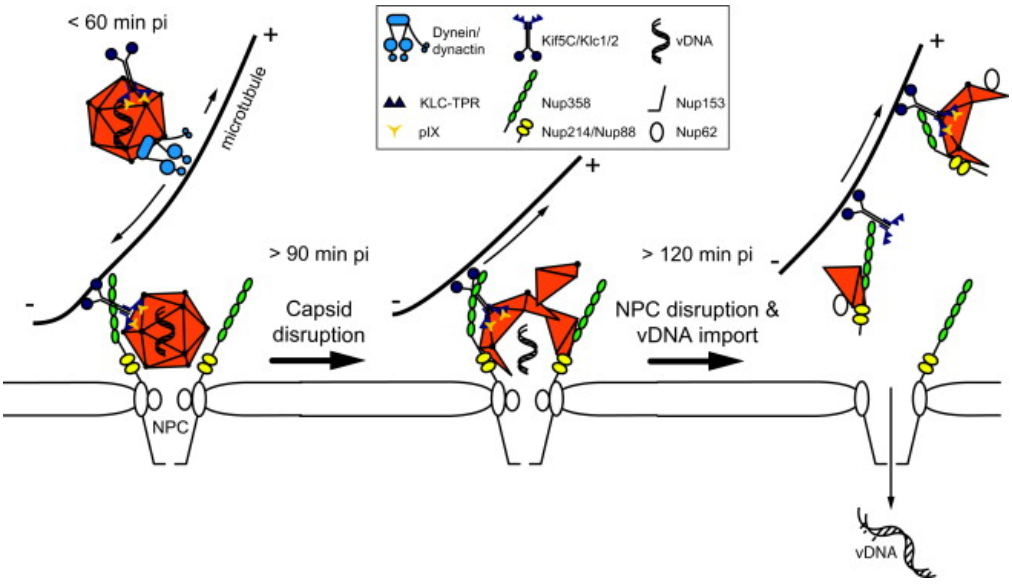

Figure 1-8: Adenovirus Genome Delivery at the NPC.

Adenovirus capsid (red) gains access to the nuclear pore complex (NPC) after dynein-mediated transport via a hexon-Nup214 (yellow) interaction. Furthermore, pIX bind KLC. KHC binding to Nup358 (green) and force generation along microtubules leads to capsid and NPC disruption and facilitated DNA entry into the nucleus (illustration from (Strunze et al., 2011)).

1.2.2.2. Gene Expression, DNA Replication and Protein Translation

Once the viral genome with associated core proteins (DNA binding protein (DBP), terminal protein (TP), mu) has entered the nucleus, a finely tuned string of events leads to viral gene expression and protein translation relying on the host transcription and translation machinery (Ginsberg and Young, 1976). The genome architecture of different adenovirus serotypes is very similar and can be divided into early class I and class II genes, involved in regulation of viral gene expression, DNA replication, and repression of host responses, and late genes encoding capsid components (Figure 1-9). Of particular importance to virus replication is the expression of the early E1A gene. It encodes the first viral polypeptides to be transcribed and can be seen as the master regulator of adenoviral infection (Pelka et al., 2008). EA1 proteins optimize the host cell environment for virus production. They are trans-acting regulators of transcription activating early genes without binding DNA. E1A can also immortalize primary cells *in vitro*, an effect potentiated by the expression of E1B (Endter and Dobner, 2004). Further early gene clusters, especially E3, have additional immune-modulating functions, which are not required for replication in cultured cells (Fessler et al., 2004; Lichtenstein et al., 2004; Windheim et al., 2004).

Replication of viral DNA requires the virus-encoded proteins TP, DBP, and the 140kDa DNA-dependent polymerase and host proteins including nuclear factor I and II (NFI and NFII), and topoisomerase I. For efficient levels of replication, all these proteins are required to bind to the origin of DNA replication (ori), the terminal 18bp of each linear viral DNA strand to form the pre-initiation complex (de

Jong and van der Vliet, 1999). Interestingly, the expression machinery for host genes is strongly inhibited during infection and 12hr p.i. virtually exclusively viral gene products are being synthesized (Bello and Ginsberg, 1967).

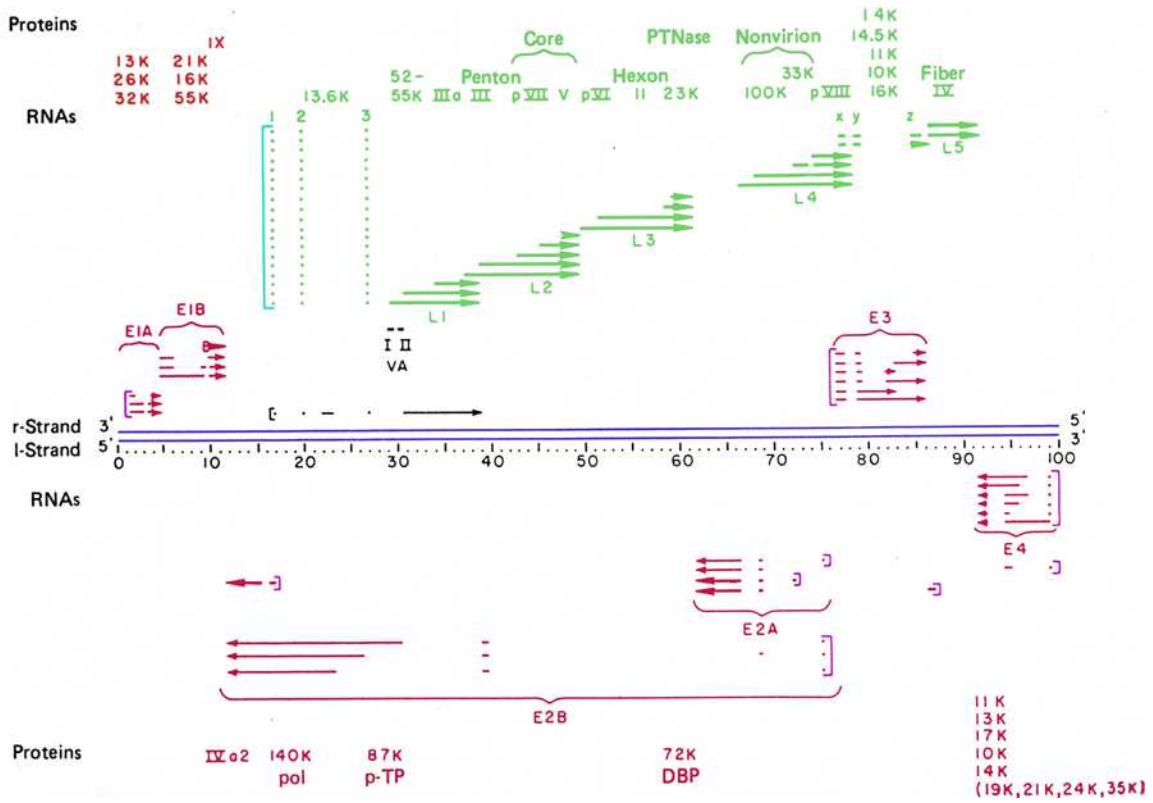

Figure 1-9: Adenovirus Transcription Map.

Schematic representation of the linear adenoviral dsDNA (purple, center) reflecting the connection between gene localization within the genome and its transcription in the course of infection. Early genes are present in 6 clusters (E1A-B, E2A-B, E3, E4, red) and expressed as early as 1h post-infection. Coping sequences in a late gene cluster (L1-L5, green) are under the control of a specific promoter and encode mostly capsid proteins required for the generation of viral progeny (illustration from (Broker, 1984)).

At the onset of DNA replication, the pattern of transcription changes radically from the early to the late genes and only newly replicated DNA is used for late gene transcription, driven primarily by the major late promoter. This promoter regulates expression of five gene clusters (L1-L5), predominantly encoding virion proteins. Similar to host proteins, translation of viral mRNA occurs in the cytoplasm. However, especially the major capsid proteins feature uncommon tertiary and quaternary structures which require the aid of the viral chaperone protein 100K for correct folding and oligomerization (Hong et al., 2005). Temperature-sensitive Ad5 mutant with compromised 100K function fails to produce hexon trimers at the non-permissive temperature, but the effect can be rescued by shifting infected cells to the permissive temperature (Oosterom-Dragon and Ginsberg, 1981).

1.2.2.3. Virus Assembly and Cell Lysis

Synthesis of viral polypeptides peaks at 15h p.i. allowing rapid capsid assembly. Assembly occurs in the nucleus, but begins in the cytoplasm when individual monomers form into hexon and penton capsomers. For nuclear localization, hexon trimers have to rely on the minor capsid protein VI, which provides the required nuclear localization signals (NLS) absent in the hexon sequence (Wodrich et al., 2003). Both members of the penton complex, penton base and fiber, in contrast, contain NLS. Inside the nucleus, the pre-formed capsid building blocks are assembled into capsids and filled with viral DNA with the help of minor capsid proteins and the virally encoded protease adenain (Weber, 1995). In a DNA- and pVI-dependent manner, adenain cleaves the capsid proteins IIIa, VI, and VIII, and the

core proteins VII, mu, and TP (Mangel et al., 1993) for correct capsid assembly. Temperature-sensitive adenovirus mutants, which lack functional adenain when grown at the non-permissive temperature are not infectious, more rigid, and their cryoEM data reveal extra-densities on the capsid inside (Perez-Berna et al., 2009; Silvestry et al., 2009). Thus, it has been hypothesized that viral DNA is packed into an empty immature virion, subsequently, adenain cleaves precursor capsid proteins resulting in a packed mature adenovirus (Ostapchuk and Hearing, 2005). Interestingly, the icosahedral capsid seems to reveal some asymmetry since protein IVa2 has been found on one vertex only and seems to act as the ATPase responsible for pulling the viral DNA into the immature capsid (Zhang and Arcos, 2005; Zhang and Imperiale, 2003). Although host cell metabolism ceases earlier in the infection, infected cells remain largely intact, round up, but many do not lyse. Unlike other viruses, adenovirus seems to rely on rather unspecific pathways for progeny virus release. Although, prolonged infection will eventually lead to cell lysis, which may be facilitated by the adenovirus "death protein" (ADP, initially E3-11.6K) (Tollefson et al., 1996), secreted penton base (Trotman et al., 2003), or fiber protein (Walters et al., 2002). Virus particles tend to accumulate in the nucleus and are visible in the microscope as eosinophilic crystals (Franqueville et al., 2008). These are thought to be the basis of occult infections in unlysed, infected cells and reactivation is caused by accidental lysis of infected cells, releasing stored virus particles.

1.3. Adenovirus Transport

1.3.1. Dynein Binding Capsid Protein

Live-cell analysis of fluorescently labeled adenovirus capsids between endosomal escape and docking to the NPC with high temporal resolution illustrates a bidirectional motility pattern of adenovirus along MT (Suomalainen et al., 1999). This indicates the engagement of active MT minus and plus end directed molecular motors, but the net movement of incoming adenovirus, however, is towards the MTOC. Weihing and coworkers identified the ability of adenovirus to interact with MTs *in vitro* (Luftig and Weihing, 1975); an interaction that is dependent on the presence of HMW MT associated proteins (MAPs) (Weatherbee et al., 1977). MT binding assays showed that the interaction between MTs and adenovirus presumably requires cytoplasmic dynein (Kelkar et al., 2004). These results suggested that dynein is required for adenovirus transport in early phases of infection, but despite the limited number of candidate proteins in the adenovirus capsid (hexon, fiber, penton base, proteins IIIa, VI, VIII, and IX), the identification of the most crucial transport determinant for virus entry is surprisingly still under debate. Knowledge of the stepwise dismantling of the virus and shedding of capsid proteins early in the entry pathway further reduces the pool of possible proteins. However, many trafficking studies have been plagued by the presence of nuclear localization sequences (NLS) in some viral proteins. At late stages of infection, NLS ensure a nuclear localization of the viral proteins for proper capsid assembly inside the nucleus. Thus, they allow for nucleus-directed movement of artificially expressed or incorporated versions of the viral protein in the cell. Subsequently,

several lines of evidence connect all major and some minor capsid proteins directly or indirectly to MT-based cytoplasmic transport of adenovirus. However, the possibility of each capsid protein to interact directly with dynein and represent the viral receptor are rarely discussed:

(1) A dodecahedron consisting of recombinant **penton base** with or without attached **fiber** molecules not only enters HeLa cells by itself and shows nuclear localization 10-20min thereafter, it can also be loaded with plasmid DNA and facilitates gene expression (Fender et al., 1997). The entry pathway of the penton base dodecahedron resembles that of the virion closely and requires an intact MT network for nuclear delivery after endosomal escape (Fender et al., 2005; Rentsendorj et al., 2006). If penton base dodecahedra properly represent the situation during an ongoing adenovirus infection is questionable, since the notion, that the pH-dependent change in hydrophobicity of penton base indicates its ability to disrupt the endosomal membrane (Seth et al., 1984), contradicts more recent work which demonstrates that the minor capsid protein VI alone facilitates this function (Wiethoff et al., 2005). This would leave the dodecahedra trapped inside the endosomal pathway without a direct engagement to the dynein motor machinery.

(2) **Protein VI** appears to be a versatile mediator of many viral functions during the intracellular life cycle. It has membrane-disrupting abilities if released from the inside of the capsid into the endosomal lumen during entry. Protein VI is also contributes to capsid assembly processes at later stages of infection. Protein VI binds closely to hexon (Matthews and Russell, 1994) and shuttles newly formed

hexon trimers from the cytoplasm into the nucleus via an importin alpha/beta-dependent mechanism (Wodrich et al., 2003). Furthermore, protein VI was very recently linked to cytoplasmic transport of adenovirus by describing a decrease in plaque formation and viral infectivity after generating an Ad5 mutant with an altered ubiquitinylation sequence in protein VI, Ad5-VI-M1 (Wodrich et al., 2010). However, the decrease in infectivity is presumably due to an indirect effect on capsid transport since protein VI stays associated with only about 5-10% of incoming wild-type virions after endosomal escape and would therefore represent an inefficient viral receptor for motor proteins. Additionally, the ubiquitinylation site is only exposed and accessible to ubiquitin ligases after protein VI dissociates from the capsid. Thus, the observed differences between wild-type Ad5 and Ad5-VI-M1 are more likely due to a delayed dissociation of protein VI from the mutant capsid and delayed endosomalysis (Wodrich et al., 2010) but not related to dynein-mediated transport of the virus.

(3) The minor capsid **protein IX** is accessible on the outside of the adenovirus capsid for host cell interactions and resides in the outside grove of adjacent hexon trimers (Akalu et al., 1999; Liu et al., 2010; Reddy et al., 2010). In addition, infection of cells with adenovirus mutants containing GFP-tagged protein IX results in green fluorescence at the nucleus 40min after infection, indicating a close association of protein IX with the virus genome until its delivery into the nucleus (Meulenbroek et al., 2004). Furthermore, adenovirus mutants without protein IX (Ad-ΔIX) show reduced infectivity in cultured 293 cells (Sargent et al., 2004). Hence, it is conceivable that protein IX represents the viral receptor for motor protein(s).

However, the reason why Ad-ΔIX shows a lower infectivity lies presumably within decreased capsid stability and effects on viral gene transcription (Parks, 2005) but not within defective motor attachment since Ad-ΔIX shows the same intracellular motility characteristics as the wild-type virus (Gazzola et al., 2009).

(4) Besides protein IX, **hexon** is the only capsid protein that has been clearly shown to remain associated with the viral DNA until virus attachment to the nuclear envelope (Greber et al., 1993; Saphire et al., 2000; Trotman et al., 2001). Hexon is present in high copy numbers per virion and is recognized by most neutralizing anti-adenovirus antibodies which act predominantly by aggregating virus particles (Wohlfart, 1988). At least one neutralizing anti-hexon antibody, however, shows post-entry effects after endosomal escape but before binding to the nuclear pore complex, presumably by affecting the capsid association with MT and MT motor proteins (Smith et al., 2008). These findings argue for an important role of hexon in motor recruitment. But microinjected purified hexon or hexon expressed in cultured cells remains spread in the cytoplasm and shows an accumulation neither at the MTOC nor the nuclear envelope (Bremner et al., 2009; Wodrich et al., 2003). This indicates that hexon itself is not actively transported in the MT minus end direction and cannot obtain nuclear localization. These results are supported by biochemical evidence that hexon and cytoplasmic dynein do not interact at physiological pH. However, short-term exposure of immunopurified hexon to acidic pH before neutralization and subsequent incubation with purified cytoplasmic dynein strongly increases its ability to bind the motor protein (Bremner et al., 2009). In a simplified model of the passage through the acidic endosomal lumen, it

could be shown that an exposure of hexon to pH≤5.4 buffer, allows detectable interaction between the capsid protein and dynein in coimmunprecipitation experiments (Bremner et al., 2009). This result argues for the necessity of adenovirus exposure to low pH in the endosome for efficient infection (Smith et al., 2010b). A pH-dependent affinity of hexon for dynein would also explain a differential behavior of acid-exposed hexon after endosomalysis and newly expressed hexon trimers later in infection, which show no directed motility by themselves but require protein VI for nuclear localization.

Taken together, this summary strongly suggests that the major capsid protein hexon constitutes the link between the incoming viral capsid and the dynein motor protein.

1.3.2. Capsid Binding Dynein Subunits

Acidified adenovirus capsid or hexon alone interact with rat brain purified dynein. To identify the dynein subunit that interacts with the virion, lysate from cultured 293A cells overexpressing individual dynein subunits were screened for hexon interaction. These studies reveal that the dynein ICs and LIC1, but not LIC2 or TcTex-1, RP3 or LC8 are able to bind to acidified immunopurified hexon (Bremner et al., 2009). These findings are insofar novel as it is the first description that two dynein subunits are able to interact with one individual protein. Both subunits reside in the tail region of the dynein motor complex and have been implicated in binding to physiological cargo (Table 1-1) and it is conceivable that the interaction with the viral capsid interferes with regular cellular transport processes.

Besides the possible analysis of a competition between pathologic and physiological cargo of dynein, a more detailed determination of the exact binding sites on the dynein subunits might open avenues for the development of adenovirus-specific therapeutic peptides. Similar to the mode of neutralization of α-defensins that prevent endosomal uncoating by low affinity binding in high copy number at sensitive sites in the peripentonal region (Smith et al., 2010a), bona fide fragments of dynein subunits might be able to block the interaction with the dynein motor and therefore neutralize the virus at a post-entry step. However, more work needs to be completed to determine the molecular mechanism of hexon binding to dynein before additional steps in regards to blockage of virus infectivity can be undertaken.

1.3.3. Cytoplasmic Adenovirus Transport

After receptor-mediated uptake into the endosome, adenovirus progression towards the nucleus depends on cytoplasmic dynein. Besides dynein-mediated transport of the virus-containing endosome (Burkhardt et al., 1997; Gastaldelli et al., 2008), virus particles show a MT- and dynein-dependent motion pattern after endosomalysis, revealed by nocodazole treatment or dynein function-blocking antibody microinjections (Bremner et al., 2009; Leopold et al., 2000; Suomalainen et al., 1999). Interestingly, Ad5 progression towards the nucleus along the MT appears to be dependent on PKA activity (Suomalainen et al., 2001). Furthermore, virus attachment to cell surface integrins has been reported to stimulate host PKA activity required for efficient dynein-mediated capsid transport (Suomalainen et al., 2001). In addition, it could be shown by immunocytochemistry that several dynein

subunits still colocalize to high levels with incoming adenovirus in the cytoplasm after endosomal escape (Bremner et al., 2009). Furthermore, two of the growing number of known cargo adaptors and regulators of cytoplasmic dynein, dynactin and NudE/EL, also colocalize with incoming virus particles in the cytoplasm. After microinjection of function-blocking NudE/EL or Lis1 antibodies or overexpression of dominant-negative constructs that disrupt the NudE/EL and Lis1 regulation of cytoplasmic dynein (Stehman et al., 2007), no change in adenovirus progression towards the MTOC was seen in infected cells. In stark contrast, interference with dynactin-mediated dynein regulation by overexpression of headless dynactin p150^{Glued} and p150^{Glued}-CC1 constructs, strongly affected virus redistribution (Bremner et al., 2009; Engelke et al., 2011). Thus, dynein is presumably under dynactin control when transporting incoming adenovirus, which would indicate a low-load, high-speed transport of the capsid. Indeed, the speed of the capsid along MT can exceed 600nm/s (Bremner et al., 2009), which is close to the maximal speed measured for mammalian dynein (800nm/s).

In strong contrast to most physiological cargos, biochemical evidence indicates that adenovirus recruits dynein directly and only the regulatory function of dynactin seems to be required for adenovirus transport. Work on herpes simplex virus (HSV) supports the finding of a predominantly regulatory function of dynactin in a non-physiological context. HSV protein(s) of the inner tegument have the ability to bind dynein directly, but dynactin is required for virus transport (Döhner et al., 2002; Radtke et al., 2010).

ZW10, an additional dynein recruitment factor (Starr et al., 1998), showed minimal colocalization with incoming adenovirus and ZW10 RNAi had no effect on virus progression towards the nucleus (Bremner et al., 2009). Recently, further dynein regulators and cargo adaptors such as BicD2, spindly, bassoon, and snapin have been identified (Cai et al., 2010; Fejtova et al., 2009; Griffis et al., 2007; Hoogenraad et al., 2001) and it is of interest to elucidate their possible contribution to adenovirus motility.

With the first movies of adenovirus motility inside an infected cell at high temporal and spatial resolution, it has become obvious that the capsid does not follow a unidirectional trajectory towards the MTOC (Bremner et al., 2009; Leopold et al., 2000; Suomalainen et al., 1999). Instead, adenovirus follows a bidirectional motion pattern with short runs in the MT minus and plus end direction. Importantly, the overall net motility is MT minus end directed and allows the virus to reach and tightly bind the nuclear pore complex before it delivers its genome into the nucleus. Interestingly, enucleated cells or cells treated with leptomycin B, which inhibits the nuclear export factor CRM1, do not show capsid accumulation at the nucleus but instead at the MTOC (Bailey et al., 2003; Strunze et al., 2005). This indicates that the MTOC is the primary target of incoming virions and the nucleus acts as a "sink" to which capsids bind with high affinity. The bidirectional motion reveals that the capsid is not only transported by cytoplasmic dynein towards the MTOC but also by kinesin(s) in the opposite direction. However, microinjections of anti-kinesin-1 monoclonal antibodies, which were shown previously to interfere with kinesin

function, have no effect on virus redistribution 1h p.i. (Leopold et al., 2000). This result argues that either the efficiency of adenovirus motility towards the nucleus is independent of kinesin, the adenovirus associated MT plus end directed motor is not kinesin-1, the correct isoform of kinesin-1 is only inadequately targeted by the function blocking antibodies, or more than one class of kinesins is responsible for the bidirectional motion of the capsid and they can substitute for each other.

Chapter 2: Control of Adenovirus-Host Interactions by a Single Motor Protein Phosphorylation

2.1. Introduction

2.1.1. Introduction

Infection of cells by all DNA viruses and most retroviruses requires their efficient transport from the cell membrane to the nucleus to overcome premature inactivation (Marsh and Helenius, 2006; Radtke et al., 2006). A number of viruses have been found to accomplish this transition using microtubules (MTs) and their associated motors (Dodding and Way, 2011; Enquist, 2012; Greber and Way, 2006; Scherer and Vallee, 2011). In uninfected cells this machinery is responsible for the redistribution of cell organelles and macromolecular complexes. At least some viruses have evolved mechanisms allowing them to masquerade as motor protein cargo (Bremner et al., 2009; Radtke et al., 2010). Transport of these viruses to the nucleus involves the microtubule minus end-directed motor protein cytoplasmic dynein, a complex of 1.5MDa (Paschal et al., 1987) and possibly its regulators, including dynactin, LIS1, NudE, and NudEL (Vallee et al., 2012).

Adenovirus is a small non-enveloped dsDNA virus with a simple capsids consisting of three major (fiber, hexon, penton base) and five minor proteins. Adenovirus enters the cell by endocytosis (Dales, 1962; Fitzgerald et al., 1983) and the acidic pH of the endosomes triggers structural rearrangements of the viral capsid allowing

endosomalysis and additionally primes hexon for dynein binding (Bremner et al., 2009; Nakano et al., 2000). After endosomalysis, the capsid recruits cytoplasmic dynein directly through its IC and LIC1 subunits (Bremner et al., 2009), and uses the motor protein to travel to the centrosome and nuclear envelope regions (Bremner et al., 2009; Leopold et al., 2000; Suomalainen et al., 1999). Dynactin, NudE, and NudEL localize to the virus particles, but, unlike many physiological cargo, are not required for dynein recruitment (Bremner et al., 2009).

Within minutes of adenovirus infection PKA and p38/MAPK activity rise. Inhibition of these pathways each resulted in a 2.5-fold decrease in the efficiency of virus transport toward the nucleus (Suomalainen et al., 2001), affecting parameters of motor protein-driven virus motility, but the kinase substrates remain unknown (Suomalainen et al., 2001). PKA signaling has been shown to modulate bidirectional movement of melanosome pigment granules in fish and amphibian chromatophore cells (Reilein et al., 1998). Although the molecular basis for the PKA effects is also incompletely understood in these systems, it is possible that virus transport takes advantage of existing physiological mechanisms.

Here we describe a novel PKA phosphorylation site in the dynein subunit LIC1, which we find to represent a crucial determinant for activating virus transport to the cell center. We have also identified a dramatic virus-activated, PKA-dependent lysosomes/late endosome dispersal, which could represent a novel host response to virus infection.

2.1.2. Materials and Methods

Cells, Viruses, and Antibodies

A549, Cos7, and 293A cells were grown in DMEM supplemented with 10% FBS. Replication-deficient Ad5 engineered to express GFP (Ad5-GFP, plaque-purified; obtained from H. Young, Columbia University) or wild-type Ad3 (VR-3, ATCC) and Ad41 (VR-930, ATCC) were propagated in 293A cells and purified by banding on two linear CsCl gradients (Lawrence and Ginsberg, 1967) and dialyzed against 10% glycerol in PBS before cryo-storage. Viral titer was obtained using fluorescent focus assays for Ad5-GFP (Thiel and Smith, 1967). Alexa546-labelling was described earlier (Bremner et al., 2009). A549 cell infections for fixed cell microscopy (MOI 20) were all performed in a low volume of DMEM without FBS at 4°C for 30 min to allow virus attachment. The cells were washed twice in warm PBS and incubated in fresh DMEM/10% FBS for 60 min at 37°C, unless stated otherwise, to allow internalization and intracellular transport. For live cell imaging, cells were infected at 100MOI with virus attachment at 37°C for 5 min.

Antibodies used included mouse monoclonal anti-hexon (Novocastra), anti-HA (clone 16B12, Covance), anti-FLAG (M2, Sigma), anti-myc (9E10, SantaCruz), anti-tubulin (Sigma), anti-p150^{Glued} (BD Bioscience) and anti-dynein IC (74.1, Chemicon), rabbit antibodies anti-LIC, and anti-LIC2 (Tynan et al., 2000b), anti-adenovirus5 (Abcam), anti-Arp1 (Sigma), anti-DHC (Mikami et al., 1993), anti-Lamp1 (abcam), anti-GFP (Invitrogen), anti-FLAG (Abcam), anti-HA (Sigma), antibodies recognizing phosphorylated PKA sites (RRXp[S/T], or RXXp[S/T], CellSignaling), and chicken anti-LIC1 (Tan et al., 2011), and anti-GFP (Milipore).

LysoTracker Green and Mitotracker Green (Invitrogen) was used to label lysosomes and mitochondria, respectively.

Plasmids, RNAi, and Molecular Methods

Mammalian expression constructs used in this work included LIC1 truncations (Tynan et al., 2000b), GFP-CD63, -Rab7 (Tan et al., 2011), -NPC1, and -NAGT (Yi et al., 2011).

Rat LIC1 was subcloned into the pEGFP-C1 vector (Clontech, Mountain View, CA) by introducing 5' XhoI and 3' KpnI restriction sites by PCR. Resistance to LIC1 RNAi was archived as described (Tan et al., 2011). LIC1 point-mutants were generated by site-directed mutagenesis (QuikChange II, Agilent Stratagene, Cedar Creek, TX) using primer sequences CCCCTCAGCGAAGAGCC**G**CGGCTGCACAGG and CCCCTCAGCGAAGAGCC**GAT**GCTGCACAGG for T213A and T213D, respectively (mutations in bold letters).

For RNAi, shRNA constructs based on the pRetro-U6G vector (Cellogenetics, MD) were used, the sequence for pRETRO-LIC1 is GTTGATTAGAGACTTCCAATT, for pRETRO-LIC2 is GCCAGAAGATGCATATGAA, and for the scrambled control is CTTCATTAGAGAGTTCCAA. The RNA sequence used for LIC1 siRNA was GUUGAUUAGAGACUUCCAATT, for LIC2 siRNA it was GGAUAGAAUGACUCGAAAAUU (Tan et al., 2011).

Transient transfections were performed using either Lipofectamine 2000 (Invitrogen) or Effectene (QIAGEN). siRNA oligos were transfected with HiPerfect (QIAGEN).

Cloning of bacterial expression constructs of his-tagged LIC1 and LIC2 constructs was described previously (Tynan et al., 2000b) and subjected to above mentioned mutagenesis. GST-tagged IC2C truncations and LC8 were described previously (McKenney et al., 2011), full-length rat IC1A and IC2C were cloned in frame with GST into the pGEX-6p vector (GE Bioscience) using BamHI/XhoI and BamHI/EcoRI sites, respectively. An additional C-terminal his-tag was introduced by PCR.

Immunofluorescence Microscopy, Live Cell Imaging, and Drugs

Cells were grown on glass coverslips and fixed in methanol at -20°C for 5 min or with 4%PFA/PBS at RT for 15min. Coverslips were blocked for >60 min in 0.5% donkey serum/PBS; incubated in primary antibody at 37°C for 1 hr; washed and incubated for 1 hr at 37°C in Cy2-, Cy3-, or Cy5-conjugated secondary antibody; then mounted using ProLong Gold antifade mounting media containing DAPI (Invitrogen) and imaged using a confocal microscope (IX-81, Olympus, Center Valley, PA) equipped with a 63x oil immersion objective. Live cell imaging experiments were described earlier (Bremner et al., 2009). Briefly, cells were grown in glass-bottomed dishes (MatTek Corp, Ashland, MA), infected with Alexa546-Ad, covered with CO2-independent medium and then processed for imaging in a 37°C chamber. Movies were acquired for 90 min p.i. at 2frames/min using a 63x oil immersion objective and a CCD camera (model C9100-12; Hamamatsu) attached to an inverted microscope (Leica) operated by Metamorph Imaging software (Molecular Devices). For image and movie analysis and particle counting ImageJ was used.

Drugs targeting PKA activity included H-89 and forskolin (FSK) purchased from Sigma-Aldrich (Saint Louis, MO), cRGD and PKI-myr from Enzo LifeSciences (Farmingdale, NY), and 3-isobutyl-1-methylxanthine (IBMX) from Santa Cruz (Santa Cruz, CA).

Proteins and Biochemical Analysis

Rat brain lysate and purified rat cytoplasmic dynein were prepared in phosphate-glutamate buffer (pH 7.0) as previously described (Paschal et al., 1987). Adenovirus hexon was either recovered from virus-depleted supernatant of the first CsCl gradient by immunoprecipitation as described (Bremner et al., 2009) or by anion exchange chromatography (Waris and Halonen, 1987). Vectors for GST- and his-tagged dynein subunits were transformed into BL21-Gold(DE3)pLysS E.coli (Agilent Stratagene, Cedar Creek, TX) and expressed for 3-5h at 20°C after 15min ice-shock of LB cultures at OD_{600}=0.6 and induction with 0.5mM IPTG. Purification was performed following standard procedures with Ni+ (Sigma-Aldrich) in buffer A (30mM TrisHCl, 150mM NaCl, 5mM imidazole, 5mM β-Mercaptoethanol, pH7.4) supplemented with protease inhibitor cocktail (Sigma-Aldrich), eluted with 450mM NaCl and 200mM imidazole, followed by buffer exchange into buffer A or Glutathione (USB) beads in buffer B (10mM TrisHC, 150mM NaCl, 1mM EDTA, 0.5mM DTT, pH7.4), and eluted with 10mM reduced glutathione or digested with R3C protease to cleave off GST. Proper protein folding was checked by size exclusion chromatography and by binding to known interaction partners. Purified proteins were flash frozen in liquid nitrogen and stored at -80°C.

For phosphatase treatment, purified dynein was incubated with λ-phosphatase (NEB) 2:1 (w/v) for 1 hr at 30°C in phosphatase buffer supplemented with MnCl2. The reaction was stopped using a phosphatase inhibitor cocktail (50mM NaF, 5mM tetra-sodium pyrophosphate, 1mM sodium ortho-vanadate, 10mM β-glyceropyrophosphate). For in vitro PKA phosphorylation, the catalytic subunit of PKA (Sigma) was incubated with purified dynein or dynein subunits at about 50:1 (unit/nmole) for 30 min at 30°C before the reaction was stopped with 67 μM H-89 (Sigma).

Mammalian cultured cell lysates were prepared in RIPA buffer (50mM Trisma-maleate, 100 mM NaCl, 1 mM EGTA, [pH 7.4]) containing protease inhibitor cocktail (Sigma) and 1% NP40, and the membrane fraction was removed by centrifugation.

Hexon binding assays were described previously (Bremner et al., 2009). Briefly, hexon was immunoprecipitated from virus-depleted infected 293A cell lysate with anti-hexon antibodies and protein A sepharose beads (GE Bioscience). The hexon beads were washed and incubated for 30 min in Tris-maleate buffer (50 mM Trizma-maleate, 10 mM NaCl, 1 mM EDTA, and 0.1% Tween 20, pH 4.4), washed in the same buffer at pH 7.4, and then incubated with purified cytoplasmic dynein or bacterially expressed polypeptides at 4°C for 1.5 hr. Following washing, the beads were analyzed for the presence of dynein or dynein subunits by immunoblotting.

Statistical Analysis

For analysis, two-sample comparisons were performed via Student's t test. Statistical significance was inferred for p values less than 0.05. Analysis and

statistical tests were performed using Excel (Microsoft, Redmond, WA) and Prism (GraphPad, La Jolla, CA).

2.2. Results

2.2.1. LIC1 phosphorylation

While screening conditions to optimize dynein binding to acidified hexon during earlier work (Bremner et al., 2009), we found that dynein treatment with a general phosphatase significantly reduces the hexon affinity of the motor complex (Figure 2-1). Regarding stimulated PKA activity upon adenoviral infection (data not shown and (Suomalainen et al., 2001)) and the reported involvement of PKA in MT minus-end directed motility of adenovirus (Suomalainen et al., 2001), we sought to rescue the dephosphorylation effect by subsequent *in vitro* PKA phosphorylation. PKA phosphorylation alone or after phosphatase treatment increases the hexon affinity compared with untreated dynein to 158% (±39%) or 168% (±65%), respectively, indicating a clear role of PKA phosphorylation in dynein binding to hexon (Figure 2-1A). In a separate experiment, we used a monospecific antibody against the phosphorylated PKA motif (RRXpS/T) for immunoblotting of rat brain purified dynein before and after PKA treatment. The antibody reacted with only two dynein subunits, strongly with the IC and to a lesser extent with LIC1 (Figure 2-1B).

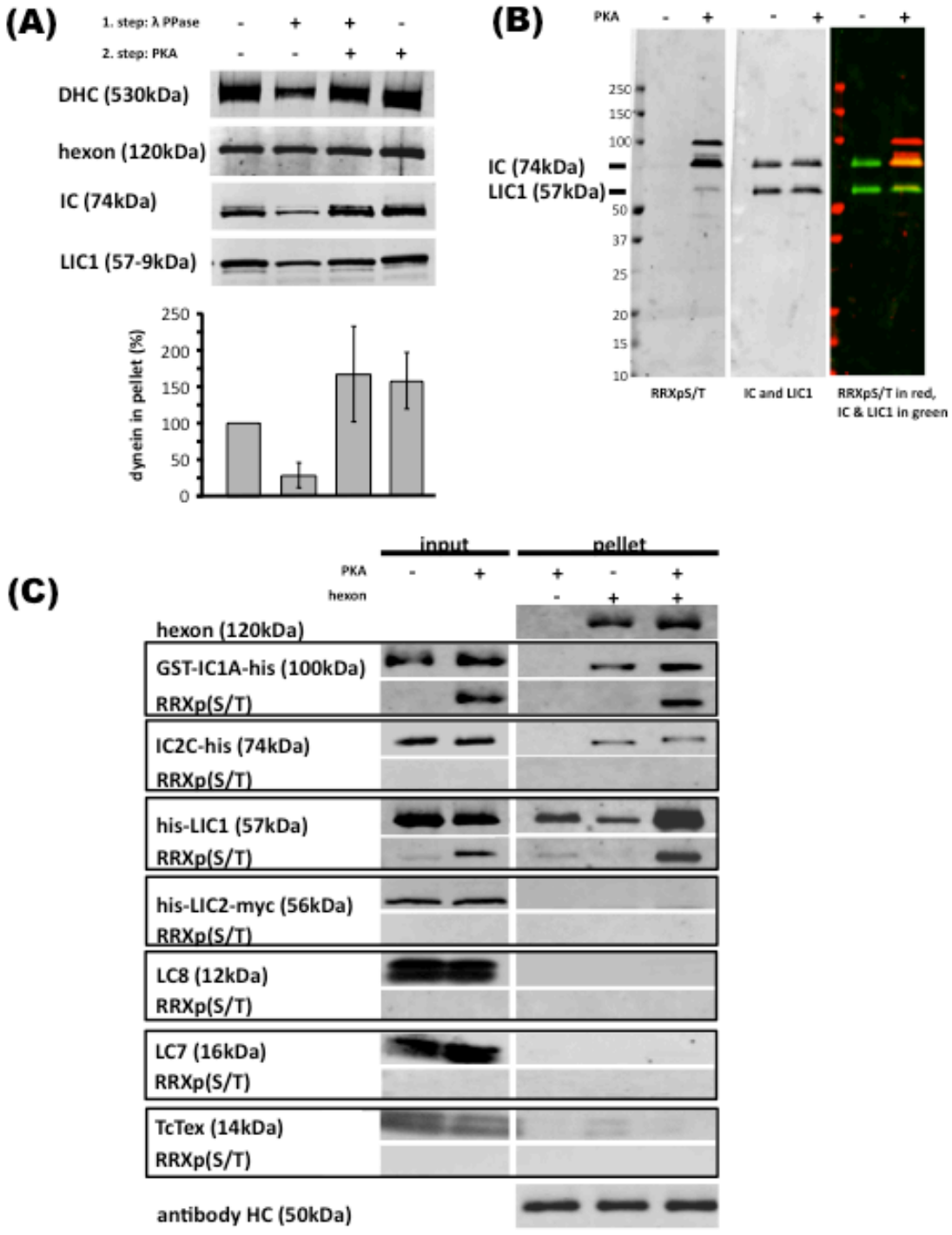
(A)
1. step: λ PPase - + + -
2. step: PKA - - + +
DHC (530kDa)
hexon (120kDa)
IC (74kDa)
LIC1 (57-9kDa)
dynein in pellet (%)
250
200
150
100
50
0
(B)
PKA - + - + - +
IC (74kDa)
LIC1 (57kDa)
250
150
100
50
37
25
20
15
10
RRXpS/T
IC and LIC1
RRXpS/T in red,
IC & LIC1 in green
(C)
input
pellet
PKA - + + - +
hexon - + +
hexon (120kDa)
GST-IC1A-his (100kDa)
RRXp(S/T)
IC2C-his (74kDa)
RRXp(S/T)
his-LIC1 (57kDa)
RRXp(S/T)
his-LIC2-myc (56kDa)
RRXp(S/T)
LC8 (12kDa)
RRXp(S/T)
LC7 (16kDa)
RRXp(S/T)
TcTex (14kDa)
RRXp(S/T)
antibody HC (50kDa)

Figure 2-1: PKA Phosphorylation of Dynein LIC1 Affects Hexon Binding.

(A) Purified rat brain cytoplasmic dynein was exposed to λ-phosphatase (PPase) and/or protein kinase A (PKA) catalytic subunit and evaluated for co-immunoprecipitation with hexon by immunoblotting of the pellets with antibodies against hexon, and dynein heavy, intermediate, and light intermediate chain (HC, IC, LIC) subunits. Lower panel, quantification of immunoblotting results: n = 3, mean ± SD, mock treated = 100%. Dynein dephosphorylation decreased, and PKA treatment enhanced binding to hexon. (B) Purified dynein was exposed to PKA catalytic subunit, and phosphorylation was evaluated by immunoblotting with antibodies against the dynein ICs, LIC1, and the phosphorylated PKA consensus sequence RRXp(S/T). Clear phosphorylation of the IC and LIC1 subunits is observed. Higher molecular weight band is contaminant in PKA preparation (data not shown). (C) Bacterially expressed full-length dynein subunits IC1, IC2, LIC1, LIC2, LC8, LC7, and TcTex were exposed to PKA catalytic subunit and tested for phosphorylation and hexon co-immunoprecipitation by immunoblotting with the anti-RRXp(S/T) antibody. LIC1 and IC1 were clearly phosphorylated, which specifically increased LIC1 binding to hexon

Of note, IC and LIC1 are the same dynein subunits that we previously identified to interact with hexon after expression in mammalian cells (Bremner et al., 2009). To elucidate which subunit is responsible for the increased affinity to hexon of the entire dynein complex, we purified recombinant full-length rat dynein IC1, IC2, LIC1, LIC2, LC8, LC7 and TcTex from bacterial lysate, mock or PKA treated the polypeptides, and performed coimmunoprecipitation experiments with acidified hexon. Using the RRXpS/T antibody, we identified only IC1 and LIC1 to be substrates of PKA, in contrast to IC2, LIC2, LC8, LC7 and TcTex (Figure 2-1C). The same results were seen using a less stringent RXXpS/T antibody (data not shown). Furthermore, IC1 and IC2 were coimmunoprecipitated with acidified hexon to a similar extent independent of their phosphorylation state, while LIC2 and LC8 were absent in the coimmunoprecipitates for both conditions (Figure 2-1C). Mock

treated, bacterially expressed LIC1 did not interact with hexon in contrast to mammalian expressed LIC1 (Bremner et al., 2009) indicating that post-translational modifications regulate the hexon affinity of this dynein subunit. In agreement with this, LIC1 is the only subunit that showed an enhanced signal in the coimmunoprecipitate after PKA treatment (Figure 2-1C).

Together, these results show that PKA phosphorylation of the dynein complex increases its hexon affinity and that one or multiple PKA sites in LIC1 are responsible for this effect.

For the identification of possible PKA sites, we aligned the protein sequences of human, rat, mouse, chicken, xenopus, and zebrafish LIC1 and screened them for the RRXS/T motif. Only one evolutionary conserved site could be identified at threonine 213 (rat, mouse, human sequence) (Figure 2-2A). Interestingly, LIC2 contains a non-phosphorylatable proline at that site.

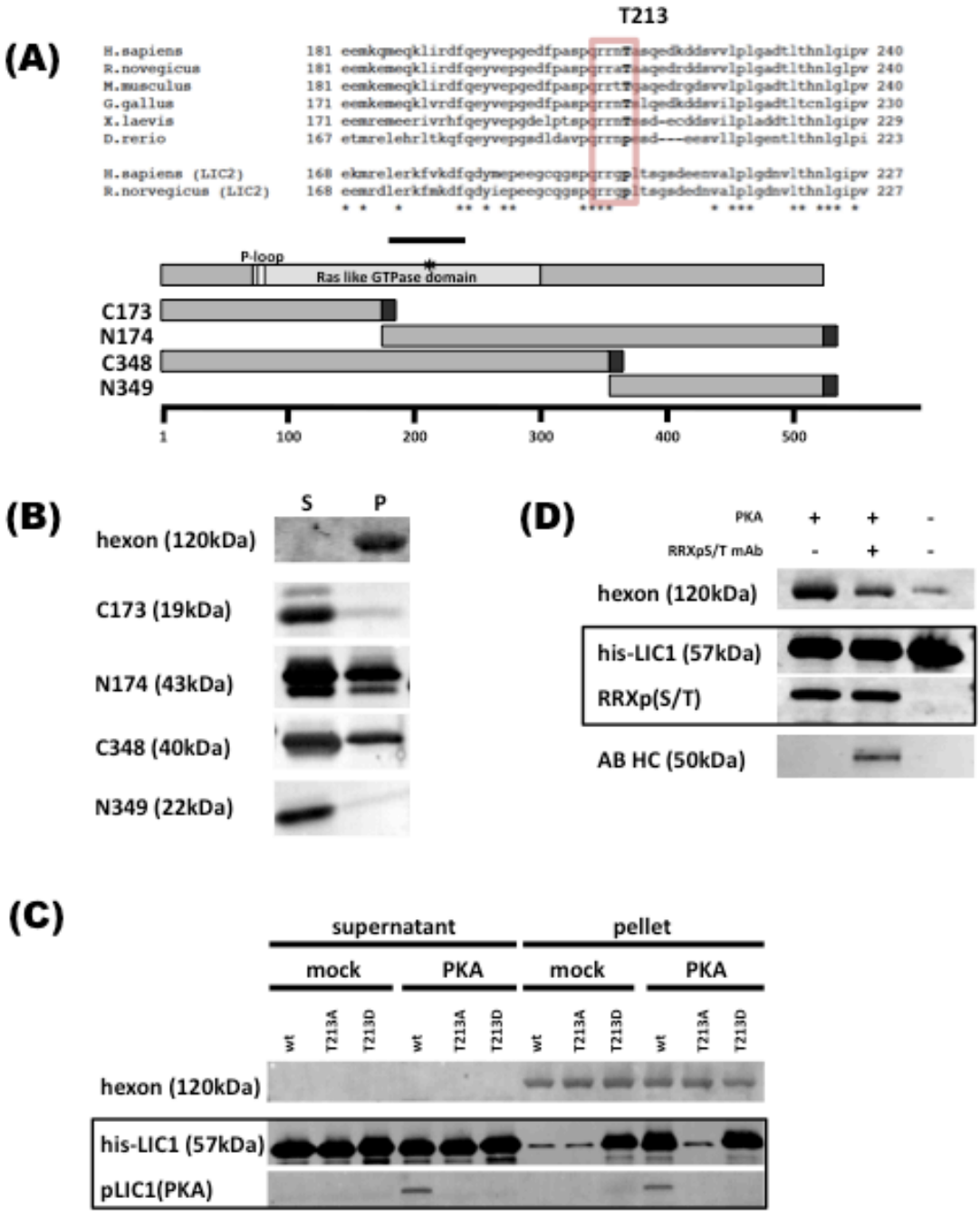
(A)
T213
H.sapiens 181 eemkqmeqklirdfqeyvepgedfpaspgrrnTaagedkddsvvlplgadtlthnlgipv 240
R.novegicus 181 eemkemeqklirdfqeyvepgedfpaspgrraTaagedrddsvvlplgadtlthnlglpv 240
M.musculus 181 eemkemeqklirdfqeyvepgedfpaspgrrtTaagedrgdsvvlplgadtlthnlglpv 240
G.gallus 171 eemkemeqklvrdfqeyvepgedfpaspgrrnTalgedkddsvilplgadtltcnlgipv 230
X.laevis 171 eemremeerivrhfqeyvepgdelptspgrrnTaad-ecddsvilpladdtlthnlgipv 229
D.rerio 167 etmrelehrltkqfqeyvepgsdldavpgrrnpaad---eesvllplgentlthnlglpi 223
H.sapiens (LIC2) 168 ekmrelerkfvkdfqdymepeegcqgspgrrgpltsgsdeesvalplgdnvlthnlgipv 227
R.norvegicus (LIC2) 168 eemrdlerkfmkdfqdyiepeegcqgspgrrgpltsgsdedsvalplgdnvlthnlgipv 227
P-loop
Ras like GTPase domain
C173
N174
C348
N349
1
100
200
300
400
500
(B)
S
P
hexon (120kDa)
C173 (19kDa)
N174 (43kDa)
C348 (40kDa)
N349 (22kDa)
(D)
PKA + + -
RRXpS/T mAb - + -
hexon (120kDa)
his-LIC1 (57kDa)
RRXp(S/T)
AB HC (50kDa)
(C)
supernatant
pellet
mock
PKA
mock
PKA
wt
T213A
T213D
hexon (120kDa)
his-LIC1 (57kDa)
pLIC1(PKA)

Figure 2-2: LIC1-T213 Represents PKA Site that Regulates Hexon Binding.

(A) LIC1 sequences of *H.sapiens* (human), *R.norvegicus* (rat), *M.musculus* (mouse), *G.gallus* (chicken), *X.laevis* (frog), *D.rerio* (zebrafish), and human and rat LIC2 were aligned to identify conserved PKA phosphorylation sites in LIC1, which are not present in LIC2. Only parts of the sequences surrounding T213 are shown (upper panel). LIC1 domain structure with P-loop sequence, ras-like GTPase domain, and location of T213 in the polypeptide are shown (middle panel). Bold line indicates sequence covered in upper panel. Delineated truncation constructs of LIC1 for mammalian expression were used to identify hexon binding site (lower panel). (B) LIC1 truncation constructs were expressed in 293A cells and were tested in hexon co-immunoprecipitation. Only fragments including the middle third of the LIC1 polypeptide show hexon binding. (C) Bacterially expressed LIC1 wild-type or the LIC1-T213A and -T213D mutants were tested for PKA phosphorylation and hexon co-immunoprecipitation. The phosphomimetic LIC1-T213D mutant alone interacted with hexon. No PKA phosphorylation was detected in the mutant polypeptides, identifying T213 as the major PKA site. (D) Monospecific antibody, which recognizes phosphorylated LIC1-T213 was tested for competition with hexon for LIC1 binding. Adding the antibody to the PKA-phosphorylated LIC1 pull-down reaction drastically reduces the amount of hexon in the pellets. Unphosphorylated LIC1 was used as negative control.

Additionally, two conserved RXXS/T sites can be found specifically in LIC1, serine 9 and 414, respectively. However, they appear to be outside the hexon-binding region of LIC1, which is in the vicinity of T213 (Figure 2-2B). Myc-tagged truncation constructs of LIC1 were expressed in mammalian cells (Tynan et al., 2000b) and used for anti-hexon coimmunoprecipitation studies. Like the full-length protein (Bremner et al., 2009), we found the C-terminal N174 and N-terminal C348 constructs, which both contain T213, to interact with hexon (Figure 2-2B). In contrast, the two N349 and C173 constructs, which lack the middle third of LIC1, show no interaction with hexon (Figure 2-2B). These results further argue for T213 as the PKA site regulating hexon binding. We mutated this residue either to aspartic acid (T213D, phospho-mimetic) or alanine (T213A, dephospho-mutant) in our

bacterial expression constructs. Even without PKA phosphorylation, LIC1-T213D was able to interact with acidified hexon, indicating that the aspartic acid successfully mimics the phosphorylated threonine at that side (Figure 2-2C). In contrast, LIC1-T213A could not be phosphorylated by PKA as indicated by an absent RXXpS/T signal and did not interact with acidified hexon above background levels (Figure 2-2C). Furthermore, the interaction between hexon and PKA phosphorylated wild-type LIC1 could be inhibited by adding RRXpS/T antibody to the reaction (Figure 2-2D).

These results illustrate that within dynein, PKA phosphorylation of LIC1-T213 represents a necessary and sufficient event to prime the motor protein for hexon binding.

We also tested the dynein LIC1 T213D and IC2C 1-250 (see chapter 4.2.3.) for competition for hexon binding and found that both accessory subunits can bind hexon to the same extent either by themselves or in combination under limiting hexon conditions, arguing against a common binding site on hexon (Figure 2-3A). However, the two subunits behaved differently in competition experiments with the dynein complex. Addition of LIC1 T213D to the binding reaction reduces the amount of dynein in the anti-hexon coimmunoprecipitates in comparison to the reaction with dynein alone but shows clear LIC1 binding to hexon (Figure 2-3B). Adding IC 1-250 to the reaction does not reduce the dynein signal in the pellet but in addition shows interacting IC fragment (Figure 2-3B).

These findings establish LIC1 as the most critical subunit of the dynein complex for hexon binding.

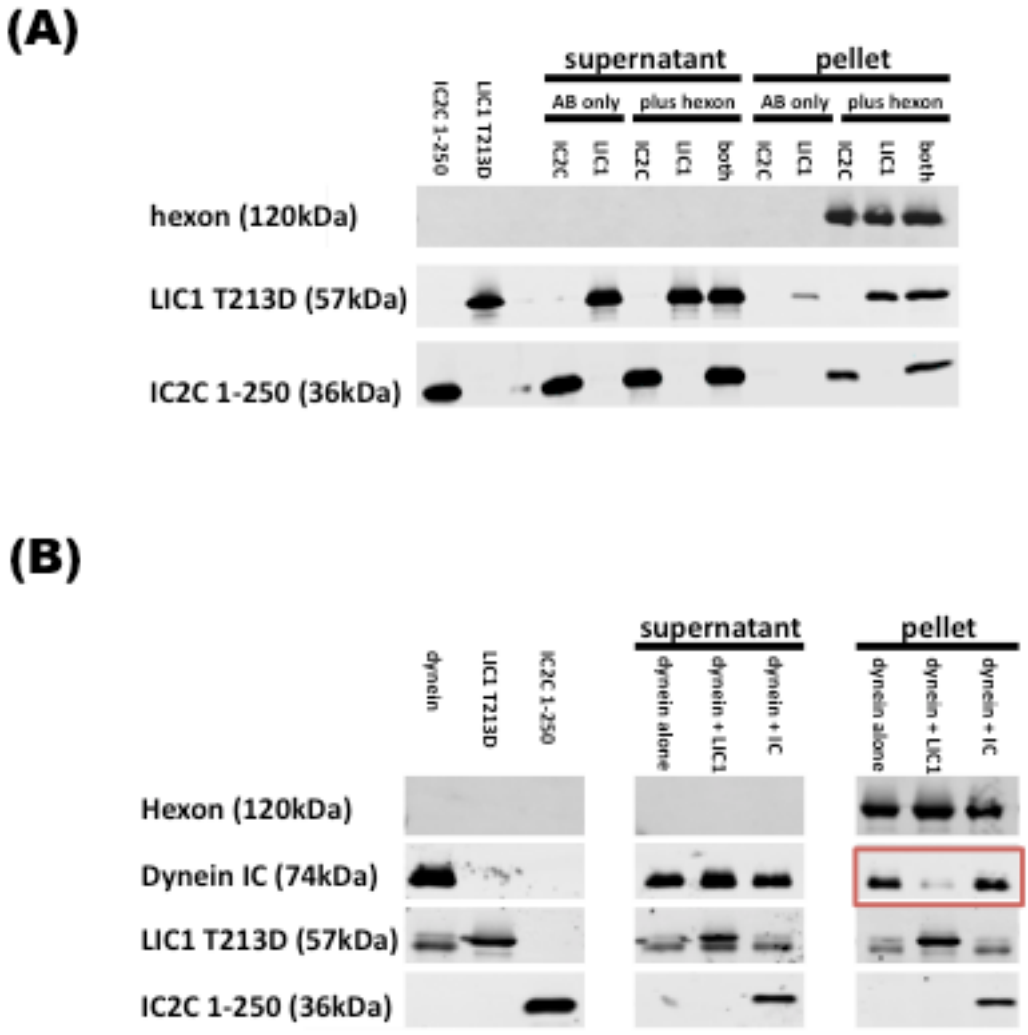

Figure 2-3: LIC1-T213D, but not IC1-250 Competes with Dynein.

(A) Bacterially expressed full-length LIC1-T213D and IC2C 1-250 fragment were tested individually and in combination for hexon binding. Both polypeptides show similar concentrations in the hexon co-immunoprecipitate independent of the presence of the other dynein subunit indicating a non-competitive interaction. (B) Purified rat brain cytoplasmic dynein was tested for pull-down with hexon in the presence of bacterially expressed LIC1-T213D or IC2C 1-250 by immunoblotting of the inputs (I), supernatants (S), and pellets (P) with antibodies against hexon, and dynein IC and LIC1 subunits. LIC1-T213D strongly reduced sedimentable dynein (red box), as indicated by a loss of IC signal, whereas LIC1-T213D can now be detected. Addition of the IC fragment has no effect on dynein co-immunoprecipitation (red box) and combined binding of IC fragment and dynein complex to hexon was detected.

To elucidate if dynein LIC1 also has a functional relevance for virus transport *in vivo,* we used vector based RNAi constructs against LIC1 and LIC2 and tested transfected A549 cells for nuclear targeting of adenovirus at 60min post-infection (p.i.) when most capsids localize at the nucleus in control settings (Bremner et al., 2009) (Greber et al., 1993; Leopold et al., 2000; Suomalainen et al., 1999). Two days of RNAi shows a clear, specific reduction of the LIC1 and LIC2 protein levels (Figure 2-4A) and for LIC1 RNAi also a striking reduction of capsids at the nucleus 60min p.i. (Figure 2-4B and C). This is, however, in marked contrast to the control or LIC2 RNAi transfected cells, which show nuclear virus targeting similar to control untransfected cells (Figure 2-4B and C).

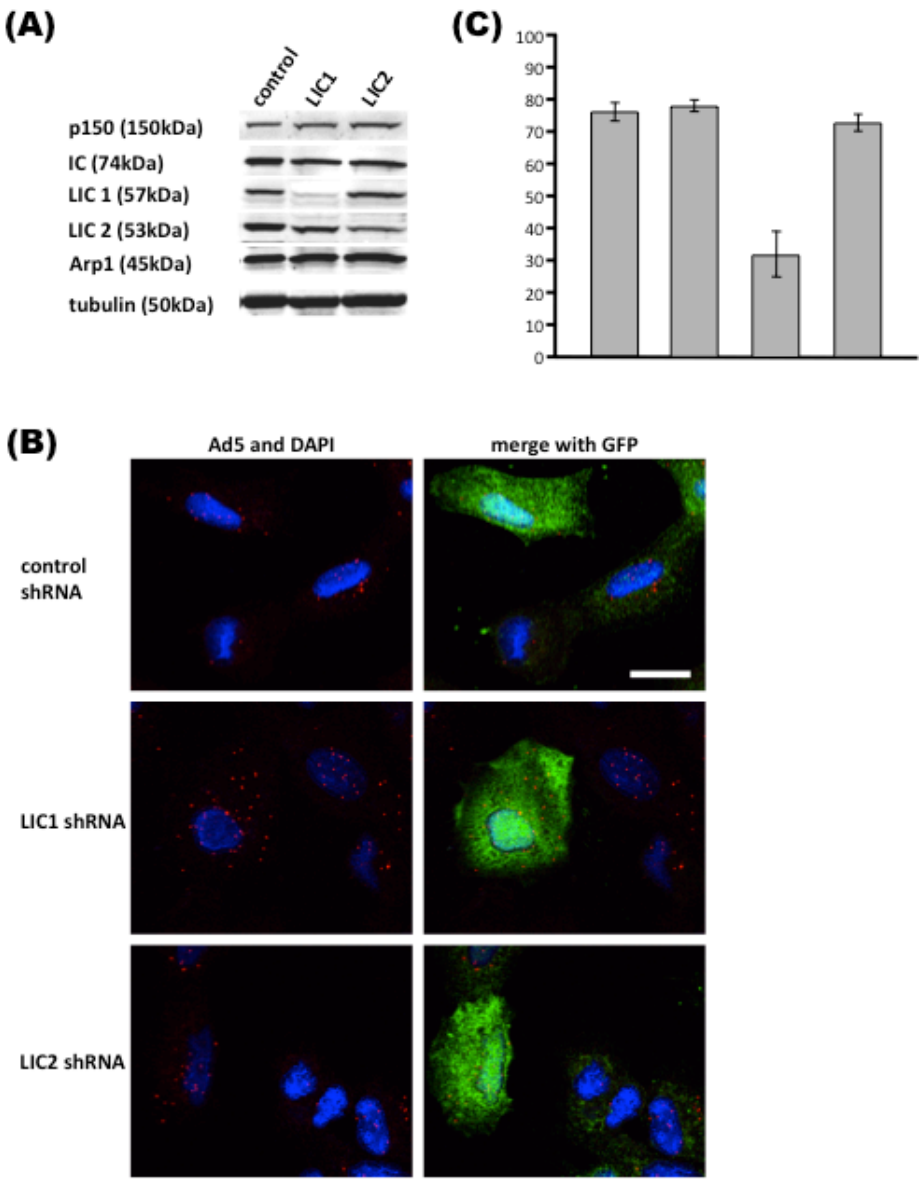

Figure 2-4: LIC1, but not LIC2 shRNA Reduces Nuclear Redistribution.

(A) Protein levels in lysates of A549 cells transfected with control, LIC1-, or LIC2-targeted shRNAs for 48h evaluated by immunoblotting using anti-p150^{Glued}, anti-IC, anti-LIC1, anti-LIC2, and anti-Arp1 antibodies, with anti-tubulin as a loading control. LIC1 was reduced by 88% and LIC2 by 65%. (B) LIC RNAi effect on adenovirus redistribution. LIC1, LIC2, or control shRNA-expressing A549 cells infected at 48 hr with Ad5 and fixed at 60 min p.i. Cells were immunostained for Ad5 and GFP, and counterstained for DNA (DAPI). LIC1 shRNA inhibited Ad5 redistribution, an effect not detected for control or LIC2 shRNA. Bar = 20 μm. (C) Quantification of virus redistribution shown in panel B. Mean percent of Ad5 particles localizing at the nucleus 60 min p.i. ± SD from three independent experiments with >30 cells each.

Furthermore, we performed rescue experiments with RNAi resistant GFP-LIC constructs, which we transfected into cells 24h after LIC1-targeted siRNAs (Figure 2-5A). At 24h of rescue construct expression, we infected the cells with adenovirus and fixed at 60min p.i. to analyze nuclear redistribution phenotypes for wild-type LIC1, LIC1-T213D, LIC1-T213A, and wild-type LIC2 compared to GFP control (Figure 2-5B and D). In accordance to the biochemical evidence, wild type LIC1 and LIC1-T213D are able to rescue the RNAi phenotype, while LIC1-T213A and LIC2 are not (Figure 2-5B and D). We have shown that our GFP-LIC1 construct successfully incorporates into the dynein complex (Tan et al., 2011) and the low expression levels during rescue presumably prevent possible dominant-negative effects. Using an inhibitor of PKA activity in the LIC1-T213D rescue condition should discriminate between LIC1 being the only PKA substrate that is required for nuclear localization of adenovirus and the presence of possible other PKA substrates critical for MT based adenovirus transport (Figure 2-5C and D). When we compared LIC1 RNAi cells treated with a highly specific PKA inhibitor (PKI-myr, 50uM), we saw an incomplete rescue of the nuclear redistribution phenotype in the LIC1-T213D expressing cells (Figure 2-5C and D).

Taken together, these results indicate that LIC1-T213 plays an important role in intracellular adenovirus motility and that other PKA substrates besides LIC1-T213 might be responsible for efficient nuclear targeting of adenoviruses.

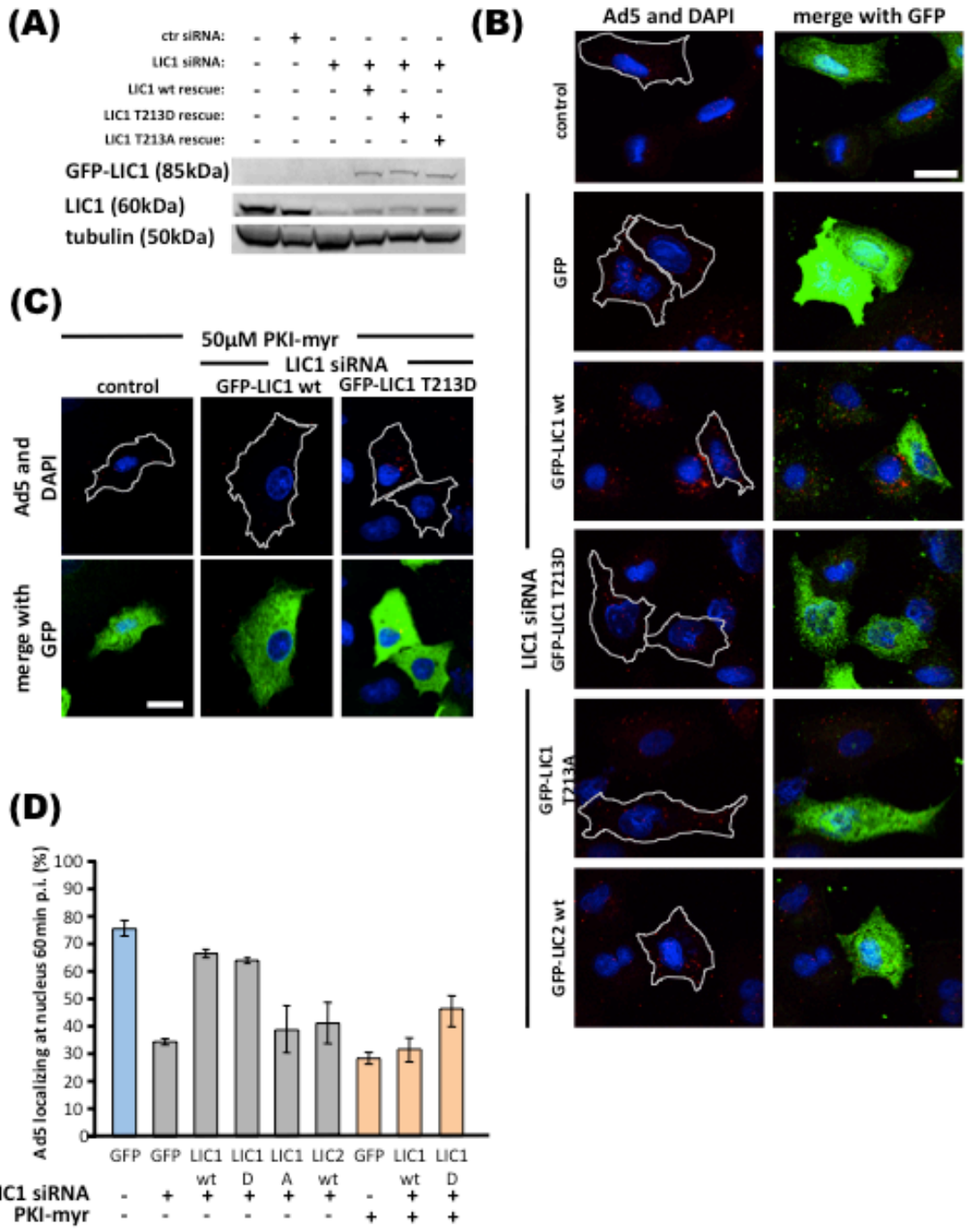
(A)
ctr siRNA:
LIC1 siRNA:
LIC1 wt rescue:
LIC1 T213D rescue:
LIC1 T213A rescue:
GFP-LIC1 (85kDa)
LIC1 (60kDa)
tubulin (50kDa)
(B)
Ad5 and DAPI
merge with GFP
control
GFP
GFP-LIC1 wt
GFP-LIC1 T213D
GFP-LIC1 T213A
GFP-LIC2 wt
LIC1 siRNA
(C)
50μM PKI-myr
LIC1 siRNA
control
GFP-LIC1 wt
GFP-LIC1 T213D
Ad5 and DAPI
merge with GFP
(D)
Ad5 localizing at nucleus 60 min p.i. (%)
GFP GFP LIC1 wt LIC1 D LIC1 A LIC2 wt GFP LIC1 wt LIC1 D
LIC1 siRNA
PKI-myr

Figure 2-5: Phosphorylated LIC1 is Required for Transport of Adenovirus to the Nucleus.

(A) Protein levels in lysates of A549 cells exposed to siRNAs (48h), and expression of RNAi resistant GFP-LIC1 (24h) evaluated by immunoblotting using anti-LIC1 and anti-GFP antibodies, with anti-tubulin as a loading control. (B) LIC1 RNAi rescue of adenovirus redistribution. LIC1 siRNA-treated A549 cells transfected at 24 hr with GFP-tagged LIC1 and LIC2 cDNAs (indicated on left) and infected at 48 hr with Ad5 for 60 min. Cells were stained for Ad5, GFP, and DNA (DAPI). Transfected cells are outlined. Adenovirus normally redistributes to the nucleus (control). LIC1 RNAi inhibits redistribution (LIC1 siRNA, GFP), an effect rescued by GFP-LIC1-wt and GFP-T213D, but not GFP-T213A or GFP-LIC2. Bar = 20 μm. (C) LIC1 RNAi rescue of adenovirus redistribution like in panel B, in presence of PKA inhibitor PKI-myr. The inhibitor alone (control) inhibited virus accumulation at the nucleus, whereas partial inhibition was observed in the RNAi rescue cells. Bar = 20 μm. (D) Quantification of virus redistribution shown in panels B and C. Mean percent of Ad5 particles localizing at the nucleus 60 min p.i. ± SD from at least two independent experiments with >40 cells each.

2.2.2. Lysosome dispersal

Unexpectedly, from an evolutionary perspective, a cellular kinase activity on dynein seems to aid viral infection. In addition, the physiological role of this phosphorylation site has not been identified. Hence, we set out to visualize the redistribution of physiological dynein cargo in response to viral infection (Figure 2-6, Figure 2-7, Table 2-1). The overall cell shape and MT array remained unaffected up to 2hr p.i. To our surprise, LysoTracker-positive lysosomes/late endosomes (lyso/LEs) and Rab7 positive late endosomes, organelles that have previously been shown to be under direct dynein and LIC1 control (Tan et al., 2011; Yi et al., 2011), show a drastic, repeatable, and robust dispersal upon viral infection (Figure 2-6, Figure 2-7, Table 2-1). Vesicles positive for the Nieman-Pick disease associated

protein NPC1, the Golgi apparatus (visualized with GFP-NAGT I), multivesicular bodies (GFP-CD63), and mitochondria (MitoTracker) maintain their perinuclear localization and early endosomes (GFP-Rab5) continue to stream from the cell periphery towards the center (Figure 2-7 and not shown). Furthermore, inhibition of PKA in combination with viral uptake reduced lyso/LE dispersal, indicative of a role of PKA in lysosome motility (Figure 2-6, Table 2-1). Furthermore, stimulating PKA outside of an adenoviral challenge with forskolin (10mM) has an effect on lyso/LEs with similar kinetics as adenoviral infection (Figure 2-6, Table 2-1). Therefore, PKA is necessary and sufficient for adenovirus induced lyso/LE dispersal.

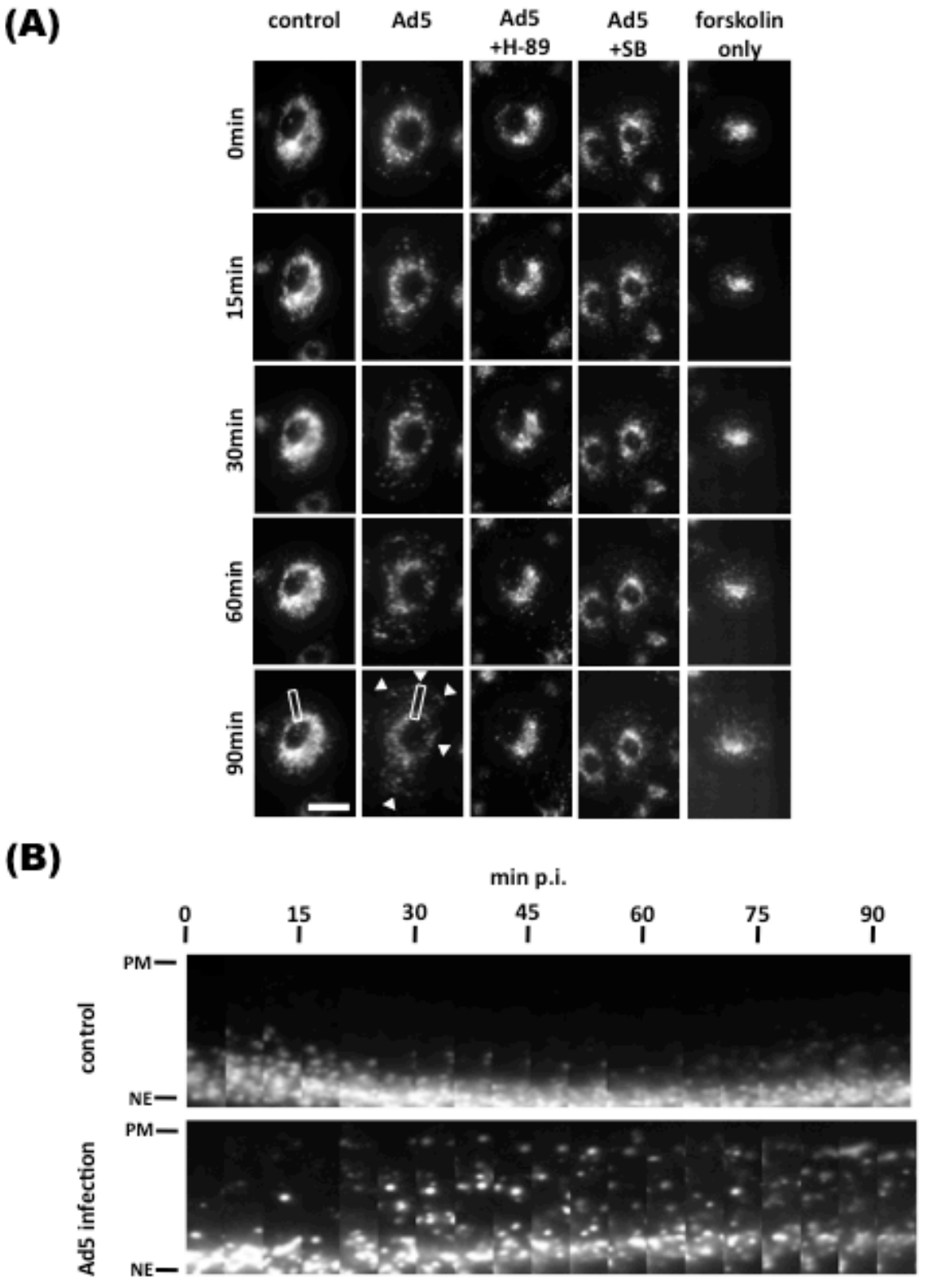
(A)
control
Ad5
Ad5 +H-89
Ad5 +SB
forskolin only
0min
15min
30min
60min
90min
(B)
min p.i.
0
15
30
45
60
75
90
PM
NE
control
Ad5 infection

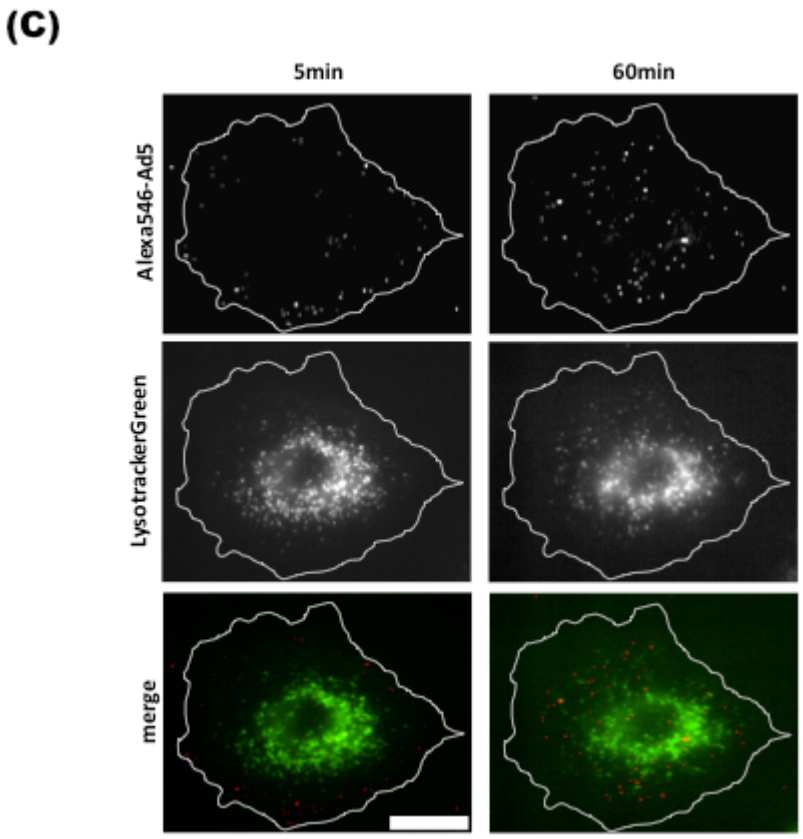

Figure 2-6: Ad5 Infection Disperses Lyso/LE.

(A) Still images of 90 min movies of LysoTracker-stained A549 cells. Controls showed an unchanging perinuclear distribution of lyso/LEs. Ad5 infection caused dramatic lyso/LE dispersal, especially notable in the appearance of individual vesicles toward the cell periphery (arrow heads). This effect was inhibited by the PKA inhibitor H-89 (5μM), but not by p38/MAP kinase inhibitor SB203580 (SB, 10μM). Treatment of uninfected cells with the adenylyl cyclase activator forskolin (10μM) caused lyso/LE dispersal with similar kinetics to those seen upon virus infection. Bar = 15 μm. (B) Series of enlarged images of boxed areas in panel A of "control" and "Ad5" movies spanning from nuclear envelope (NE) to the plasma membrane (PM). Frames every 5min. (C) Relative changes in live behavior of Alexa-546 labeled Ad5 (red) and LysoTracker-labeled lyso/LEs (green) in same A549 cell at 5 min and or 60 min p.i. Ad5 progression towards the cell center is visible while lyso/LEs disperse through the cytoplasm. Bar = 15 μm.

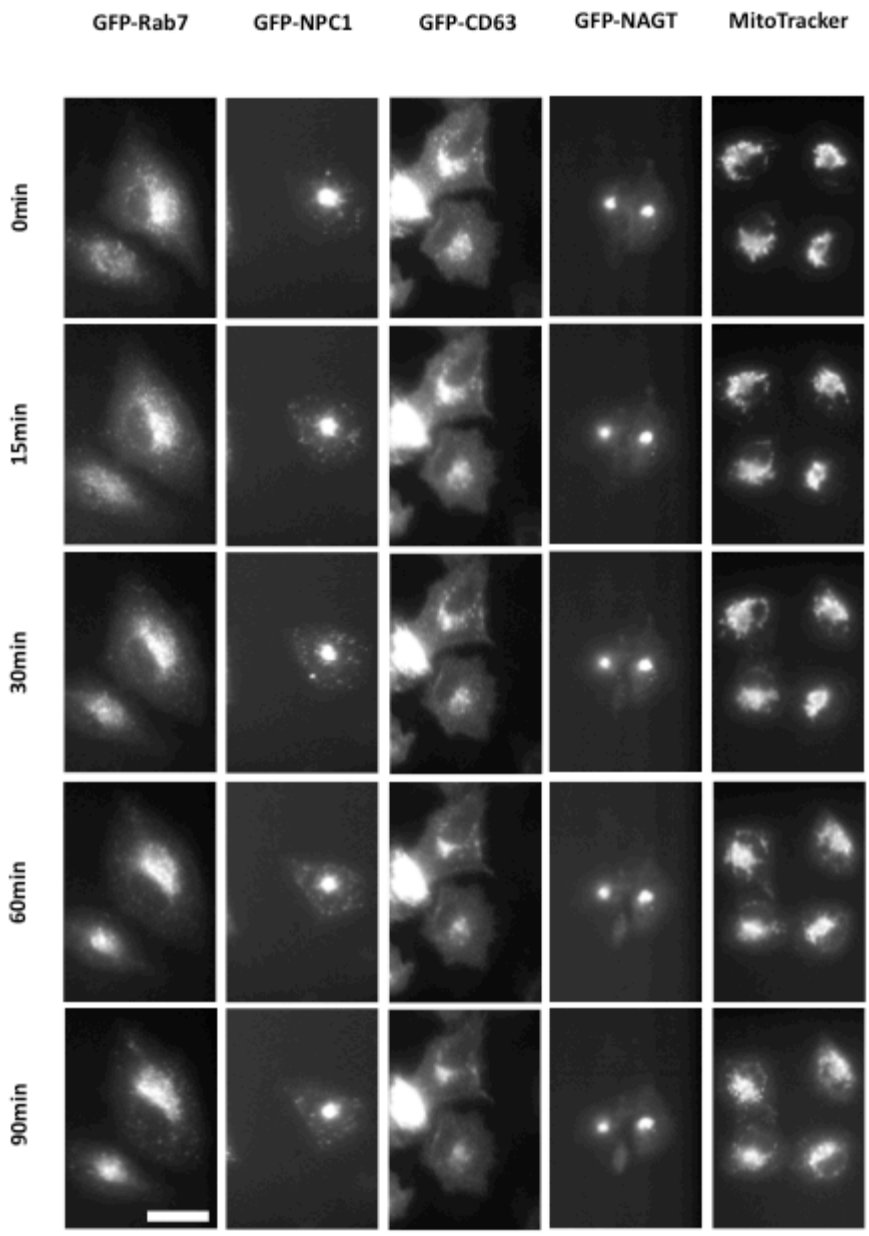

Figure 2-7: Effects of Ad5 Infection on Membranous Organelles.

Still images of 90 min movies of A549 cells expressing GFP-tagged marker proteins for lyso/LE (Rab7, NPC1), multi-vesicular bodies (CD63), Golgi elements (NAGT) or treated with MitoTracker to specifically label mitochondria. Ad5 infection caused dramatic lyso/LE dispersal, whereas the localization of other membranous organelles remains unaffected. Bar = 15 μm

Table 2-1: Effect of Adenoviruses and PKA-targeting Drugs on the Dispersal of Membranous Organelles.

Dispersal was scored based on 90min time-lapse movies.

organelle marker	virus	drug	# of cells	# of cells showing organelle dispersal	cells showing organelle dispersal (%)
LysoTracker	none	none	31	5	16.1
LysoTracker	Ad5	none	46	39	84.8
LysoTracker	Ad5	H-89 (5μM)	31	11	35.5
LysoTracker	Ad5	SB203580 (10μM)	20	16	80.0
LysoTracker	Ad5	cRGD (8.5μM)	15	6	40.0
LysoTracker	none	FSK (10μM)	32	25	78.1
LysoTracker	Ad3	none	57	41	71.9
LysoTracker	Ad3	H-89 (5μM)	32	5	15.6
GFP-Rab7	Ad5	none	10	7	70.0
GFP-NPC1	Ad5	none	6	5	83.3
GFP-CD63	Ad5	none	7	0	0.0
GFP-NAGT	Ad5	none	13	0	0.0
MitoTracker	Ad5	none	20	1	5.0

We employed two additional adenovirus serotypes to identify the upstream initiation of the PKA signaling. Ad3, a subgroup B adenovirus, which does not bind to CAR but interacts with alpha5 integrins like Ad5. Subgroup B adenoviruses remain in the endo-lysosomal pathway much longer than Ad5 (Miyazawa et al., 2001) but still induces lyso/LE dispersal; indicative of integrin but not CAR binding or endosomal escape to trigger the effect (Figure 2-8). Ad41, a member of the

enteric subgroup F, cannot interact with cell surface integrins since its penton base protein lacks the required RGD motif (Albinsson and Kidd, 1999). It still binds to CAR but fails to induce lyso/LE dispersion as seen with Ad3 and Ad5 (Figure 2-8).

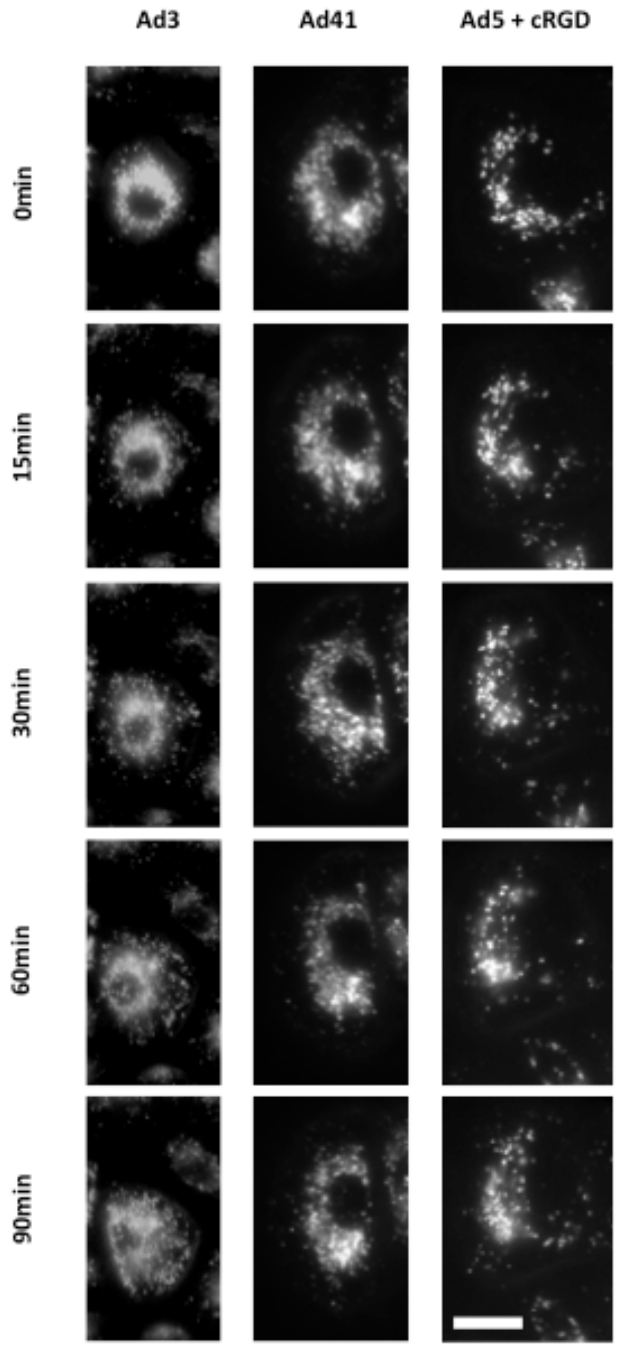

Figure 2-8: Lyso/LE Dispersal by Additional Adenovirus Serotypes.

Still images of 90 min movies of LysoTracker-labeled A549 cells infected with Ad3, Ad41, or Ad5 in combination with 8.5 μM cyclic-RGD peptide (cRGD) to block integrin signaling. Ad3 infection caused lyso/LE dispersal, whereas lyso/LE maintain their perinuclear cluster during Ad41 infection, which cannot interact with integrins, or Ad5 infection plus integrin inhibition. Bar = 15 μm

Hence, upstream integrin binding by capsid penton base seems to initiate a host cell response leading to PKA activation and lyso/LE dispersal. To further test these results, we used cyclic RGD peptide (cRGD) during Ad5 infection to block integrin signaling. Lyso/LE dispersal was completely inhibited with 8.5μM cRGD added to the medium during Ad5 infection (Figure 2-8, Table 2-1). To test for a specific role of LIC1-T213 phosphorylation in lyso/LE dispersal, we again used LIC RNAi. LIC1 and LIC2 RNAi disrupted lyso/LE organization (Tan et al., 2011), with clear dispersal observed in the A549 cells used here (Figure 2-9A). Expression of wild-type LIC1 rescued lyso/LE dispersal (Tan et al., 2011), as did LIC1-T213A, though LIC1-T213D was significantly less effective (Figure 2-9B). In Ad5 infected cells LIC1-T213A strongly inhibited both lyso/LE dispersal and virus transport to the nucleus, whereas rescue with LIC1 wild type allowed organelle dispersal and capsid progression towards the cell center (Figure 2-9C and D).

These results connect evidence for a possible PKA regulation of Lyso/LE to dynein recruitment and clearly indicate a role of LIC1-T213 in the motility of this particular class of organelles.

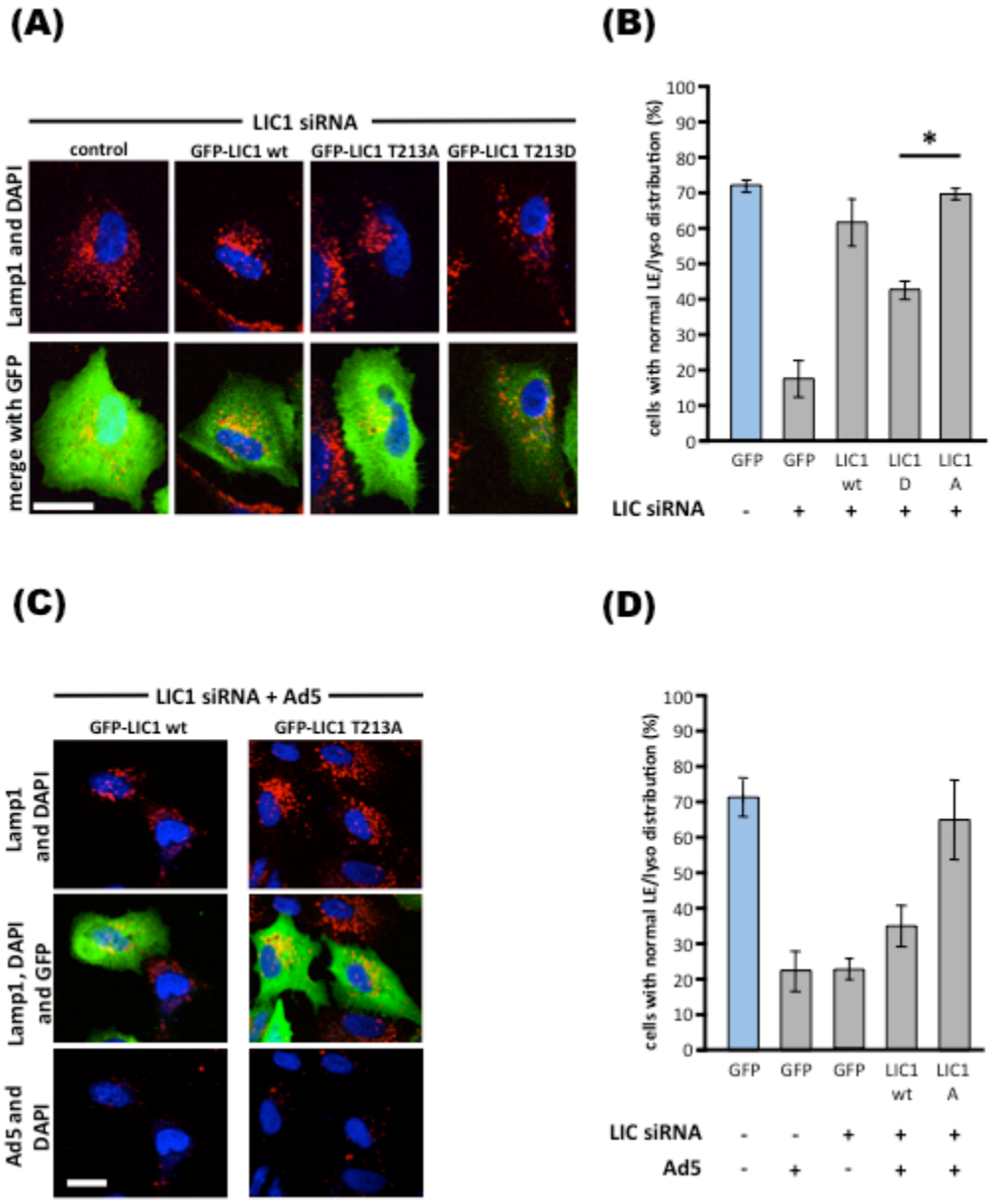
(A)
LIC1 siRNA
control
GFP-LIC1 wt
GFP-LIC1 T213A
GFP-LIC1 T213D
Lamp1 and DAPI
merge with GFP
(B)
cells with normal LE/lyso distribution (%)
100
90
80
70
60
50
40
30
20
10
0
*
GFP
GFP
LIC1 wt
LIC1 D
LIC1 A
LIC siRNA - + + + +
(C)
LIC1 siRNA + Ad5
GFP-LIC1 wt
GFP-LIC1 T213A
Lamp1 and DAPI
Lamp1, DAPI and GFP
Ad5 and DAPI
(D)
cells with normal LE/lyso distribution (%)
100
90
80
70
60
50
40
30
20
10
0
GFP
GFP
GFP
LIC1 wt
LIC1 A
LIC siRNA - - + + +
Ad5 - + - + +

Figure 2-9: Role of LIC1-T213 in Lysosome Dispersal.

(A) Rescue of LIC1/LIC2 RNAi-induced lyso/LE dispersal by overexpression of GFP (control), GFP-LIC1-*wt*, -T213A or -T213D in A549 cells shown by immunostaining for GFP (green) and LAMP1 (red). Bar = 20 μm. Rescue was observed with GFP-LIC1-*wt* and LIC1-T213A, but not with LIC1-T213D. (B) Quantification of data in panel *A*. Mean of at least two independent experiments with >40 cells each, error bars represent SD, * indicates $p < 0.05$. (C) Involvement of LIC1-T213 in Ad5-induced lyso/LE dispersal. Rescue of LIC1/LIC2 RNAi-induced lyso/LE dispersal as in panel *A,* but in Ad5-infected cells. The non-phosphorylatable LIC1-T213A mutant still rescues lyso/LE dispersal. Bar = 10 μm. (D) Quantification of data in panel *C.* Mean of at least two independent experiments with >40 cells each, error bars represent SD.

2.3. Discussion

2.3.1. Role in Virus Transport

These results reveal a remarkable use of a highly specific phosphorylation mechanism, involving a single PKA site within a specific LIC isoform, for opposite purposes by host and pathogen (Figure 2-10). Enhanced virus transport toward the cell center is likely caused by increased recruitment of the phosphorylated dynein to adenovirus particles. Enhanced Lyso/LE transport toward the cell periphery appears to be due to inhibition of dynein recruitment to these structures or dynein activity. These organelles normally undergo short inward and outward movements driven by the opposing activities of dynein and kinesin, respectively (Herman and Albertini, 1983; Soppina et al., 2009). Dynein inhibition causes kinesin-driven outward movements to predominate, resulting in Lyso/LE dispersal (see chapter 1.1.2.2. and Julie Yi, personal communication).

This behavior may increase the ability of Lyso/LE to reach incoming viruses before they exit to the cytoplasm, perhaps to inhibit escape. Ad3 and Ad41 are, in fact, known to remain within endosomal organelles for prolonged periods, an effect correlated with reduced infectivity (Albinsson and Kidd, 1999; Miyazawa et al., 2001). However, similar to *Trypanosoma cruzi* (Tardieux et al., 1992), which induces lysosome redistribution to the cell periphery for enhanced infection, fitness of some adenovirus serotypes might gain from Lyso/LE dispersal and premature endo-lysosomal fusion through faster escape from the organelle. Nevertheless, whether adenovirus-induced Lyso/LE dispersal represents an effective defense mechanism or, instead, a vestigial response remains to be shown (further discussed in chapter 2.3.3.). Surprisingly, adenovirus appears to have evolved to use the same underlying phosphorylation mechanism to reach the nucleus quickly after endosomalysis, avoiding intracellular innate immunity responses and degradation (Mallery et al., 2010). It will be interesting to test a broader field of additional viruses, known to passage through the endosomal compartments during entry, for PKA activation and lysosome dispersal. In this regard, Ebola virus infectivity has recently been found to depend on the endo-lysosomal fusion complex HOPS and NPC1, but a dependence on PKA activity has not been reported (Carette et al., 2011; Cote et al., 2011).

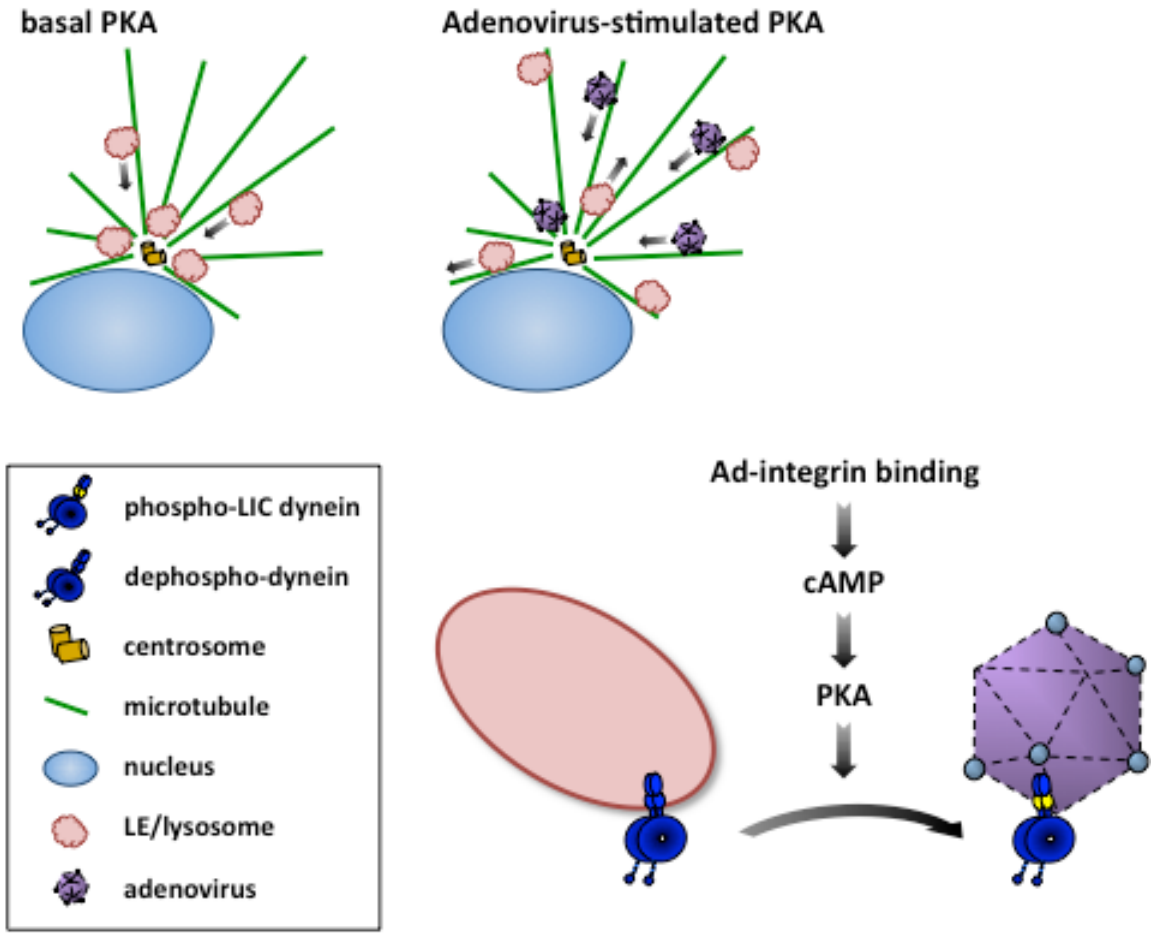

Figure 2-10: Schematic Representation of Adenovirus-induced Effects on Dynein-mediated Lyso/LE Distribution.

At basal PKA activity levels in uninfected cells, lyso/LE cluster around the centrosome. At the onset of infection, adenovirus binds integrins, increasing cAMP levels and PKA activity. PKA phosphorylation of the dynein LIC1 subunit promotes virus transport to the centrosome and nucleus, while dispersing lyso/LEs in a novel mechanism for host-virus competition.

Furthermore, possible therapies against adenoviral infections might be developed to target the post-entry hexon – LIC1 interaction. Expression of LIC1-T213D, which results in attenuated nuclear targeting of the virions, indicates a significant dominant-negative effect on motor recruitment. Hence, it becomes plausible that

short LIC1-T213D peptides containing the hexon binding site might block the interaction even when added during the viral attachment phase. Following co-uptake of viral capsids and blocking peptide into the endosome, acidification renders hexon susceptible for peptide binding, which presumably will cover all available LIC1 binding sites if administered in high doses. After endosomal escape, the blocking peptides compete with dynein for capsids capsid binding which would drastically affected nuclear redistribution and reduce infectivity.

2.3.2. Role in Organelle Transport

Our identification of a LIC1-mediated dynein regulatory mechanism may have general implications. PKA activates dispersal of pigment granules in vertebrate chromatophores (Marks and Seabra, 2001; Reilein et al., 1998; Rodriguez et al., 1997) and although the target of PKA phosphorylation is unknown, LIC1 now emerges as a likely candidate. We also note that the site of PKA phosphorylation in LIC1, T213, is near S207 (S197 in Xenopus LIC1), a Cdk1 phosphorylation site correlated with dynein dissociation from membranes during mitosis (Addinall et al., 2001; Dell et al., 2000; Niclas et al., 1996). Hence, the possibility exists, that the part of the LIC1 structure, which contains S207 and T213 represents a functional element in the dynein motor complex regulating membrane recruitment. At this point, however, no detailed structural information of either LIC is available as is definite proof of the direct involvement of these phosphorylation sites in dynein recruitment to Lyso/LE. However, S207 and T213 are located in a hydrophilic

region of the LIC1 polypeptide and may be responsible to switch functional states of LIC1 and the dynein complex.

2.3.3. Evolutionary Origins

Given the robust host response to adenoviral infections, this mechanism has likely been fine-tuned in the course of evolution. Lyso/LE dispersal has presumably evolved as a protective measure for host cells and it has been reported now for pathogens of multiple kingdoms that infection leads to Lyso/LE dispersal or exocytosis on the cellular level (this work and (Andrews, 1995)). Hence, the physiological role of Lyso/LE dispersal and exocytosis, providing additional phospholipids for cell membrane repair (Reddy et al., 2001; Roy et al., 2004), was expanded and adapted to pathogen defense. In the case of the tested adenovirus serotypes, only Ad5 exits the endo-lysosomal pathway within 15mins, whereas Ad3 and Ad41 stay within vesicular structures for prolonged periods of time and shows low rates of infectivity in cultured cells (Albinsson and Kidd, 1999; Miyazawa et al., 2001). We have been able to visualize co-translocation of Alexa546-Ad3 with LysoTracker Green labeled Lyso/LE in cells (not shown), which have been pre-labeled with the dye. These results indicate either re-uptake of capsids into Lyso/LE after endosomalysis or fusion of the virus-containing organelle with Lyso/LE and thus an active protective mechanism against Ad3 and Ad41 infection. Ad5, however, appears to have evolved specific counter-measures avoiding re-uptake into a Lyso/LE or, more likely, enabling rapid escape from the acidic organelle. In addition, Ad5 has evolved to profit from this vestigial host defense mechanism in an

additional way. The same phosphorylation event that leads to Lyso/LE dispersal is also used by the virus for transport towards the nucleus. This represents a remarkable manifestation of pathogen adaptation to host responses.

Further analysis of these phenomena should shed important light on innate responses to virus infection and, potentially, a wide range of important feature of intracellular transport.

Chapter 3: Adenovirus Penton Base Interaction with Kinesin-1

3.1. Introduction

3.1.1. Introduction

Most adenoviruses enter the cell via receptor-mediated endocytosis but are able to escape the endosomal vesicle shortly after uptake (Dales, 1962; Greber et al., 1993; Wiethoff et al., 2005). Subsequently the virus makes use of the microtubule (MT)-based motor machinery for active transport towards the cell center. Interestingly, adenoviruses show bidirectional motility at high temporal resolution (Bremner et al., 2009; Leopold et al., 2000; Suomalainen et al., 1999), indicating the involvement of MT minus- and plus-end directed motor proteins in virus transport. MT plus end-directed motility at rates measured for adenoviruses (~600µm/sec; Bremner et al., 2009; Suomalainen et al., 1999) are highly indicative of kinesin transport, which can be unmasked by treating cells with dynein function-blocking reagents (Yi et al., 2011). Candidate kinesins possibly involved in capsid transport are kinesin-1 (Kif5), kinesin-2 (Kif3, Kif17), kinesin-3 (Kif1), and kinesin-4 (Kif4), which all are regulating vesicle transport, interacting with physiologic cargo through their heavy chain or accessory light chains (Okada et al., 1995; Sekine et al., 1994; Setou et al., 2000; Sheetz et al., 1986; Yamazaki et al., 1995).

Some of these kinesins have also been reported to play a role in viral infections (Dodding and Way, 2011; Greber and Way, 2006). Human Immunodeficiency Virus

(HIV) Gag protein, which promotes viral particle production at the plasma membrane, is being delivered to its site of action by kinesin-4 (Martinez et al., 2008; Tang et al., 1999). Expression of dominant-negative tail constructs of kinesin-4, but not kinesin-3, severely disrupted gag trafficking to the plasma membrane and kinesin-4 RNAi inhibits virus production (Martinez et al., 2008). Inner tegument proteins of Herpes Simplex Virus (HSV) have been implied in recruiting kinesin-1 and kinesin-2 to the non-enveloped cytoplasmic from of the virus (Radtke et al., 2010)(Radke et al., PLoS Pathogen, 2010). VP1/2 (pUL36), one of the inner tegument proteins required for virus egress (Luxton et al., 2006), represents a strong candidate for virus binding, especially since it contains WD/E repeats which have recently been implicated in modulating kinesin-1 binding (Dodding et al., 2011; Morgan et al., 2010). However, it is unclear at the moment, if the heavy or light chains of kinesin-1 and kinesin-2 is able to interact with HSV (Dodding and Way, 2011). Progeny of vaccinia virus assembles close to the nucleus and leaves the infected cell via MT- and actin-dependent processes. From the perinuclear site to the plasma membrane, intracellular enveloped virus (IEV) relies on kinesin-1 for efficient transport during egress (Moss and Ward, 2001). The viral membrane protein A36 appears crucial for this motility since A36-deficient viruses show no MT-based transport during egress but remain clustered at their perinuclear site of assembly (Rietdorf et al., 2001). In fact, residues 81–111 of A36 are capable of interacting directly with the cargo binding TPRs of KLC (Ward and Moss, 2004), supporting an important role of A36 in recruiting kinesin-1 to IEV.

The role of kinesins during adenovirus entry remains controversial. Agreement exists that bidirectional MT-based transport of cytoplasmic capsids involves at least one class of the kinesins (Bremner et al., 2009; Leopold et al., 2000; Scherer and Vallee, 2011; Suomalainen et al., 1999; Yi et al., 2011). However, the function of bidirectional MT-based transport during early adenoviral infections remains unknown, since microinjection of kinesin function-blocking antibodies into infected cells fails to block nuclear capsid redistribution (Leopold et al., 2000). Similarly, the identity of the responsible kinesin remains to be elucidated. However, a second, transport-independent role of kinesins has been reported to affect adenoviral fitness. Kinesin-1 (Kif5c) seems to function after viral capsid are attached to the nuclear pore complex (NPC) by generating force to disrupt the virus capsid and facilitate injection of the viral genome into the nucleus (Strunze et al., 2011). Kif5c RNAi leads to slightly decreased rates of infectivity (Strunze et al., 2011), does not affect viral redistribution to the nucleus, but reduces the accumulation of empty capsid shells in the cell periphery after genome delivery. The mechanism entails a direct KLC interaction with the minor capsid protein IX and Kif5c heavy chain binding to the nuclear pore protein Nup358 (RanBP2). Furthermore, adenovirus hexon binds to Nup214 (Trotman et al., 2001) and in this tightly interlocked constellation, it has been hypothesized, Kif5c generates sufficient force to structurally compromise viral capsid and NPC to allow efficient genome transfer (Strunze et al., 2011).

Here, we present biochemical work supporting a role of kinesin-1 mediated transport in the cytoplasmic phase of Ad5 entry. The major capsid protein penton base, which largely remains with viral DNA until the capsid reaches the nucleus, interacts directly and independent of KLC with immunopurified kinesin-1. Furthermore, additional data show that a minimal motile virus-like particle, the penton dodecahedron (Pt-Dd) (Fender et al., 1997; Norrby and Skaaret, 1967), shows kinesin binding and motility in cultured hippocampal neurons.

3.1.2. Materials and Methods

Cells, Viruses, and Antibodies

293A cells were grown in DMEM supplemented with 10% FBS. Embryonic hippocampal neuron cultures were generated from E18–E19 rat embryos as described (Grabham et al., 2007). Briefly, hippocampi were dissected in HBSS containing 10 mM HEPES, trypsinized, and triturated in the plating medium DMEM containing 10% FBS, 0.5 mM L-glutamine, and 1 mM sodium pyruvate. After trituration the cells were plated in 50 mm MatTek (Ashland, MA) imaging dishes that were pre-coated with 0.5 mg/ml poly-D- lysine in borate. Once the cells had adhered to the substrate, the medium was removed completely and replaced with Neurobasal medium (Invitrogen) containing B-27 supplement (Invitrogen) and 0.5 mM L-glutamine. Cultures were grown for 5 DIV before prepared for infection and live cell imaging. Replication-deficient Ad5 engineered to express GFP (Ad5-GFP, plaque-purified; obtained from H. Young, Columbia University) and modified Ad5 with FLAG-tagged protein IX (Ad5pIXflag, kind gift of Igor Dmitriev, University of

Alabama) were propagated in 293A cells and purified by banding on two linear CsCl gradients (Lawrence and Ginsberg, 1967) and dialysed against 10% glycerol in PBS before cryo-storage. Viral titer was obtained using fluorescent focus assays for Ad5-GFP (Thiel and Smith, 1967). Hippocampal neuronal cell incubations with Alexa546-Pt-Dd for live cell imaging were all performed in a low volume of Neurobasal medium with B-27 at 37°C for 15 min to allow particle attachment. The cells were washed twice in warm PBS and prepared for live cell imaging.

Antibodies used included mouse monoclonal anti-hexon (Novocastra), anti-HA (clone 16B12, Covance), anti-FLAG (M2, Sigma), anti-myc (9E10, SantaCruz), anti-tubulin (Sigma), anti-kinesin-1 H1 and H2 (Millipore), anti-p150^{Glued} (BD Bioscience) and anti-dynein IC (74.1, Chemicon), rabbit antibodies anti-LIC, and anti-LIC2 (Tynan et al., 2000b), anti-adenovirus5 (Abcam), anti-GFP (Invitrogen), anti-FLAG (Abcam), anti-HA (Sigma), and chicken anti-LIC1 (Tan et al., 2011).

Plasmids, and Molecular Methods

Mammalian cell expression constructs used in this work included HA-tagged penton base, GFP-100K, and untagged hexon described in (Bremner et al., 2009). Protein IX tagged with FLAG and GFP (pIX-flag-GFP) was cloned from purified adenovirus 5 DNA. Viral DNA was separated from capsid proteins by boiling ~10^{10} purified virus particles at 100°C for 5min in 1%SDS and subsequent MiniPrep (Qiagen). Protein IX was cloned into the pEGFP-N1 vector (Clontech, Mountain View, CA) by introducing 5' EcoRI and 3' AgeI restriction sites by PCR. The additional C-terminal FLAG-tag

was introduced during PCR. Mutations in the sequence and in-frame cloning was tested for by 5' and 3' sequencing.

Transient transfections were performed using Lipofectamine 2000 (Invitrogen).

Live Cell Imaging

Hippocampal neuronal cells grown in glass bottom dishes and incubated with Alexa546-Pt-Dd were covered with CO2-independent medium and then processed for imaging in a 37°C chamber. Movies were acquired between 15- 90 min thereafter at video frame rate (16frames/min) for 1min using a 63x oil immersion objective and a CCD camera (model C9100-12; Hamamatsu) attached to an inverted microscope (Leica) operated by Metamorph Imaging software (Molecular Devices). For image and movie analysis and particle counting ImageJ was used.

Proteins and Biochemical Analysis

Rat brain lysate and purified rat cytoplasmic dynein were prepared in phosphate-glutamate buffer (pH 7.0) as previously described (Paschal et al., 1987). Kinesin was enriched for by sucrose gradient density centrifugation of the GTP release of the dynein preparation protocol on 5-20% linear sucrose gradients. Fractions containing kinesins-1, -2, and -3 but no dynein were chosen for further analysis. Adenovirus hexon was either recovered from virus-depleted supernatant of the first CsCl gradient by immunoprecipitation as described (Bremner et al., 2009) or by anion exchange chromatography (Waris and Halonen, 1987). Initial steps of penton dodecahedra (Pt-Dd) purification followed the protocol described in (Waris and

Halonen, 1987). Additionally, the first eluding peak of the anion exchange step was pooled, concentrated using spin columns (Milipore), and poured over a Superose 6 10/300 GL column equilibrated with PBS. Pt-Dd containing fractions eluted close to the void volume were pooled and concentrated. Labeling with Alexa546 as described for adenoviral capsids (Bremner et al., 2009; Leopold et al., 2000). Briefly, ~1mg purified Pt-Dd was dialysed in 500µl dialysis cassette (10MWCO, Thermo Scientific) against 8mM sodium carbonate, 92mM sodium bicarbonate, pH9.3 for 4h at 4°C, incubated with 2µg Alexa546 (Invitrogen) for 30min at 25°C, and separated from uncoupled dye by sixe exclusion chromatography. Purified proteins were flash frozen in liquid nitrogen and stored at -80°C.

Mammalian cultured cell lysates were prepared in RIPA buffer (50mM Trizma-maleate, 100 mM NaCl, 1 mM EGTA, [pH 7.4]) containing protease inhibitor cocktail (Sigma) and 1% NP40, and the membrane fraction was removed by centrifugation. Adenovirus capsid and hexon binding assays were described previously (Bremner et al., 2009). Briefly, virus or hexon was immunoprecipitated with anti-hexon antibodies and protein A sepharose beads (GE Bioscience) from purified virus stock or virus-depleted infected 293A cell lysate, respectively. The beads were washed and incubated for 30 min in Tris-maleate buffer (50 mM Trizma-maleate, 10 mM NaCl, 1 mM EDTA, and 0.1% Tween 20, pH 4.4 or pH 7.4), washed in the same buffer at pH 7.4, and then incubated with purified kinesins at 4°C for 1.5 hr. Following washing, the beads were analyzed for the presence of dynein or dynein subunits by immunoblotting. In reciprocal experiments, anti-kinesin antibodies H1, H2, or Kif5b

were used to immunopurify kinesin-1, which was subsequently incubated with purified virus stock, virus-depleted infected 293A cell lysate, or 293A cell lysate expressing viral capsid components.

Microtubule Gliding Assay

Unlabeled and rhodamine-labeled tubulins (Cytoskeleton) were mixed at a ratio of 1:1 (total concentration of 5mg/ml) in BRB80 buffer (80 mM PIPES, pH 6.8, 1 mM EGTA, 1 mM MgCl2, 1 mM GTP, 3% glycerol). The mixture was polymerized at 37°C for 15 min and then stabilized by adding prewarmed BRB80/T buffer (BRB80 buffer plus 20 μM taxol)and microtubules were stored at room temperature in the dark. For chamber assays, microtubules were diluted in PMEE buffer (35 mM PIPES, 5 mM MgSO4, 1 mM EGTA, 0.5 mM EDTA, pH 7.4) supplemented with 20 μM taxol. For *in vitro* MT gliding assays, flow chambers were assembled from a glass slide and acid-washed cover slip, using double-sided adhesive tape (chamber volume, approximately 10 μl). All solutions were incubated for 10 min. The chamber was first incubated with 5 mg/ml BSA (bovine serum albumin), washed twice with 20 μl PMEE buffer, incubated with kinesin-enriched fraction, washed twice, then incubated with rhodamin-labelled MT and washed twice again with PMEE buffer containing 5 μM taxol. Motility was initiated with the addition of 500 μM ATP diluted in PMEE buffer, and imaging was performed in a inverted microscope (Leica) operated by Metamorph Imaging software (Molecular Devices) at 25°C, equipped with a 63x oil immersion objective and a CCD camera (model C9100-12; Hamamatsu). For image and movie analysis and particle counting ImageJ was used.

Statistical Analysis

For analysis, two-sample comparisons were performed via Student's t test. Statistical significance was inferred for p values less than 0.05. Analysis and statistical tests were performed using Excel (Microsoft, Redmond, WA) and Prism (GraphPad, La Jolla, CA).

3.2. Results

3.2.1. pH-independent binding of Ad5 to Kinesin-1

A striking phenomenon of adenovirus transport during the cytoplasmic phase of entry represents the bidirectional motility behavior (Bremner et al., 2009) (Suomalainen et al., 1999). Thus far, the only functional interaction between a MT plus-end directed motor and the virion has been reported for capsid disassembly at the NPC. A weak interaction of Kif5c light chains with protein IX was reported, which, apparently, had no relevance to in MT-based transport (Strunze et al., 2011). To test for kinesin binding to the capsid during the cytoplasmic transport phase of Ad5, we used A549 cell lysate at 40min p.i. infected with 1000pa/cell of a modified Ad5 virus containing FLAG-tagged protein IX (Ad5pIXflag) to. Immunoprecipitation with anti-flag antibody reveals binding of cytoplasmic dynein to Ad5 and a weaker, but detectable signal for kinesin-1 (Fig 3-1A).

For further analysis of the interaction between kinesin-1 and the viral capsid or capisd components, we relied on rat brain kinesins obtained by MT binding and GTP release as part of the dynein purification protocol, followed by sucrose gradient

centrifugation (Fig 3-1B). The kinesin peak fraction contained active kinesin, as tested for by MT gliding. MTs show a speed of ~800nm/sec, characteristic for kinesin-1 propelled MT (Fig 3-1C).

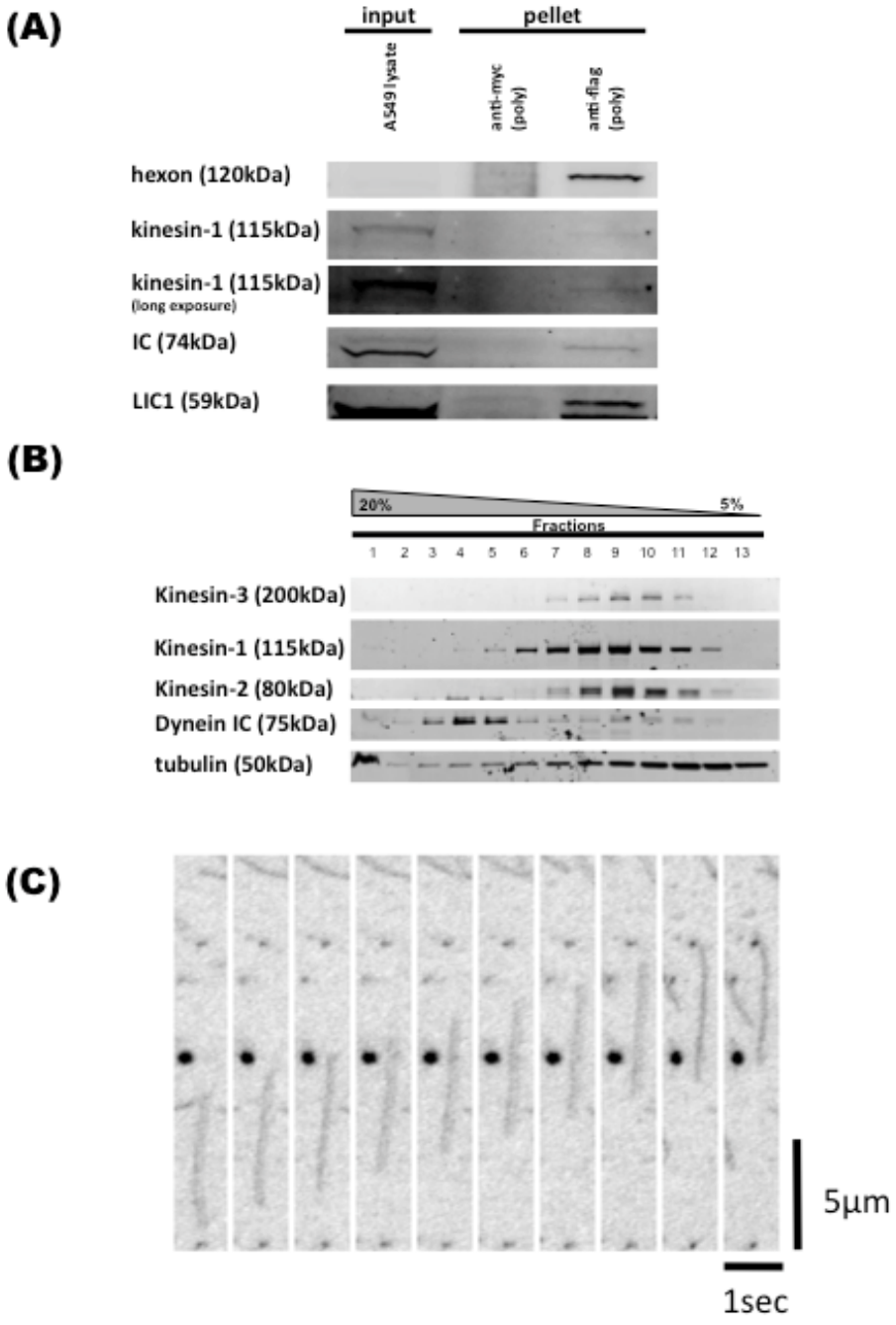

Figure 3-1: Kinesin-1 Binds Incoming Ad5 Capsid and Kinesin Enrichment.

(A) Ad5pIXflag was immunoprecipitated from infected A549 cell lysate 40min p.i. with a polyclonal anti-flag antibody and the pellets were immunoblotted using anti-dynein IC and LIC1 or anti-kinesin-1 (clone H2) antibodies. Dynein and kinesin-1 were present in the pellets. Note that the hexon signal in the input sample was below the detection limit but was visible in the concentrated pellet. (B) Kinesin was enriched for by sedimenting the GTP release fraction of a dynein preparation in a linear sucrose gradient (5-20%). Gradient fractions were immunoblotted with anti-kinesin-1, -2, and -3, and anti-dynein IC and anti-tubulin antibodies, which shows a clear separation of the kinesins (peak fraction 9) from cytoplasmic dynein (peak fraction 4). (C) Still images of a time-lapse acquisition following an individual microtubule (MT) in a MT gliding assay over 10frames (1frame/sec). The assay chamber was incubated with kinesin-enriched fraction 9 of the sucrose gradient in B before rhodamine labeled MTs and ATP was added and the chamber was prepared for imaging at 37°C.

Binding of components of this kinesin-enriched fraction to immunopurified Ad5 capsid or hexon exposed to either neutral or acidic pH was tested in pull-down experiments. We find a clear interaction of kinesin-1 with Ad5 capsid (Fig 3-2A), whereas other plus-end kinesins, kinesin-2 and -3, showed no clear evidence of virus binding, possibly reflecting their lower concentrations in the input samples. Remarkably, in contrast to cytoplasmic dynein, the kinesin-1 interaction with Ad5 was independent of hexon and unaffected by exposure to low pH levels, suggesting independent recruitment mechanisms for kinesin and dynein (Fig 3-2A). Reciprocally, we also performed kinesin-1 pull-downs, and found clear binding of intact Ad5, but not hexon (Fig 3-2B and C). We also tested the behavior of the capsid protomer penton, which consists of penton base and fiber. Although fiber is lost early during entry (Nakano, JVI, 2000), penton base has been observed cytochemically to remain associated with capsids throughout early infection at

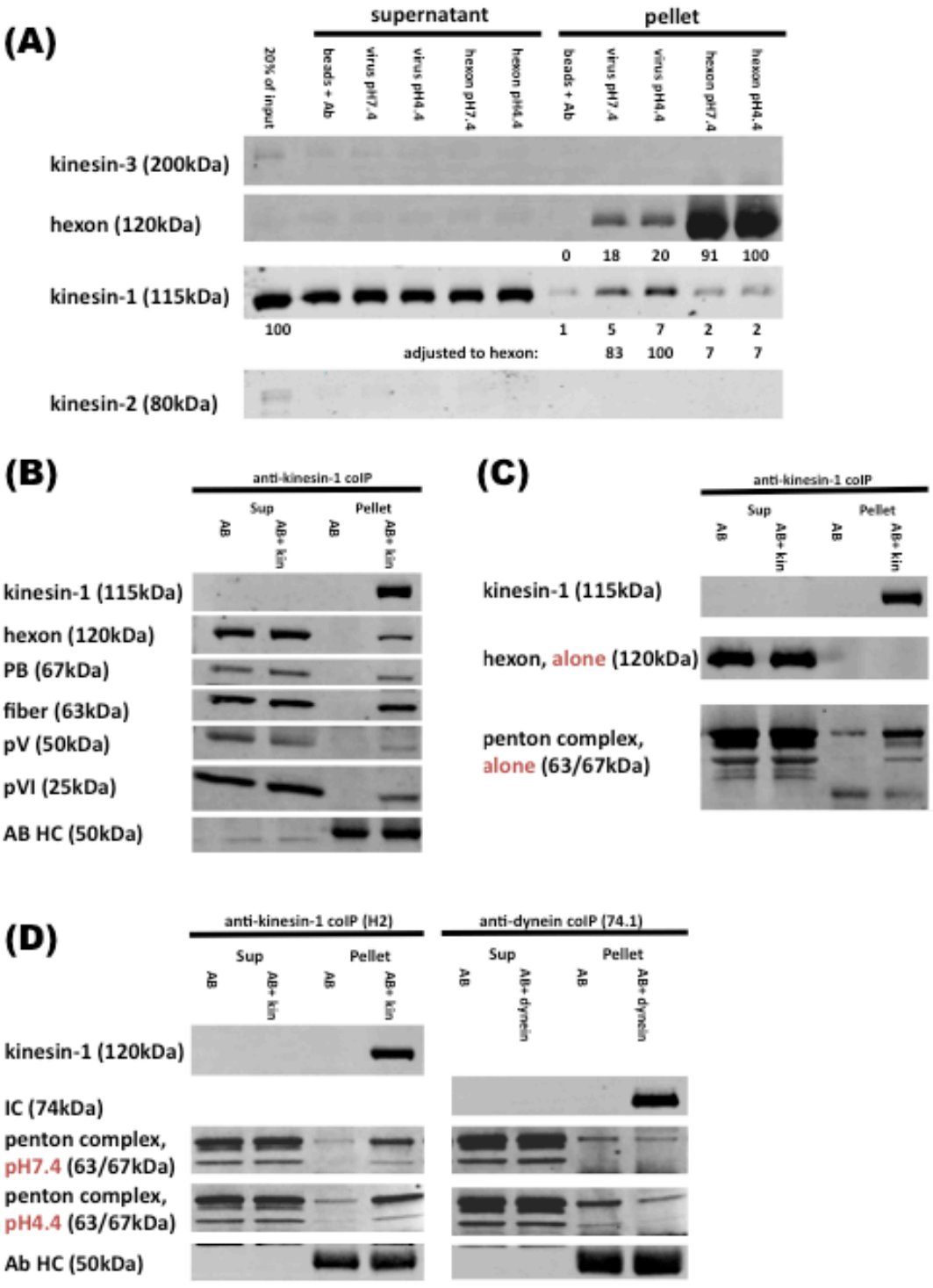
(A)
supernatant
pellet
20% of input
beads + Ab
virus pH7.4
virus pH4.4
hexon pH7.4
hexon pH4.4
beads + Ab
virus pH7.4
virus pH4.4
hexon pH7.4
hexon pH4.4
kinesin-3 (200kDa)
hexon (120kDa)
0 18 20 91 100
kinesin-1 (115kDa)
100 1 5 7 2 2
adjusted to hexon: 83 100 7 7
kinesin-2 (80kDa)
(B)
anti-kinesin-1 coIP
Sup
Pellet
AB
AB+ kin
AB
AB+ kin
kinesin-1 (115kDa)
hexon (120kDa)
PB (67kDa)
fiber (63kDa)
pV (50kDa)
pVI (25kDa)
AB HC (50kDa)
(C)
anti-kinesin-1 coIP
Sup
Pellet
AB
AB+ kin
AB
AB+ kin
kinesin-1 (115kDa)
hexon, alone (120kDa)
penton complex,
alone (63/67kDa)
(D)
anti-kinesin-1 coIP (H2)
anti-dynein coIP (74.1)
Sup
Pellet
AB
AB+ kin
AB
AB+ kin
Sup
Pellet
AB
AB+ dynein
AB
AB+ dynein
kinesin-1 (120kDa)
IC (74kDa)
penton complex,
pH7.4 (63/67kDa)
penton complex,
pH4.4 (63/67kDa)
Ab HC (50kDa)

Figure 3-2: Kinesin-1 Interacts with Penton Complex.

(A) Kinesin-enriched fraction was tested for pull-down with hexon or Ad5 capsid exposed to either neutral or acidic buffer conditions before the incubation by immunoblotting of the kinesin input, supernatants, and pellets with antibodies against hexon, and kinesin-1, -2, and -3. Kinesin-1 interacts with the adenoviral capsid clearly above background and 12-14fold better with the capsid than with hexon alone only (binding fraction adjusted to the amount of hexon present in the pellet samples). Kinesin-2 and -3 were only detectable in the input. Of note, capsid acidification has only a minor effect on kinesin-1 binding, indicating a different recruitment mechanism for kinesin-1 and cytoplasmic dynein. Numbers below each lane indicate relative signal intensity. (B) Purified Ad5pIXflag was tested for co-immunoprecipitation with kinesin-1 using the monoclonal H2 antibody. Supernatant (Sup) and pellets were immunoblotted with anti-kinesin and anti-adenovirus antibodies. Clear pull-down of Ad5pIXflaf was observed. In addition, the ratio of hexon to penton base was higher in the supernatants than in the anti-kinesin co-immunoprecipitate indicating possible free hexon protomers in the input sample, which do not interact with kinesin. (C) Same as in B, except MonoQ purified hexon or purified Penton-Dodecahedra (Pt-Dd) were tested for kinesin-1 co-immunoprecipitation. Pt-Dd are present in the pellets, whereas hexon was not pulled-down. (D) After incubation in either neutral or low pH buffer, Pt-Dd was tested for binding to cytoplasmic dynein or kinesin-1 by immunoblotting of supernatants (Sup) and pellets. Pt-Dd was present in anti-kinesin pellets independent of pH at the pre-incubation step, but was absent in the anti-dynein pellets.

relatively constant levels (Bremner et al., 2009; Greber et al., 1996; Martin-Fernandez et al., 2004), consistent with a potential role in early adenovirus transport. As one test for kinesin-1 binding we produced penton dodecahedrons (Pt-Dd), stable complexes of penton base with fiber subunits found in lysates of adenovirus-infected cells (see chapter 3.2.2.1. (Fender et al., 1997; Norrby and Skaaret, 1967). We observed pH-independent pull-down of Pt-Dd with kinesin-1, but not cytoplasmic dynein (Fig 3-2D).

We also expressed individual capsid subunits in 293A cells and found that penton base alone interacted with kinesin-1 (Fig 3-3A), while no apparent interaction with protein IX was observed, the only previously reported kinesin-1 interacting

adenovirus capsid protein, though that interaction appeared to be weak (Strunze et al., 2011). In this assay, hexon was also negative for kinesin-1 binding. Furthermore, we tested a polyclonal Kif5b-specific antibody in immunoprecipitations of rat brain kinesin-1 and penton base binding (Fig 3-3B). Surprisingly, this antibody pulled-down less KLC1 than the monoclonal H2 antibody, but the amount of bound penton base was comparable. These data suggest a potentially KLC1-independent interaction between penton base and Kif5b. However, the contribution of other kinesin family members, especially Kif5a and Kif5c, in cytoplasmic adenovirus motility cannot be ruled out.

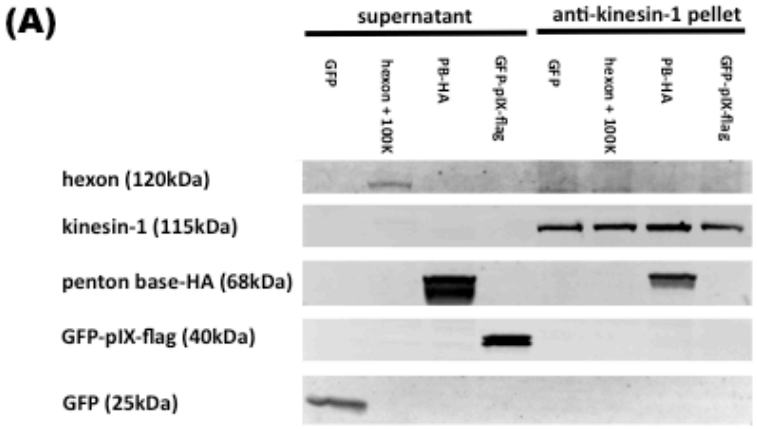

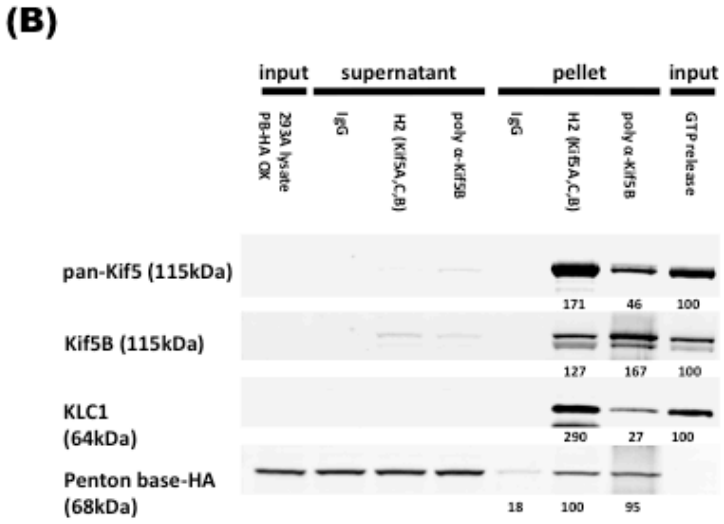

Figure 3-3: Kinesin-1 Pulls-Down Penton Base.

(A) Pull-down of virus components with kinesin-1 as in Figure 3-2, but using lysate from 293A cells expressing either GFP, hexon and GFP-100K, GFP-pIX-flag, or HA-tagged penton base. Penton base alone binds kinesin-1, whereas all other capsid proteins were negative for motor binding. (B) Pull-down of HA-tagged penton base expressed in 293A cells with kinesin-1 immunopurified with monoclonal H2 antibody (similar to panel A) or polyclonal Kif5B antibody. Inputs, supernatants and pellets were immunoblotted with anti-HA, anti-kinesin HC (H2 and Kif5B) and LC (KLC1) antibodies. Similar amounts of penton base were present in the pellets independent of the antibody used for the immunoprecipitation and the co-immunoprecipitated amount of KLC1. Numbers below each lane indicate relative signal intensity.

3.2.2. Intracellular Penton Dodecahedron Motility

Penton dodecahedra (Pt-Dd), subviral particles consisting exclusively of penton base and fiber (Norrby and Skaaret, 1967), have been proposed as possible gene delivery vectors, since they show nuclear accumulation in cultured cells (Fender et al., 1997). They can be loaded with extra-genomic DNA leading to gene expression 48h p.i. (Fender et al., 1997). Thus far, Pt-Dd have only been described for recombinant baculovirus expressed adenovirus 3 pentons purified by sucrose gradient centrifugation (Fender et al., 2008). In addition, visualization of intracellular translocating Pt-Dd, revealing their transport mechanism, is still lacking. Here, we describe a two-step purification process for Pt-Dd from Ad5 infected cell lysate and the intracellular transport characteristics of Alexa546-dye labeled Pt-Dd incubated with cultured hippocampal neurons.

3.2.2.1. Penton Dodecahedron Purification

Penton base and fiber undergo a structural change during penton complex formation (Zubieta et al., 2005). The assembly of twelve pentons to form a Pt-Dd

requires proteolytic cleavage of the N-terminal 37 residues of penton base, 60 copies of which cannot fit into the interior volume of the Pt-Dd (Fuschiotti et al., 2006). Proteolysis can be achieved by incubating virus-depleted cell lysate of infected cells for 7days at 4°C. Under mildly acidic conditions (pH 6.8), which are optimal for Pt-Dd formation (Fuschiotti et al., 2006), we subjected the lysate to anion-exchange chromatography (AEC), following protocols for hexon purification adjusted for MonoQ columns (Waris and Halonen, 1987) (Figure 3-4A).

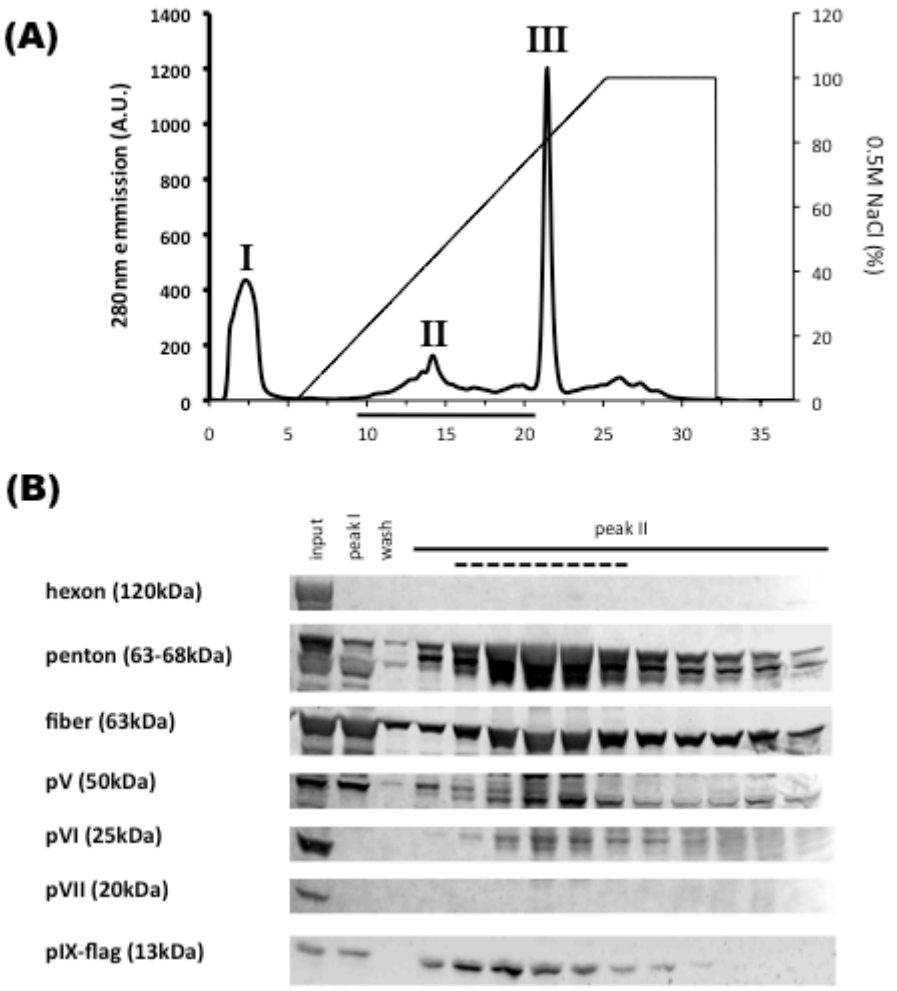

Figure 3-4: Anion Exchange Chromatography of Ad5pIX-flag Infected A549 Cell Lysate.

(A) Virus-depleted lysate of Ad5pIXflag infected 293A cells 2-3 days p.i. was incubated at 4°C for 7 days before poured over a MonoQ anion exchange column and eluted with 0.5M NaCl at pH6.5 (Waris and Halonen, 1987). Besides the flow-through (peak I) and the hexon peak (III) an additional peak (II) elutes at approximately 0.2M NaCl. Solid line indicates fractions used for SDS-PAGE and immunoblotting in B. Protein levels are measured by absorbtion at 280nm (thick line), salt concentration (thin line) is indicated on the right. (B) Total lysate, fraction of peak I, wash, and anion exchange fractions of peak II were tested for the presence of adenoviral capsid proteins by immunoblotting with anti-adenovirus and anti-Flag antibodies. Penton base, fiber, pV, pVI, pVII, and pIX are eluting in peak II, whereas hexon is absent in these fractions. Fractions indicated by the dashed line were pooled and subjected to size exclusion chromatography.

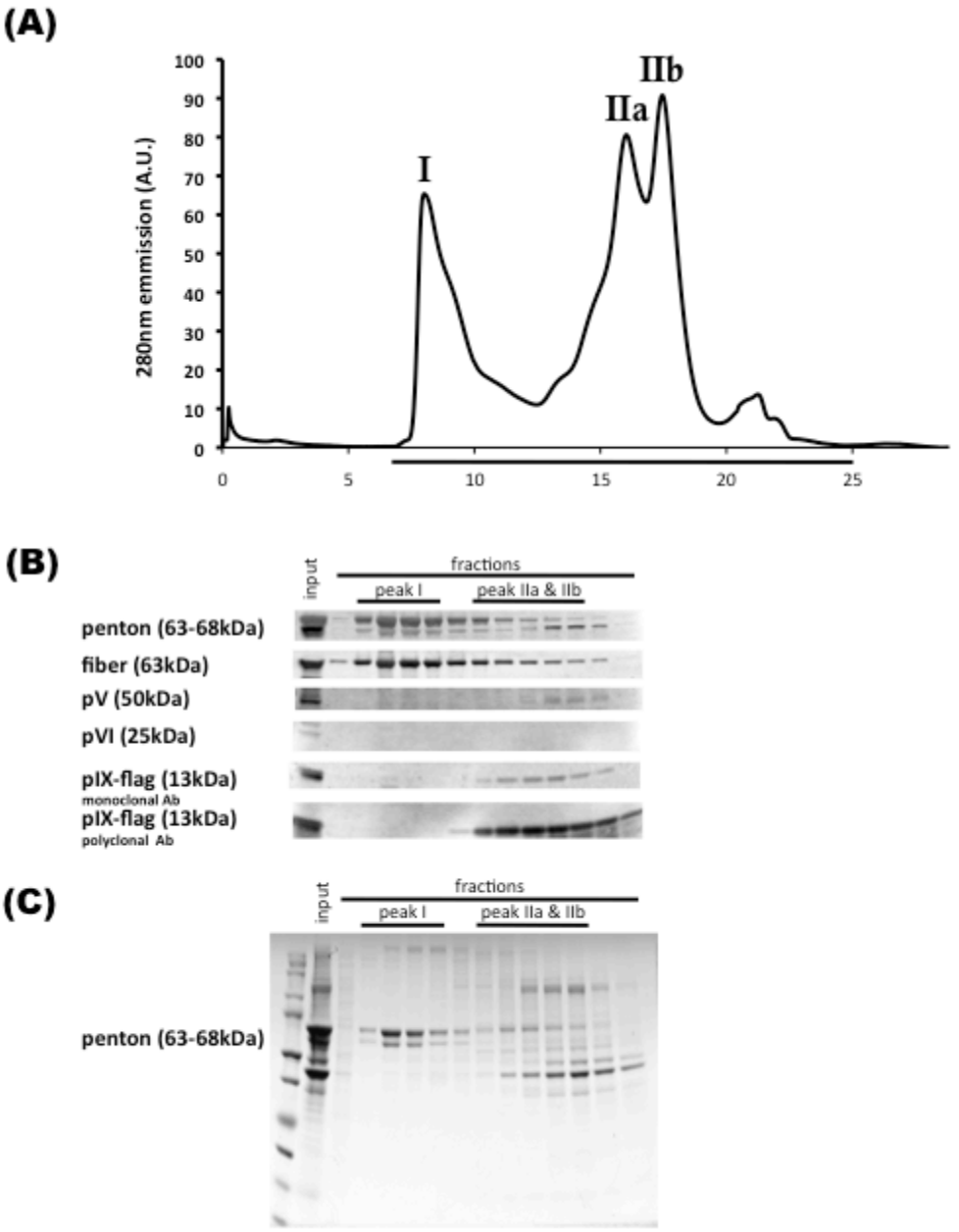

Figure3-5: Size Exclusion Chromatography.

(A) Pooled fractions of anion exchange chromatography were poured over size exclusion column and protein levels were measured at 280nm. One individual peak (I) elutes at the void volume before an additional double peak (IIa and IIb). Solid line indicates fractions used for SDS-PAGE and immunoblotting in B and C. (B) Immunoblotting with anti-adenovirus and anti-flag antibodies or (C) Coomassie-staining of input and elution fractions indicate a high concentration of penton base and fiber in peak I, which can be separated from most cellular and viral contaminants.

The first peak eluting at low salt concentrations was devoid of hexon but contained the viral proteins penton, fiber, and proteins V, VI, and IX (Figure 3-4B).

We pooled fractions with high penton concentration and poured them over a size-exclusion chromatography (SEC) column, which resulted in two major peaks (Figure 3-5A). Peak I eluted at the void volume and only contained penton, fiber and a high molecular weight contaminant (Figure 3-5B and C). Peak II contained the minor capsid components and further host cell contaminants (Figure 3-5B and C).

Using this method, we enriched for Pt-Dd by 280% from the initial cell lysate to SEC elution (Figure 3-6A and B, Figure 3-7A and B).

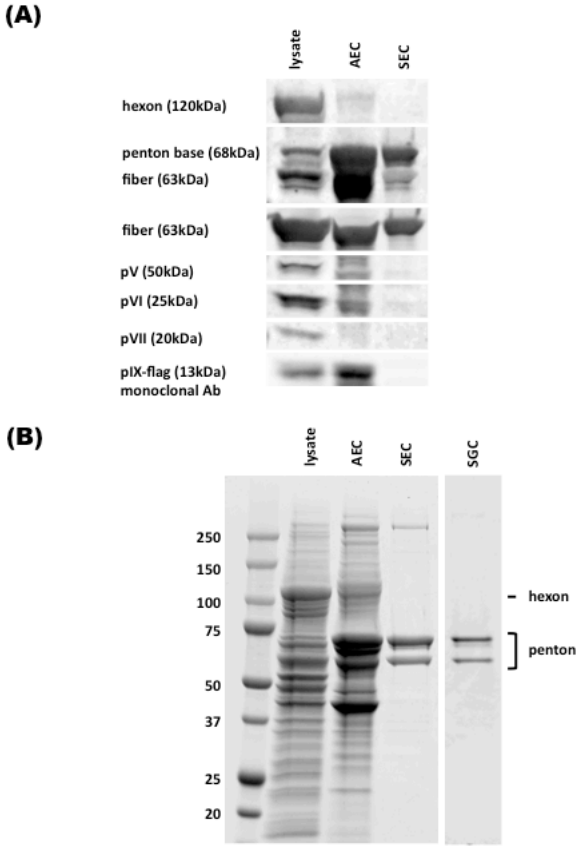

Figure 3-6: Pt-Dd Purification.

(A) Immunoblotting with anti-adenovirus and anti-Flag antibodies or (B) Coomassie-staining of virus-depleted lysate of infected 293A cells (lysate), peak fractions of anion exchange chromatography (AEC), size exclusion chromatography (SEC), and sucrose gradient centrifucation (SGC) indicate an increasing purity of the Pt-Dd and the absence of any other adenoviral polypeptides in the final sample.

Sucrose density gradient centrifugation clearly reveals the identity of Pt-Dd in the preparation, which can also be separated from the high molecular weight by this method (Figure 3-7C). The final purity of Pt-Dd after sucrose density gradient centrifugation was 99.0% (Figure 3-6B).

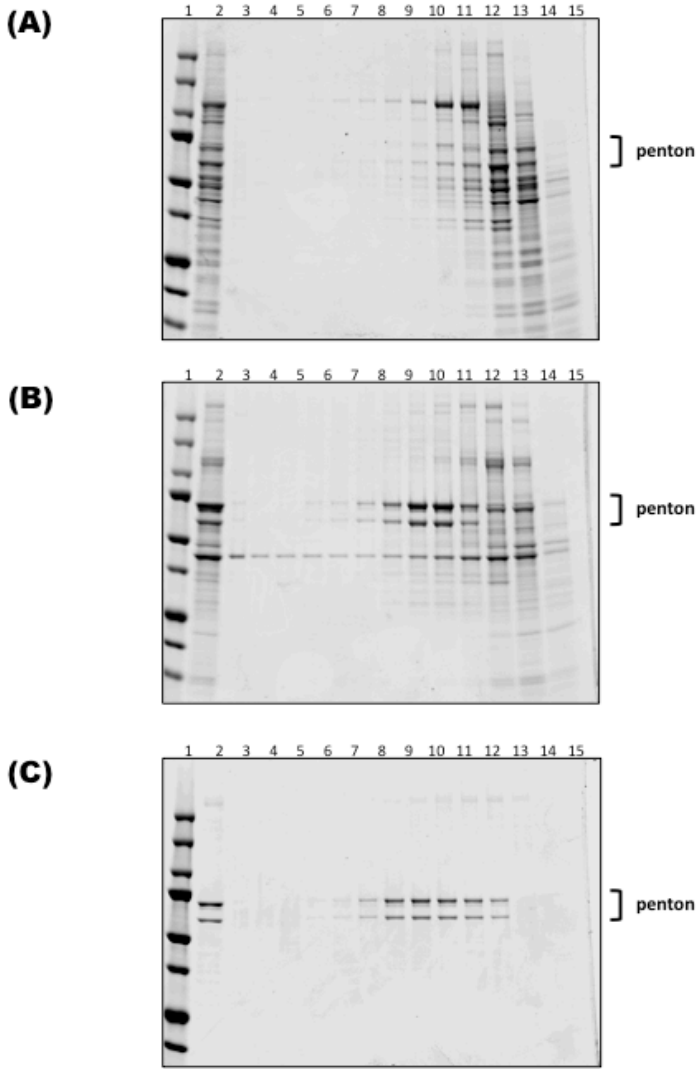

Figure 3-7: Sucrose Gradients of Pt-Dd Purification.

Coomassie-stained SDS-PAGE gels after centrifugation through 5-20% sucrose gradient of (A) virus-depleted lysate of infected 293A cells, (B) anion exchange chromatography peak fraction, and (C) size exclusion chromatography peak fraction indicate increasing purity of the Pt-Dd (bracket "penton"), which maintains its sedimentation coefficient throughout the purification process. 1: protein marker, 2: 10% of input, 3-15: fractions with decreasing sucrose concentration.

3.2.2.2. Motility in Cultured Hippocampal Neurons

We also tested intracellular motility of Alexa546 dye-labeled Pt-Dd in 5DIV cultured hippocampal neurons. Attachment was performed in the cold to synchronize uptake, and live cell imaging with streaming acquisition was used to visualize intracellular movements (Figure 3-8).

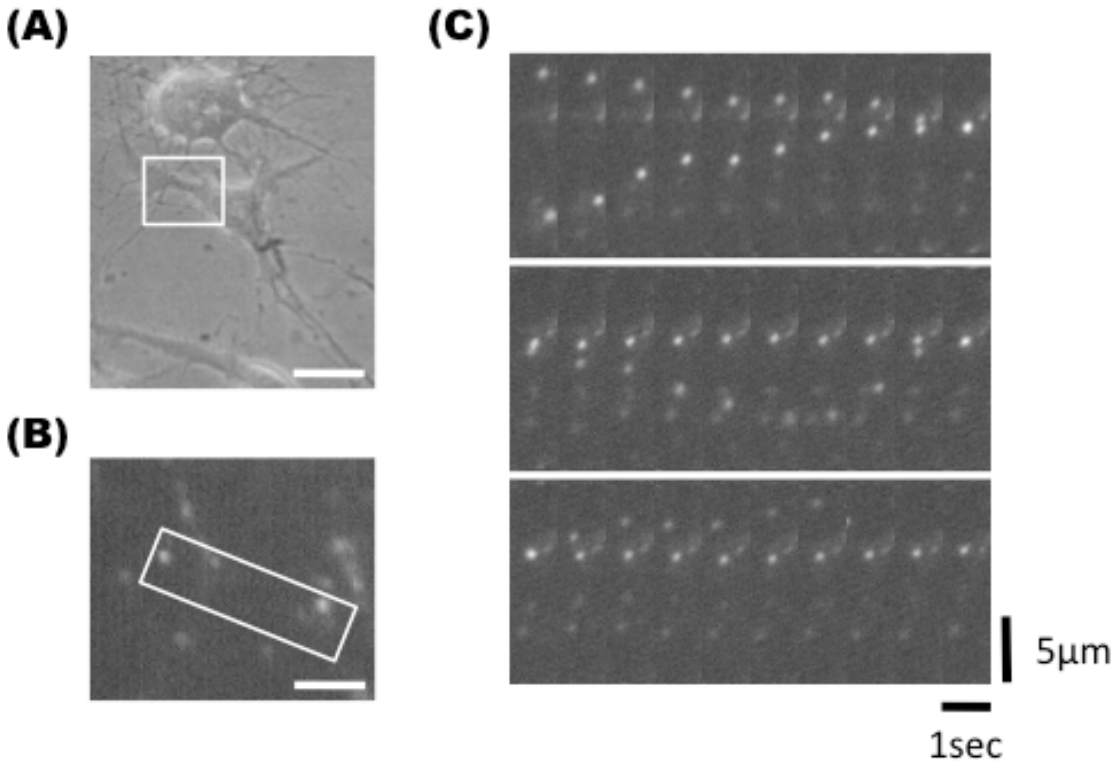

Figure 3-8: Intracellular Alexa546-Pt-Dd Motility in Hippocampal Neurons.

Alexa546-Pt-Dd motility was tested in hippocampal neurons by live cell imaging of cells incubated with Alexa546-Pt-Dd at 10frames/sec. (A) DIC image of neuronal cell chosen for imaging (upper panel). Box indicates area of high Alexa546-Pt-Dd motility. Bar = 20µm. (B) Magnified view of box in panel A in Alexa546 channel shows distinct Alexa546-Pt-Dd signals. Box indicates area used for montage in panel C. Bar = 5µm. (C) Montage of boxed area in panel B, shows clear, bidirectional movement of two Alexa546-Pt-Dd particles in this part of the neuronal cell. Images every 10 frames.
Hippocampal neurons were a generous gift of Shahrnaz Kemal.

Almost all Alexa546-Pt-Dd were motile up to 1.5h after synchronous uptake was initiated. The movements were fast with speeds up to 1.7 µm/sec and bidirectional, especially close to the cell body and in thicker portions of cell processes. Almost no movement was observed in thinner parts of dendrites or axons. However, caution has to be taken interpreting these results since uptake of Pt-Dd has not been investigated to the same detail as for the adenovirus capsid. Hence, it is possible that the crucial step of endosomalysis occurs much later or even never for Pt-Dd and the described movements are representative of Pt-Dd inside vesicular structures.

3.3. Discussion

3.3.1. Role of Kinesin in Virus Entry

Besides the work presented here, which indicates a direct interaction of kinesin-1 with the viral capsid protein penton base, roles of kinesin transport in adenoviral entry has been investigated in various contexts (Leopold et al., 2000; Strunze et al., 2011; Yi et al., 2011), Jie Zhou, personal communication).

In early entry phases, kinesin-1 is presumably responsible for lysosome/LE (lyso/LE) dispersion upon virus-induced PKA stimulation, which reduces dynein attachment to this class of organelles and rapidly increases their kinesin-driven MT plus-end motility (see chapter 1.1.2.2. and 2.3.1.). A clear host cell protection mechanism for lyso/LE dispersal could not be shown for subgroub C adenoviral infections since they leave the endosomal pathway early. However, subgroup B and F adenoviruses stay inside vesicles for prolonged periods of time, a phenotype correlated with lower infectivity (see chapter 2.3.3). Here, kinesin-mediated lyso/LE redistribution might represent a host defense mechanism, which employs degradative organelles to inactivate incoming adenoviral particles.

In contrast, the kinesin-1 isoform Kif5c has been reported to improve infectivity by aiding injection of the viral genome into the nucleus (Strunze et al., 2011).

Kinesin is also involved in the cytoplasmic transport of incoming adenovirus particles which can be unmasked by acute dynein inhibition (Yi et al., 2011). Reports that microinjection of function-blocking kinesin-1 antibodies has no effect on nuclear targeting of Ad5 (Leopold et al., 2000) might be of limited relevance, since direct effects on viral motility were not examined and the possibility remains that kinesin-1 is involved in viral movements away from the nucleus and its inhibition leads to an increased redistribution of capsids to the nucleus. Furthermore, various other kinesins might substitute for kinesin-1. We did not detect interactions of kinesin-2 or kinesin-3 with the viral capsid or penton base by the described methods. However, abundance of these kinesins was low in the starting material for the binding studies and we might have missed a possible low

affinity interaction, which might have further been masked if kinesins complete for binding sites on the capsid. Using recombinant penton base constructs expressed in Sf9 cells (Wickham et al., 1993) and kinesin full-length or truncation proteins for further binding analysis might reveal additional interactions and also elucidate clearly which part of kinesin-1 interacts with the viral capsid. Mapping of the penton base binding site on kinesin-1 might allow the generation of specific dominant-negative approaches blocking exclusively the capsid – kinesin-1 interaction and affecting virus transport while physiological transport processes remain unaffected. This would also allow investigations regarding a possible protective role for MT plus-end directed transport during viral infections (see below).

Interestingly, preliminary data show a complete inhibition of virus motility in cells expressing the cargo- and light chain interacting tail domain of Kif5b indicative of a possible dominant-negative effect (Jie Zhou, personal communication). This construct also seems to localize to viral capsids in their cytoplasmic entry phase between 15-45min p.i., in accordance with kinesin-1 reactive antibodies also staining cytoplasmic capsids (Jie Zhou, personal communication).

The biochemical and live cell imaging data together with these immunocytochemical results indicate that kinesin-1 is a very strong candidate responsible for MT plus-end directed capsid motility through a direct interaction with the major capsid protein penton base.

3.3.2. Bidirectional Capsid Transport

We are only beginning to understand the puzzling result that adenovirus is not only transported by a minus-end directed motor but shows plus-end directed transport as well.

Bidirectional motility might represent an evolutionary safety mechanism by which infected host cells are trying to prevent the virus from gaining access to the nucleus. Kinesin-inhibited cells still show virus redistribution to the nucleus (Leopold et al., 2000), implying kinesin-function to be part of the host defense. In contrast to dynein, which is clearly needed for viral transport purposes towards the nucleus (Bremner et al., 2009; Leopold et al., 2000; Suomalainen et al., 1999). Rates of nuclear localization and high resolution imaging during cytoplasmic transport of Ad5 in kinesin-inhibited cells might reveal more striking support for a role of kinesin in host defense.

However, given the evolutionary pressure on adenoviruses to traverse the cytoplasm quickly after endosomal escape avoiding innate immune defense mechanisms mediated through TRIM21 leading to intracellular capsid degradation (Mallery et al., 2010), it seems more likely that bidirectional motility supports viral fitness. Based on the virus population motility inside the cytoplasm, an assisted diffusion or “random-walk” model has been proposed. Here, capsids explore wide cell areas as quickly as possible until they encounter binding partners at the nuclear pore complex to which they bind with high affinity. According to this model, similar MT minus- and plus-end directed motilities would be beneficial for viral fitness. In enucleated cells, however, adenovirus clearly accumulates at the MTOC with highly

similar kinetics as nuclear localization occurs in mock treated cells (Bailey et al., 2003) and does not stay dispersed in the cytoplasm, indicating a MT minus-end directed bias of population motility. It cannot be ruled out, that bidirectional capsid movement enhances viral motility in general by increased flexibility to circumnavigate obstacles on MT and to reduces the possibility that the processivity of a particular motor becomes limiting (Suomalainen et al., 2001), despite the observation that most particles show predominantly bursts of motility in the course of a 60min infection period (Bremner et al., 2009; Scherer and Vallee, 2011). Similarly, the ability to use both types of motors might be beneficial for Ad entry into polarized cells with altered MT orientations (Suomalainen et al., 1999). The transport step from the MTOC to the nucleus might also require kinesins, but others and we have not identified significant MTOC accumulation of viral capsids in kinesin-inhibited cells ((Leopold et al., 2000), Jie Zhou, personal communication).

Lastly, bidirectional MT-dependent transport might be an intrinsic characteristic of MT-based transport since opposite polarity motors are intrinsically present together at their cargo through a cargo-independent association. For the dynein-dynactin supercomplex two possible modes of interaction with kinesins have been reported. Biochemical assays and immunostaining indicated that kinesin-1 can directly interact with dynein IC (Ligon et al., 2004). Intermediate chain residues 120-283 interact with kinesin light chain 1 and 2, an *in vitro* finding further supported by the presence of WD repeats in the IC sequence, a motif which has previously been associated with KLC binding (Dodding et al., 2011; Morgan et al., 2010). A functional relevance was shown by co-localization of dynein IC and

kinesin-1 on some but not all vesicles inside fixed cells and co-fractionation of both motor proteins with membranous vesicles in flotation sucrose gradient centrifugations in an ATP-dependent manner (Ligon et al., 2004). In addition, dynactin has also been shown to interact with the kinesin-2 light chain KAP in biochemical experiments with Xenopus proteins (Deacon et al., 2003). According to these data, residues 530-793 of KAP interact with the dynactin p150^{Glued} subunit residues 600-811. Interestingly, this site in p150^{Glued} has also been implied in dynein IC binding and a steric competition was postulated (Deacon et al., 2003). However, in light of more recent data, this p150^{Glued} binding site seems only secondary to a N-terminal binding site (McKenney et al., 2011; Morgan et al., 2011), leaving the possibility of simultaneous interaction of dynein and kinesin-2 with the dynactin complex.

In the case of the adenoviral capsid, a more detailed picture of motor recruitment emerges. The two capsid proteins hexon and penton base interact directly with the opposite polarity motors dynein and kinesin-1, respectively. Dynactin is required for dynein regulation but presumably not for motor recruitment. This would allow for studies investigating the role of mechanical strain based (tug-of-war) or signaling mechanisms during bidirectional runs. In contrast to models proposing the role of dynactin as a platform and switch of bidirectional transport, bidirectional capsid motility seems to follow different mechanisms. If reversals in run directions represent indeed a strain- or tension-controlled mechanism, the force-sensing element has to be an intrinsic characteristic of the motor complexes themselves (Mallik et al., 2004), independent of cargo adaptors or recruitment factors. If local

signaling events control bidirectional behavior immediately as proposed recently (Yi et al., 2011), studies on capsid motility might facilitate the identification of this mechanism since the biochemical results presented here reveal a decreased complexity compared to physiological cargoes.

Further work on MT plus-end directed adenovirus motility, employing high temporal and spatial resolution imaging techniques, is required to elucidate the underlying principle how incoming adenovirus simultaneously engages opposite polarity motors. In addition, to determine the identity of the plus-end motor(s) is crucial for any kind of cell-based assays to test their importance and function in adenovirus infection.

Chapter 4: Structural Change of Adenovirus Hexon Dependent on pH

4.1. Introduction

4.1.1. Introduction

Adenoviral capsids protect the viral genome and ensure its rapid delivery to the nucleus of permissible host cells. The highly symmetric proteinaceus capsids self-assemble from hexon and penton protomers with the help of cement proteins into icosahedral structures (Liu et al., 2010; Reddy et al., 2010). The facets of the icosahedra mainly consist of the major capsid protein hexon, which represents extremely tightly packed homotrimers that require the viral chaperon protein 100K for correct folding (Hong et al., 2005; Oosterom-Dragon and Ginsberg, 1981). Hexon trimers feature a double-jelly-roll fold which consists of two eight-stranded β-barrels joined by a linker region and can be found in multiple capsid proteins of other viruses (Krupovic and Bamford, 2011). It is thought to give them the required resistance against environmental influences such as temperature, pH, radiation, and oxidation (Rexroad et al., 2003). The structural rigidity, the large abundance of soluble, non-capsid associated hexon in the lysate of infected cells and the advance in single-step ion-exchange based purification protocols (Boulanger and Puvion, 1973; Rux and Burnett, 2007; Waris and Halonen, 1987), greatly facilitated crystallographic work on hexon (Rux and Burnett, 2000; Rux and Burnett, 2007; Rux et al., 2003). The structure of one hexon monomer can be divided into eight

domains: two eight-stranded viral jellyroll domains, V1 and V2, in the base, which also includes a 55-residue loop at the N-terminus, NT, and a 53-residue "viral jelly-roll-connector" domain, VC, that holds the V1 and V2 domains apart. The loops forming the top of the molecule (FG1 and 2, DE1 and 2) are named for the β-strands in V1 and V2 that they connect (Rux and Burnett, 2000). Seven loops extending from the FG and DE domains are not structurally resolved indicating their flexibility and are termed hypervariable regions (HVR). HVRs differ in length and sequence between serotypes and presumably contain the majority of serotype-specific residues (Rux and Burnett, 2000).

We reported earlier that brief capsid or hexon exposure to low pH conditions, significantly increased cytoplasmic dynein binding (Bremner et al., 2009). There are several lines of evidence that link low pH exposure of the adenovirus capsid in general and hexon in particular to biochemical changes presumably by affecting the structural conformation. It was found that not only the virus capsid but also all three major capsid proteins hexon, penton base, and fiber individually exhibit a pH-dependent hydrophobicity indicating a structural rearrangement between pH6.0-5.0 (Seth et al., 1985). Expanding on these findings, it was shown that the capsid structure loosens after low pH exposure as indicated by an increased accessibility of the viral DNA to an intercalating fluorophore below pH5.5 and by a facilitated dissociation of most capsid proteins from the viral genome (Wiethoff et al., 2005). According to this model, only hexons residing in the facets of the capsid remain bound to the viral genome after low pH exposure while the peripentonal hexon, the penton complex and protein VI dissociate from the virion to varying extents. These

results contradict an earlier view of the interaction between hexon and protein VI, since hexon showed an increased affinity for protein VI in low pH incubation buffer during Blot Overlay experiments with a maximal affinity at pH5.5 (Matthews and Russell, 1994). Interestingly, below pH5.5 hexon becomes susceptible to dispase proteolysis, which results in 15kDa and 85kDa cleavage products (Everitt et al., 1988). The 15kDa fragment covers the amino-terminal 135 to 150 residues including the NT domain and parts of the V1 and DE1 domains, which are involved in quartary structure formation of the hexon trimer (Rux et al., 2003). Antibodies raised against this 15kDa fragment show strong adenovirus neutralizing capabilities (Varga et al., 1990). A predicted dispase cleavage site is on the amino-terminal side of W135 and therefore in the hinge sequence of HVR1 of hexon containing an acidic stretch of residues (133–161) with 16 glutamate and 4 aspartate residues in the Ad2 sequence (Rux and Burnett, 2000). It has been speculated, that HVR1 plays an important role in histone H1 binding during passage of hexon and viral DNA through the NPC (Trotman et al., 2001).

In addition to histone H1 binding, hexon also interacts with Nup214 and cytoplasmic dynein (Bremner et al., 2009; Trotman et al., 2001). Dynein can be structurally divided into a force generating head and a cargo binding tail region. The tail contains the accessory subunits intermediate chain (IC), light intermediate chain (LIC) and IC binding light chains (LC) (Figure 1-1). It has been shown, that IC and LIC1 are responsible for motor recruitment to the viral capsid, presumably by forming a continuous binding surface for the hexon trimer (Bremner et al., 2009; Scherer and Vallee, 2011).

Here, we present data indicating a reversible subtle structural change within hexon at low pH, which changes the homotrimeric structure leading to SDS sensitive monomerization. Furthermore, we show that hexon-IC binding can be controlled by the presence of LCs *in vitro*.

4.1.2. Materials and Methods

Cells, Viruses, Plasmids, Molecular Methods, and Antibodies

293A cells were grown in DMEM supplemented with 10% FBS. Replication-deficient Ad5 engineered to express GFP (Ad5-GFP, plaque-purified; obtained from H. Young, Columbia University) were propagated in 293A cells and purified by banding on two linear CsCl gradients (Lawrence and Ginsberg, 1967) and dialysed against 10% glycerol in PBS before cryo-storage. Viral titer was obtained using fluorescent focus assays for Ad5-GFP (Thiel and Smith, 1967).

Truncation constructs of GST-tagged dynein intermediate chain 2C and LC8 were described earlier (McKenney et al., 2011). Bacterial expression constructs for TcTex and LC7 from Sarah Weil (unpublished).

Snapin was cloned form full-length cDNA (Thermo Scientific) into the pGEX-6p vector (GE Bioscience) by introducing 5' BamHI and 3' EcoRI restriction sites by PCR. The additional C-terminal FLAG-tag was introduced during PCR. Mutations in the sequence and in-frame cloning were tested for by sequencing.

Antibodies used included mouse monoclonal anti-hexon (Novocastra) and anti-dynein IC (74.1, Chemicon), rabbit antibodies anti-adenovirus5 (Abcam), anti-LC8 (Santa Cruz), anti-HA (Sigma), and anti-TcTex (S.Weil, unpublished).

Proteins and Biochemical Analysis

Adenovirus hexon was either recovered from virus-depleted supernatant of the first CsCl gradient by immunoprecipitation as described (Bremner et al., 2009) or by anion exchange chromatography (Waris and Halonen, 1987).

Hexon was incubated with a six-fold molar excess of neutral protease (dispase; Worthington Biochemicals, Freehold, NJ) in dispase buffer (100mM Trizma-maleate, 120mM NaCl, 2.5mM $CaCl_2$), pH adjusted to either pH 7.4 (neutral) or pH4.4 (acidic) for 5min at 37°C until the reaction was stopped either by addition of protein sample buffer or 5mM EDTA.

Sucrose gradient density centrifugation of hexon preparation was performed on linear 5-20% sucrose gradients with a total volume of 1.4ml. Sucrose was dissolved in Tris-maleate buffer (50 mM Trizma-maleate, 10 mM NaCl, 1 mM EDTA, and 0.1% Tween 20) at indicated pH values. Sample (100µL) was added on top and gradients, which were centrifuged for 3h at 54,000 rpm in a TL- 55 rotor at 4°C and fractionated into 14 fractions of equal volume. Dynein (20S) and BSA (4.4S) were used as calibration standards.

For time-dependent SDS sensitivity assays, hexon was exposed to 250mM Trizma-maleate at indicated pH for 30min on ice before protein sample buffer (final concentration: 60mM TrisHCl, 1.5% SDS, 5% glycerol, 0.1M DTT, 20µg/ml bromphenol blue, pH6.8) was added for incubation at room temperature for indicated amount of time.

Purification of dynein IC fragments and LC8 were described earlier (McKenney et al., 2011). Briefly, purifications were performed following standard procedures with Ni+ (Sigma-Aldrich) in buffer A (30mM TrisHCl, 150mM NaCl, 5mM imidazole, 5mM β-Mercaptoethanol, pH7.4) supplemented with protease inhibitor cocktail (Sigma-Aldrich), eluted with 450mM NaCl and 200mM imidazole, followed by buffer exchange into buffer A or glutathione (USB) beads in buffer B (10mM TrisHC, 150mM NaCl, 1mM EDTA, 0.5mM DTT, pH7.4), and eluted with 10mM reduced glutathione or digested with R3C protease to cleave off GST. Snapin was purified using glutathione beads and buffer B only. Purified proteins were flash frozen in liquid nitrogen and stored at -80°C. Roadblock and TcTex protein was a generous gift of Sarah Weil.

Hexon binding assays were described previously (Bremner et al., 2009). Briefly, hexon was immunoprecipitated and hexon beads were washed and incubated for 30 min in Tris-maleate buffer (50 mM Trizma-maleate, 10 mM NaCl, 1 mM EDTA, and 0.1% Tween 20, pH 4.4), washed in the same buffer at pH 7.4, and then incubated with purified bacterially expressed dynein subunits at 4°C for 1.5 hr. Following washing, the beads were analyzed for the presence of dynein polypeptides by Coomassie staining or immunoblotting.

4.2. Results

4.2.1. pH-dependent Monomerization of Hexon

Adenovirus capsids remain unaffected by extreme environmental conditions, maintaining their icosahedral structure even over pH4-8 from 10°C to 85°C (Rexroad et al., 2006). The most abundant adenovirus capsid protein hexon shows high structural complexity (Figure 4-1A) (Rux et al., 2003) but presumably represents the main factor ensuring structural capsid integrity and stays with the viral genome until its delivery into the nucleus (Greber et al., 1993; Wiethoff et al., 2005). Strikingly, low pH exposure of purified hexon, an effect reflecting endosomal passage during cell entry, primes the viral polypeptide for binding to the intermediate and light intermediate chains of cytoplasmic dynein (Bremner et al., 2009). This behavior can be explained by a low pH-induced structural change exposing the dynein binding site. Purification of hexon trimers to a high degree (Figure 4-1B) allowed tests if low pH exposure affects hexon trimers leading to their monomerization, we incubated purified hexon (Figure 4-1C) over night in pH7.4 or pH4.4 buffer and prepared unboiled gel samples for SDS-PAGE. We noticed, that the samples differed in their migration pattern, indicating changed electrophoretic characteristics. After low pH incubation hexon becomes monomeric while neutral pH does not affect the hexon trimer (Figure 4-1C) as previously reported (Fortsas et al., 1994). However, the monomerization could be induced either by acidic pH alone or by acidic pH treatment in combination with exposure to protein sample buffer.

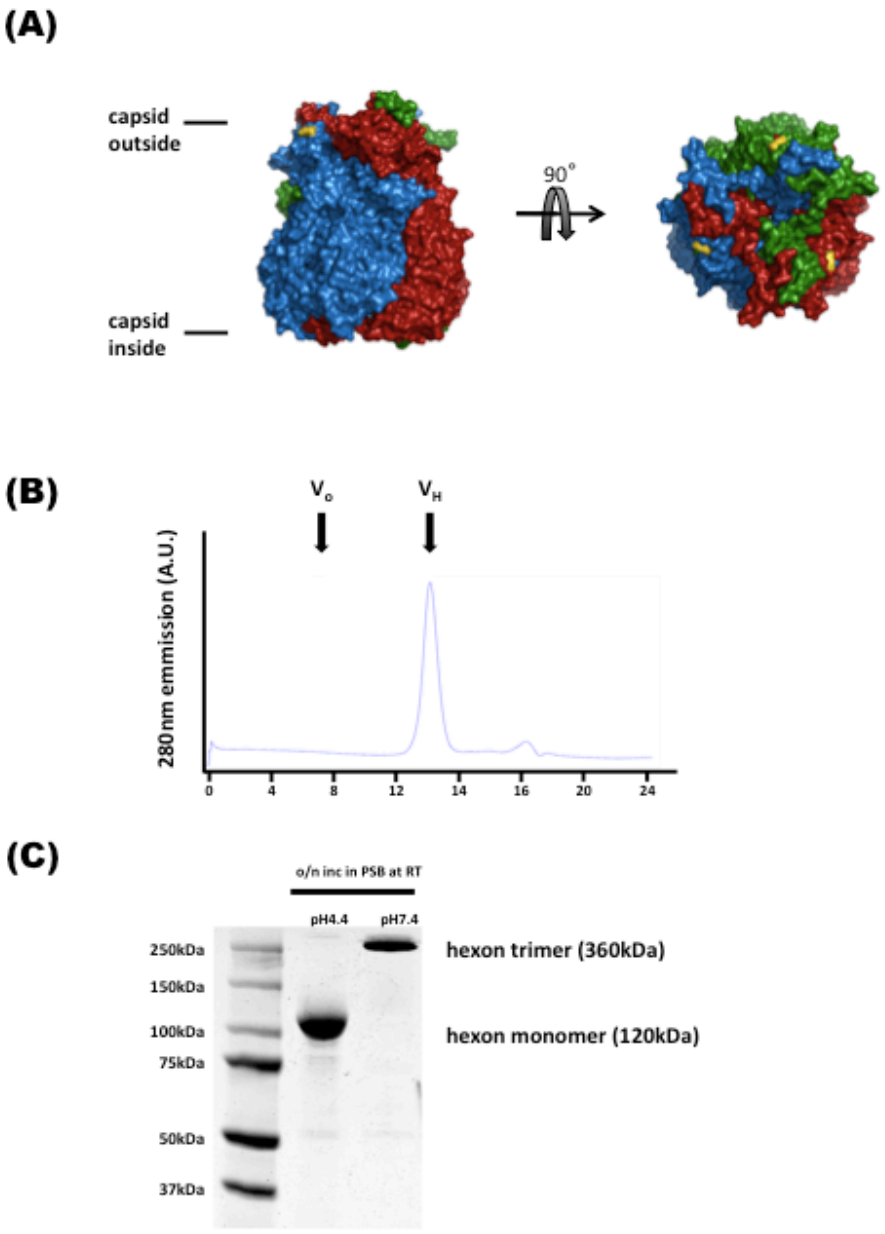

Figure 4-1: Purified Hexon Reacts to Low pH.

(A) X-ray crystal structure of hexon trimer (PDB ID: 1P30) with monomers colored in red, green, and blue and possible dispase hydrolysis site at W135 in yellow. Side and top views are shown. Illustration was generated with PyMol. (B) MonoQ purified hexon from virus-depleted infected 293A lysate was poured over size exclusion column and protein levels were measured at 280nm. One individual peak elutes at 366kDa (theoretical trimer size: 360kDa). Ferritin, BSA, and Ovalbumin were used as size standards. (C) Purified hexon was tested for monomerization after low pH treatment by incubation in protein sample buffer (PSB) over night and SDS-PAGE of unboiled samples. Monomerization was detected on Coomassie-stained gel for the pH4.4 condition but not for pH7.4.

Therefore, we tested if hexon monomerization occurs by low pH exposure alone and compared sedimentation coefficients of hexon on sucrose gradients poured with pH7.4 or pH4.4 buffers. Strikingly, independent of pH, hexon remains trimeric, sedimenting at 12S (Figure 4-2A and B), as reported earlier (Velicer and Ginsberg, 1970). Strikingly, unboiled hexon samples of the low pH gradient migrated at the monomeric size on the SDS-PAGE gel, while neutral pH hexon samples remained trimeric.

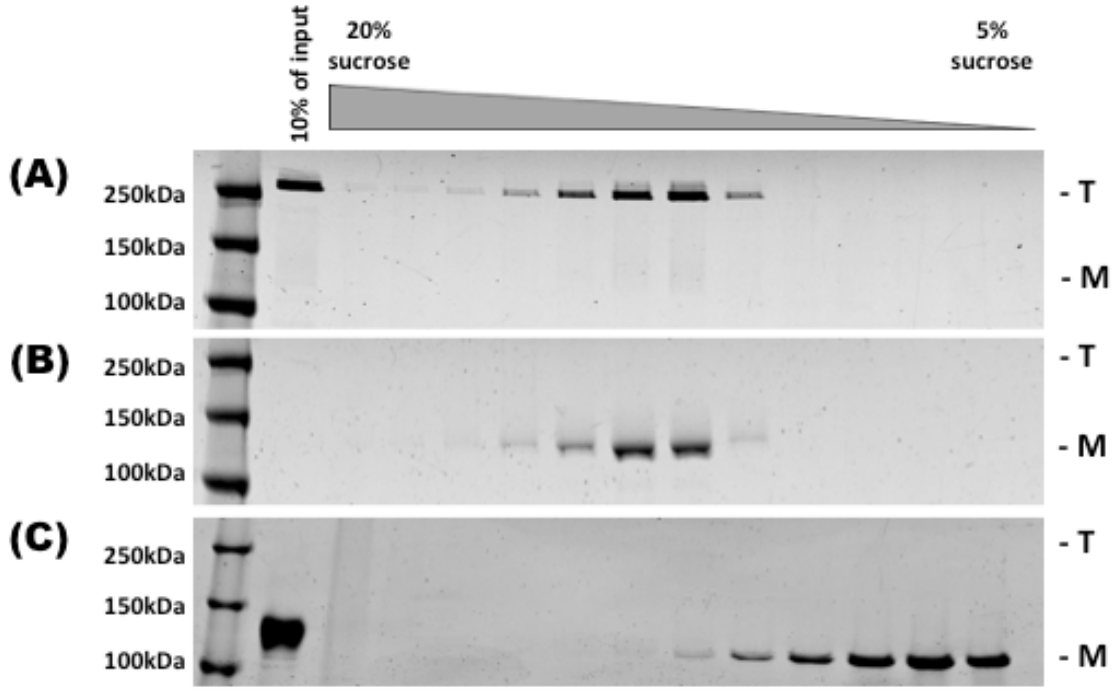

Figure 4-2: Hexon Monomerization by Low pH and SDS.

Purified hexon was tested for monomerization after low pH treatment by sedimentation on linear sucrose gradients (5-20%) at (A) pH7.4, (B) pH4.4, or (C) pH7.4 but hexon was boiled in 1% SDS before loading on gradient. SDS-PAGE of unboiled fraction samples and Coomassie-stained gels show pH-independent sedimentation coefficient for pH7.4 and pH4.4 conditions but monomerization induced by SDS at pH4.4. Boiling in SDS prior to sucrose gradient centrifugation leads to sedimentation profile of hexon monomers. T: trimer; M: monomer.

These results indicate that acidification of hexon leads to subtle structural changes, which do not affect the trimeric hexon structure but manifests itself by strongly increased SDS-sensitivity to monomerization.

Since boiling of hexon in 1% SDS at 100°C prior to loading onto the gradient at neutral pH results in the sedimentation profile of the monomeric polypeptide (Figure 4-2C), it is plausible that the SDS-containing protein sample buffer crucially contributes to acid-induced hexon monomerization.

To test the kinetics of SDS induced monomerization of acidified hexon, we investigated the time-dependency of hexon monomerization after acidification. Hexon was incubated a low pH for 30min and than treated with protein sample buffer for 0-25min before all samples were simultaneously loaded onto a SDS-PAGE gel without prior boiling. Under these conditions, SDS sensitivity of acidified hexon is time-dependent and full hexon monomerization occurs not before 20 min (Figure 4-3A).

We also tested the reported effects of hexon acidification on dispase cleavage and furthermore on dispase cleavage inducing monomerization. Dispase proteolyses hexon into 85kDa and 15kDa digestion products only at pH4.4 but not pH7.4 confirming earlier results (Figure 4-3B; (Everitt et al., 1988)). Interestingly, hexon remains trimeric after low pH digest (Figure 4-3B), indicating that dispase proteolysis strongly inhibits SDS-sensitivity of hexon after low pH treatment. In addition, these data indicate that the N-terminal fragment removed by dispase treatment is an integral part of the core of the hexon trimer and cannot be clipped off to rest of the structure.

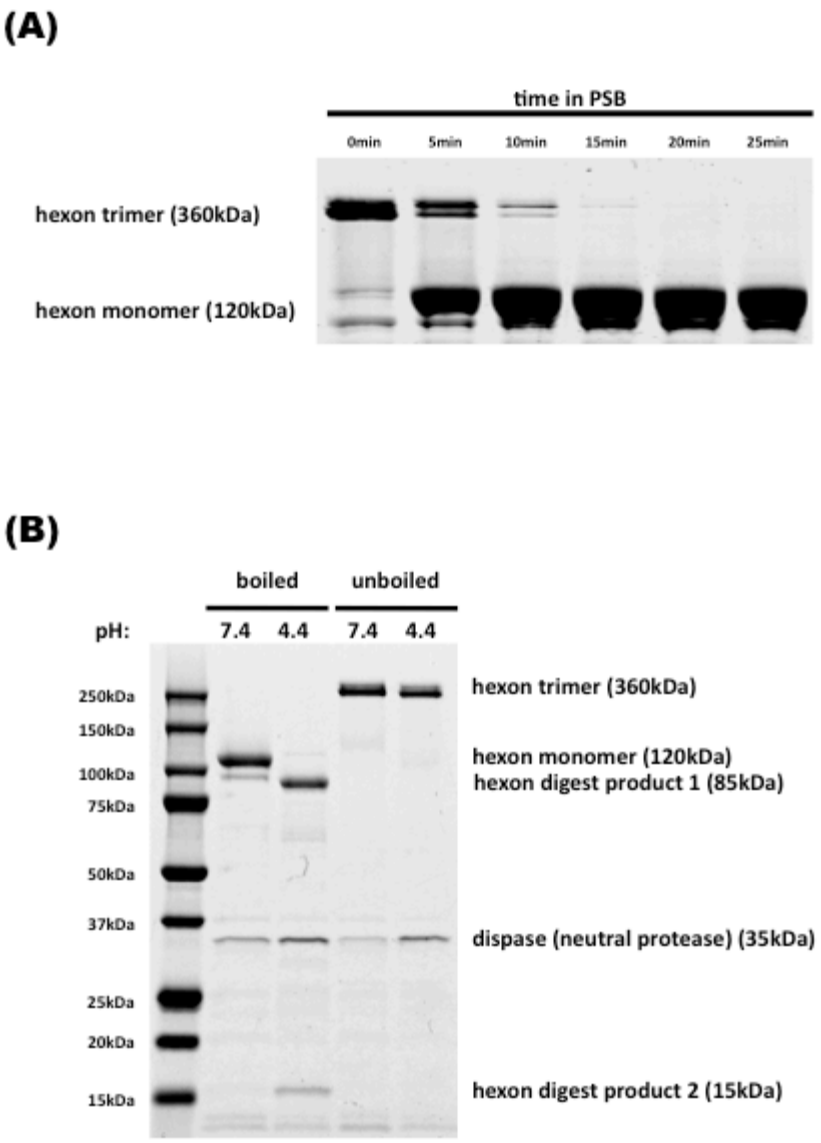

Figure 4-3: Hexon SDS-Sensitivity Kinetics and Inhibition by Dispase Hydrolysis.

(A) Kinetics of low pH-induced hexon SDS-sensitivity were tested after purified hexon was pH4.4 treated for 30min by protein sample buffer (PSB) incubation for indicated times durations and SDS-PAGE of unboiled samples. Monomerization was detected as early as 5min after the addition of PSB, a complete effect was seen after 20min, indicating a gradual SDS effect. (B) Purified hexon was tested for monomerization after dispase treatment. Dispase hydrolyses hexon in low pH conditions resulting in two major digestion products (85kDa and 15kDa) visible by Coomassie staining of SDS-PAGE boiled samples. Unboiled samples show hexon trimers in the digested and undigested condition and no digestion products, indicating that the hexon trimer remains inact even after dispase hydrolysis and low pH treatment.

Together, these results indicate that low pH treatment of hexon alone does not disrupt the trimeric structure but monomerization of the polypeptide requires the additional exposure to SDS and, for a full effect, SDS treatment needs to exceed 20min. In addition, a likely site of subtle pH-induced structural change in the hexon trimer surrounds a dispase proteolysis site N-terminal of HVR1 since dispase treatment inhibits SDS sensitivity.

4.2.2. Reversible Monomerization

We further asked if the effect of low pH and SDS-induced monomerization could be reversed by raising the pH before addition of SDS. Therefore, we incubated purified hexon at pH4.4 for 30min on ice before subjecting it to sucrose density gradient centrifugation on a linear 5-20% gradient poured at pH7.4. As expected, hexon still sedimented at 12S (Figure 4-4). Strikingly, unboiled gel samples run exclusively at hexon trimer size on SDS-PAGE (Figure 4-4), revealing a complete reversal of the low pH induced effect.

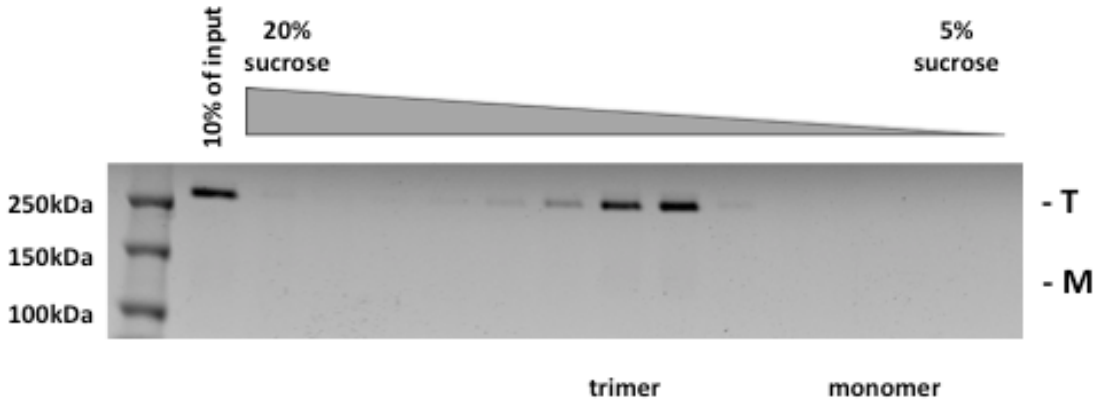

Figure 4-4: Low pH-induced Hexon SDS Sensitivity Is Reversible.

Purified hexon was tested for reversibility of SDS-sensitivity for monomerization by pH4.4 treatment before sedimentation on linear sucrose gradients (5-20%) at pH7.4. SDS-PAGE of unboiled fraction samples and Coomassie-stained gels show the sedimentation coefficient and SDS-PAGE sedimentation of the trimeric hexon molecule indicating full reversibility of the low pH effect leading to increased SDS sensitivity. T: trimer; M: monomer.

4.2.3. Hexon Binding to Dynein IC

We also continued hexon binding screens with IC2C truncation constructs expressed in bacteria (McKenney et al., 2011) to elucidate the minimal binding region for hexon and possible overlap with the dynein regulatory factors dynactin and NudE/EL which both seem to interact with the N-terminal 70 residues (McKenney et al., 2011). Interestingly, only the 1-250 construct interacted with hexon whereas the 1-150 and shorter fragments did not pull-down significant amounts (Figure 4-5A and B).

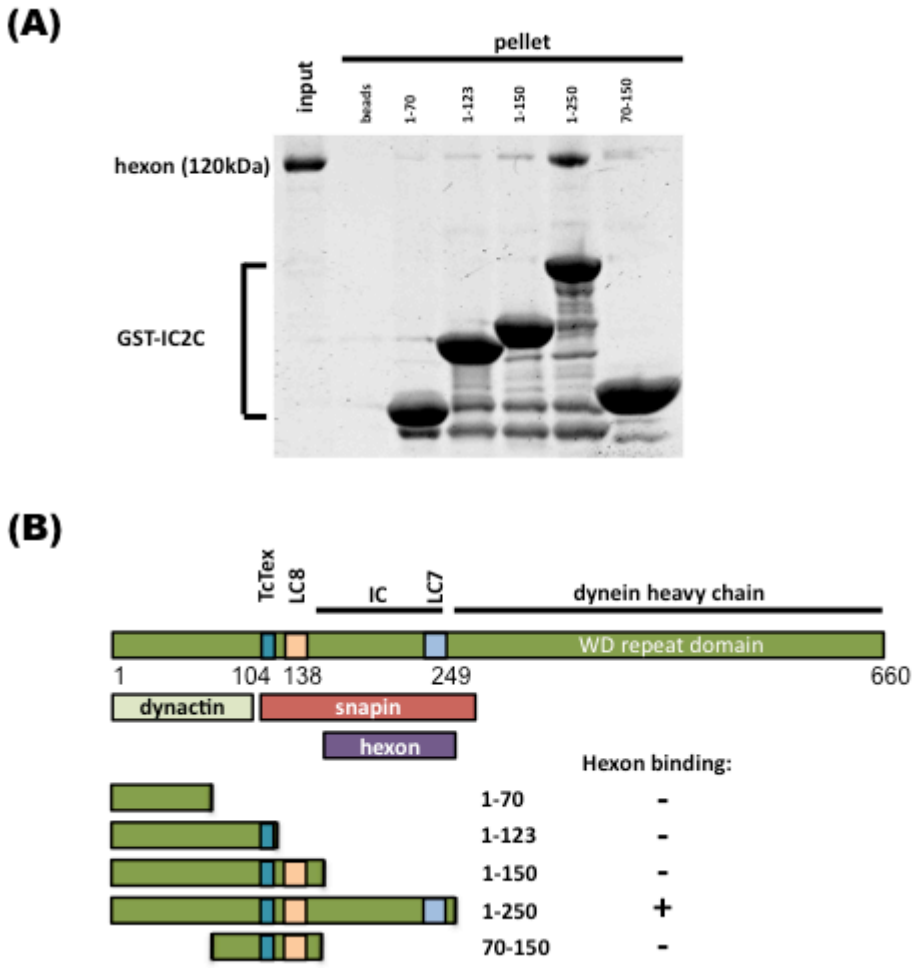

Figure 4-5: Hexon Binding to Dynein Intermediate Chain.

(A) MonoQ purified and acidified hexon was tested in pull-down experiments with bacterially expressed GST-tagged truncation constructs covering the N-terminal part of the dynein IC2C. The hexon binding site could be mapped to IC residues 150-250. (B) Diagram of the dynein IC with binding sites for light chains (TcTex, LC8, LC7), dynactin, snapin, and, dynein heavy chain and the IC-IC dimerization domain. The hexon binding region overlaps with the reported snapin binding site but not dynactin or NudE.

Furthermore, the IC-hexon interaction could be modulated by the addition of different classes of light chains. Roadblock/LC7 reduced the amount of IC in the hexon pellet (Figure 4-6A and C), whereas LC8 and TcTex-1 increased it in an additive fashion (Figure 4-6B and C). Importantly, none of the light chains by themselves bind to hexon ((Bremner et al., 2009), and Figure 2-1C).

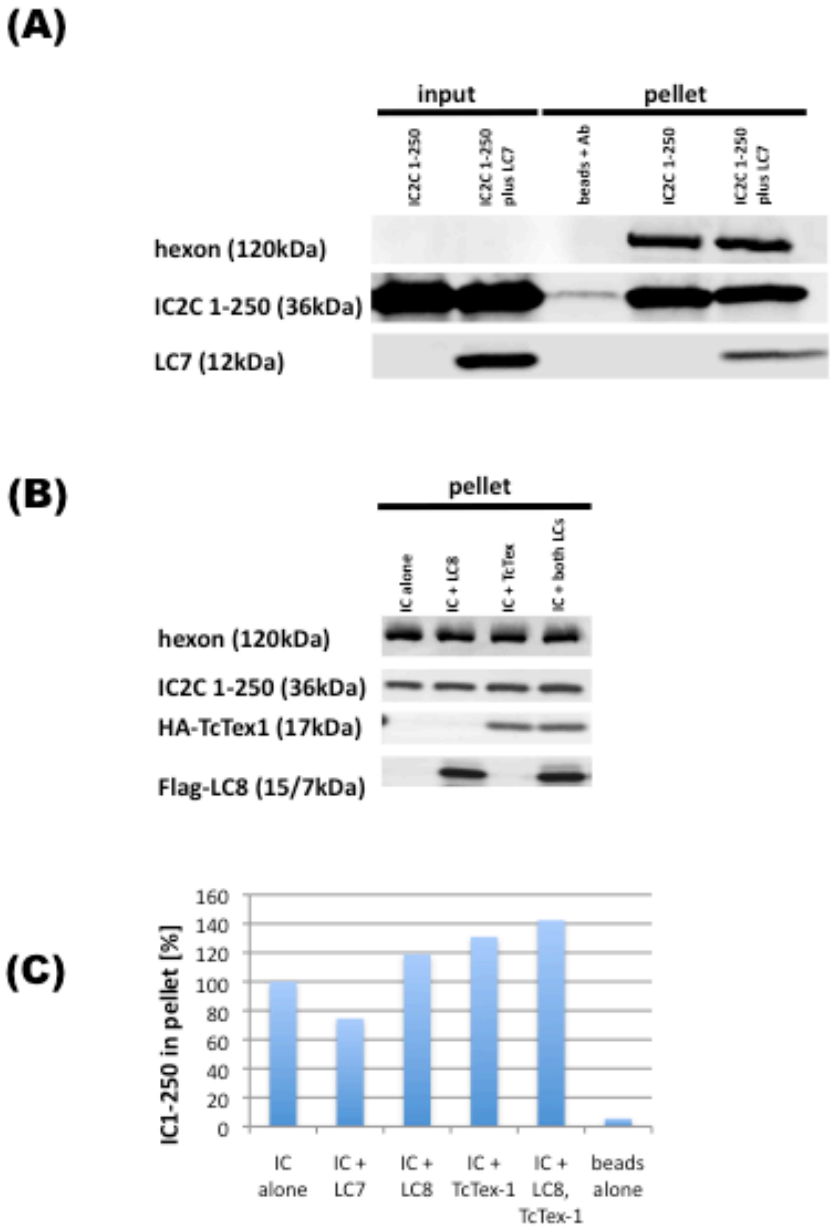

Figure 4-6: Light Chains Affect Hexon - IC Binding.

Bacterially expressed dynein light chains were tested for affecting the affinity of the IC2C fragment 1-250 to hexon by addition of IC fragment with (A) roadblock/LC7 or (B) HA-TcTex and Flag-LC8 separately or combined to the hexon pull-downs and immunoblotting of inputs (panel A) and pellets (panels A and B) with anti-hexon, anti-IC, anti-LC7, and anti-tag antibodies. (C) Quantification of hexon-bound IC fragment shows that LC7 has an inhibitory effect on the hexon affinity, reducing the amount of interacting IC fragment by ~30%, whereas TcTex and LC8 increase the affinity by up to 45%.

Since hexon does not interact within the N-terminal 70 residues of the IC, it remains possible that dynein regulators and the viral capsid bind to the motor complex simultaneously. Interestingly, antibodies, which interfere with dynein-dynactin and dynein-NudE binding (McKenney et al., 2011) do not affect the dynein-hexon interaction (Bremner et al., 2009). However, recently, a small protein of the lysosomal pathway, snapin, was shown to interact with the IC 108-268 (Cai et al., 2010), similar to the hexon binding. We conducted competition experiments between snapin and hexon and saw a reduction of dynein signal in the anti-hexon coimmunoprecipitates if snapin was added compared to the snapin free condition indicative of overlapping binding sites of hexon and snapin in the IC (Figure 4-7).

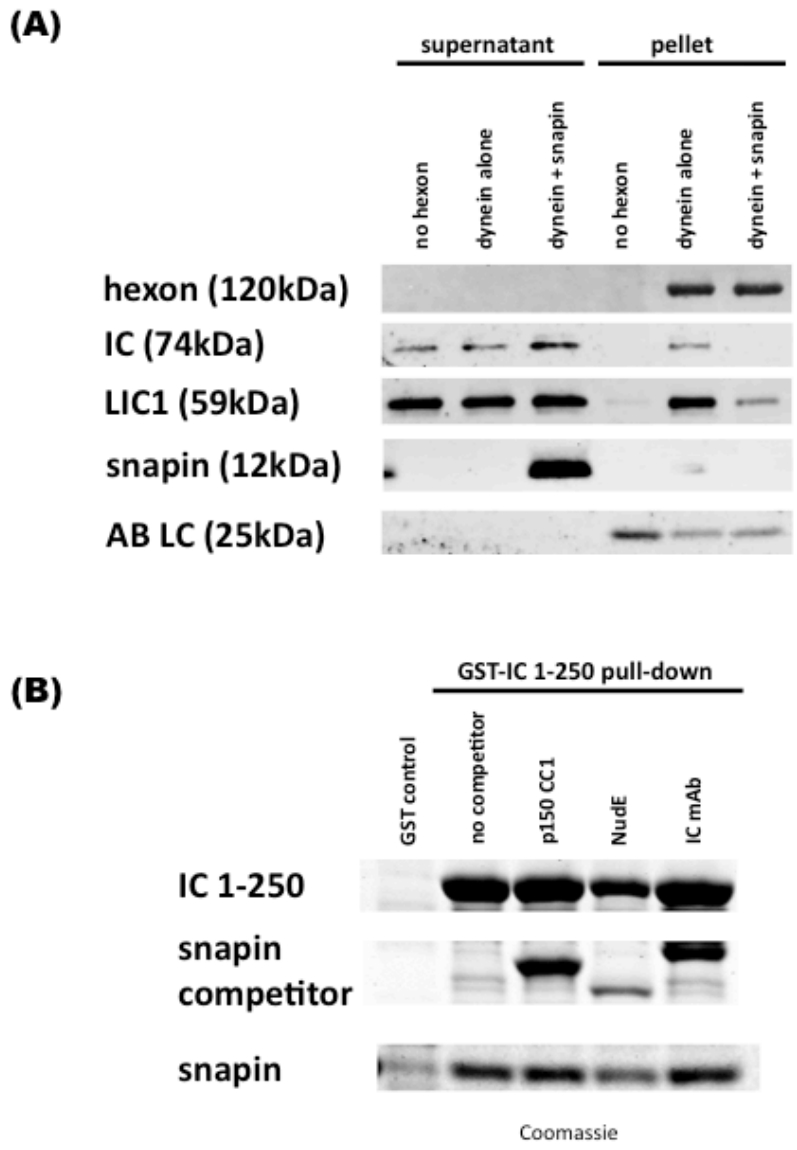

Figure 4-7: Lysosomal Dynein Recruitment Factor Snapin Competes With Hexon for Dynein.

(B) Purified rat brain cytoplasmic dynein was tested for pull-down with hexon in the presence of bacterially expressed snapin by immunoblotting of the supernatants and pellets with antibodies against hexon, snapin, and dynein IC and LIC1 subunits. Snapin strongly reduced sedimentable dynein, as indicated by a loss of IC and LIC1 signal. (B) Snapin was tested for pull-down with IC2C 1-250 fragment in the presence of dynein IC binding proteins p150^{Glued}-CC1, NudE, and 74.1 monoclonal antibody (IC mAb) by Coomassie staining of SDS-PAGE gel. None of the tested binding partners reduced the amount of pull-down snapin, indicating independent IC binding sites. All proteins expressed in bacteria.

These results demonstrate a further interaction between the dynein complex and the major adenoviral capsid protein hexon in additional to LIC1 (chapter 2.2.1.). The described hexon-IC interaction can be modulated by the presence of dynein light chains and is sensitive to competition with the small lyso/LE associated protein snapin.

4.3. Discussion

4.3.1. pH Effects on Hexon Tertiary Structure

The results presented here indicate a reversible, subtle but reproducible structural effect of low pH exposure on the hexon trimer. We can only speculate, if the pH effects obtained with purified hexon are representative of structural rearrangements of capsid-associated hexon (Figure 4-8).

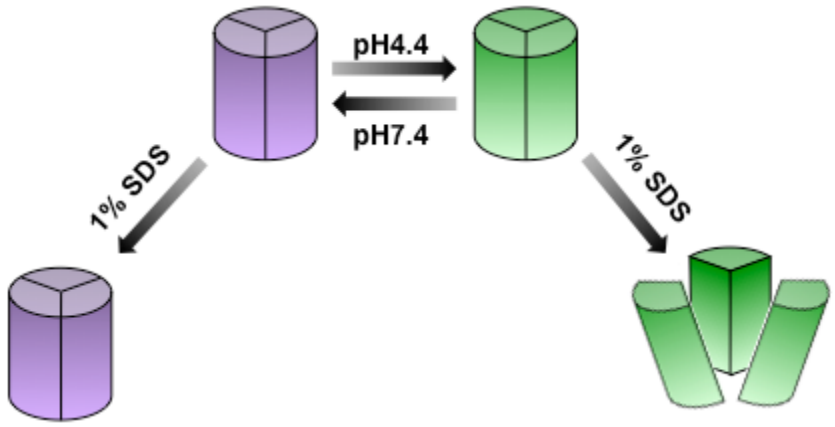

Figure 4-8: Model of pH-Sensitive Hexon Monomerization upon SDS Treatment.

Diagram illustrating different structural states of the hexon trimer dependent on pH leading to SDS sensitivity. The hexon trimer at neutral pH (purple) is resistant to SDS and remains monomeric after addition of 1% SDS. Acidified hexon (green) maintains the trimeric state. However, low pH treatment induces subtle changes, which lead to strongly increased dynein affinity (Bremner et al., 2009) and SDS sensitivity resulting in monomerization but which can be fully reversed by raising the pH.

However, interestingly, the reported pH-dependent structural change in the hexon trimer, which appears to unmask a dispase hydrolysis site at low pH, presumably affects the external loop sequence HVR1 (Everitt et al., 1988). This rearrangement is possible in the individual hexon trimer and also in capsid-associated hexons (Everitt et al., 1988). Hence, it is very likely that the low pH effect leading to increased SDS sensitivity represents a structural change possible in free and capsid-incorporated hexon trimers, as well. Furthermore, low pH exposure also leads to increased hydrophobicity of the viral capsid and capsid proteins (Seth et al., 1985). The effect is maximal at pH<5.5 and reversible by addition of pH7 buffer (Seth et al., 1985). Of note, hydrophobicity effects on hexon are pronounced after low pH dispase cleavage (Everitt et al., 1988). At this point, however, it remains to be shown if effects of low pH exposure leading to increases in dynein binding, hydrophobicity, and dispase- and SDS-sensitivity have separate or distinct molecular causes in the hexon structure. Nevertheless, hexon HVR1 and surrounding sequences emerge as a likely candidate region of the polypeptide mediating the reported low pH effects since dispase treatment strongly reduced low-pH induced SDS sensitivity. HVR1 represents the N-terminal part of the DE1

domain, which connects the two halves of the viral jellyroll domain V1 and covers large portions of the external hexon surface. It would be interesting to test cells expressing DE1 for binding between this hexon fragment and dynein or for possible effects on virus motility.

4.3.2. Role in Virus Transport

During regular adenovirus infection, capsid acidification occurs while the capsid passages through the endosome. The effects on infectivity remain under debate (Smith et al., 2010b), but several lines of evidence indicate that fitness is increased for subgroup C adenoviruses by low pH priming inside the endocytic vesicle. Endosomalysis, dynein binding, and efficient microtubule-based transport seem to require low pH exposure of the capsid (Bremner et al., 2009; Wiethoff et al., 2005). Interestingly, two dynein subunits, which have both been implicated in cargo binding, also mediate the interaction with adenovirus hexon (Bremner et al., 2009). Dynein light intermediate chain 1 (LIC1) appears to be the dominant binding partner but intermediate chain (IC) also contributes to the interaction (see chapter 2.2.1 and 4.2.3.). IC alone can bind to acidified hexon but the affinity seems to be increased in the presence of the dynein light chains LC8 and TcTex-1. Both light chains have been implied in cargo recruitment (Table 1-1), but they show no interaction with hexon (Bremner et al., 2009) and Figure 2-1C). This implies indirect effects of the LCs on hexon binding by structurally modulating IC. In fact, LC8 and TcTex-1 have been found to function in structural stabilization and dimerization of the IC (Barbar, 2008; Makokha et al., 2002; Williams et al., 2007).

Trapping experiments to sequester LCs from the dynein complex have effects on cargo transport and mitosis (Varma et al., 2010). Hence, it is conceivable that upon LC8 and TcTex-1 binding, the conformation of IC is altered to a state more favorable for hexon binding, inducing IC-IC dimerization and increasing stability. The role of the third class of dynein light chains, Roadblock/LC7, is less understood (Bowman et al., 1999). They are also implied in cargo recruitment but seem to be less crucial for IC-IC dimerization. Their mode of interaction with the IC also differs from LC8 and TcTex, which act like a molecular clamp, bringing two IC monomers in close contact. Roadblock/LC7, however, is binding between two IC monomers, increasing their distance (Hall et al., 2010; Song et al., 2005). Therefore, the here presented reduction in IC affinity for hexon by addition of Roadblock/LC7 might be due to a disruption of the hexon binding site or similarly is due to competition between hexon and Roadblock/LC7 for IC binding.

We detected competition for the dynein IC between hexon and snapin. Snapin is reported to associate with lysosomes and late endosomes (Cai et al., 2010) and functions by dynein recruitment to these organelles via a direct IC interaction. It remains to be tested, if snapin might also have additional regulatory control over the dynein complex. Hence, hexon might not only replace snapin on the IC sterically, recruiting more dynein from a lysosome/late endosome associated motor pool, but also bind to a critical functional element in the dynein motor complex.

CONCLUSIONS

The here presented work combines research in two fields, motor proteins and host-pathogen interactions. It reveals how MT-dependent motor processes play a pivotal role in virus attack and cellular host defense.

Our data connects the effects of adenovirus stimulated PKA activity on MT minus-end directed transport with a specific role of dynein LIC1-T213 in recruitment of the motor complex to the viral capsid. This has implications on the future design of adenovirus based gene vectors, which should keep their ability to induce a cellular PKA response to ensure efficient capsid transport to the nucleus to maintain their infectivity. Furthermore, we have determined the independent hexon binding sites within the dynein IC and LIC1 polypeptides. In contrast, the parts of hexon interacting with the dynein subunits are still unknown. Testing recombinant hexon fragments for IC or LIC1 bindig might give additional insight in the molecular mechanism of capsid – motor binding. We suspect flexible surface loops of the trimeric hexon structure to mediate the interaction. Unfortunately, none of them could be resolved in x-ray crystallographic studies and structural information on possible pH-dependent reorientations is lacking at this time as well. Another caviat of the use of hexon fragments is the closely packed structure of the full-length polypeptide. Presumably, hexon fragments will most likely fail to fold properly leaving them of limited use. Another possibility is proteolytic digest of purified hexon at specific hydrolysis sites. It should be possible to extract parts from the hexon structure, isolate and purify them, and test them in dynein IC or LIC1 pull-

downs. Good protease candidates recognize a limited number of hydrolysis sites in hexon such as trypsin or dispase. It would be interesting to test additional proteases in hexon digests and to identify their affinity to dynein subunits.

An additional method to determine IC and LIC1 binding regions in hexon is cryoEM using purified Ad capsid either alone or pre-incubated with fragements of dynein subunits. Additional protein mass might indicate the localization of capsid-interacting proteins as has been done with defensins (Smith et al., 2010a).

In addition to facilitating smarter Ad vector design by keeping the dynein binding parts of hexon intact, this information can also be used to develop hexon-based peptides that block the capsid – motor interaction specifically and might prevent Ad infection in a post-entry step. Similarly, using fragements of IC or LIC1, which contain the hexon binding site, might also lead to a post-entry block of infection. However, this approach presumably results in less specific effects, since physiological dynein interacting proteins are known to compete with hexon for the same dynein binding sites and might also be affected.

Intracellular adenovirus transport might serve as a model system for various reported characteristics of MT-based motility of physiological cargos.

Intruigingly, Ad also moves in a bidirectional fashion and the work presented here indicate independent recruitment of the opposite polarity motors cytoplasmic dynein and kinesin. Hence, the Ad capsid might emerge as an ideal pseudo-cargo studying transport processes at the single molecule level with high temporal and special resulution inside living cells. At this point, more and more evidence emerges

that opposite polarity motors coordinate their activity not only through a mechanical tug-of-war. Possible regulatory mechanisms such as signaling, binding of regulatory factors, or MT track based phenomena might be easier to study using Ad which gives a distinct bright fluorescent signal without any concerning background than using endogenous cargo.

The role of MT in bidirectional transport has been addressed only inadequately. We can see several Ad tracking along the same linear part during entry in short temporal succession, which might indicate the preferred use of particular MT inside the cell. It would be interesting to elucidate the specific characteristics of these MT, if they are more dynamic or more stable, their role in Ad transport and possibly the general role of MT stability in intracellular transport procceses.

Furthermore, the binding of regulatory factors might determine the bidirectional behavior of cargo transport. We and others have shown that Ad relies on the dynein regulatory complex dynactin for cytoplasmic motility but not NudE, Lis1, or ZW10. This makes Ad transport a reasonable model for dynactin-regulated transport and therefore dynactin function *in vivo*. For instance, it is still under debate, what roles the different parts of dynactin-p150^{Glued} play in dynein mediated motility. It is unknown if the p150^{Glued} MT binding site is active during runs and if it contributes to increased dynein processivity. Another unanswered question represents the dynein recruitment mechanism to cargo before runs and if dynactin might also act as a loading station. Furthermore, is the minimal p150^{Glued} binding region with the dynein IC, p150^{Glued}-CC1, able to regulate dynein by itself or are additional parts of the dynactin complex reguired for its complete function.

In addition, it would be interesting the visualize co-localization and co-transport of fluorescently tagged dynein regulators with the incoming capsid. Stable cell lines, constitutively expressing GFP-tagged kinesin, dynein, or dynactin subunits and additional dynein regulators at low levels, might indicate a dynamic presence of motors or regulators at the viral capsid during or in between runs.

Importantly, results presented above indicate that dynein-based Ad motility is dependent on stimulated PKA activity, which facilitates dynein recruitment to the capsid and hence links Ad transport to established models of PKA-regulated transport systems such as melanosome movements in pigment cells. Here, increased PKA activity leads to melanosome dispersal and it has been postulated that an increase in kinesin run-length is responsible for this effect. However, dynein effects regarding possible cargo recruitment mechanisms, as seems to be the case with the Ad capsid, cannot be ruled out. To our surprise, we also found lysosomes/late endosomes (lyso/LE) to be affected be Ad entry in a PKA dependent fashion. Lyso/LE disperse through the cytoplasm upon Ad5 infection or PKA stimulation, leading to strong peripheralization within 30-60 minutes. For both transport systems, Ad capsid and lyso/LE, we were able to identify the same conserved PKA site, LIC1-T213, to mediate these effects. Hence, LIC1-T213 becomes an intruiging candidate to be tested in established PKA regulated transport systems and might reveal a role of dynein recruitment to other classes of organelles dependent on LIC1 phosphorylation by PKA.

If PKA activity represents a general mechanism for bidirectional transport remains to be elucidated. However, given the rather slow response time to external cues like

Ad5 binding or forskolin treatment and a rather gradual effect on lysosome redistribution in the course of several minutes, might indicate that bidirectional transport is regulated by different means, since reversals occur on the millisecond time scale.

Questions more specific to Ad motility, but maybe also general cytoplasmic pathogen movements evolve around the function of kinesin during entry. Continuing our studies to elucidate the identity of the MT plus end-directed motor should give inside into whether it functions as part of the host defense machinery or is part of the viral attack and required for rapid nuclear targeting of adenoviral capsids. To this end, we will employ dominant-negative constructs disrupting known kinesin – cargo interactions and kinesin targeting RNAi. However, the complex nature of the kinesin family and the possibility of additional familiy members substituting for the preferred capsid-trasnporting kinesin, might hamper a rapid identification process. However, the here presented biochemical evidence indicates that kinesin-1 is a very likely candidate in Ad motility and that cell biological efforts should focus on this motor protein. We here show that a sub-viral particle consisting of penton base and fiber, penton dodecahedron (Pt-Dd), can enter cells and exhibits fast linear movements. It is unclear, however, if the Pt-Dd can escape the endo-lysosomal pathway, but given their affinity for kinesin-1 even microinjected particles should move inside cells. MT plus end directed motility of Pt-Dd or dedocahedra consisting of penton base exclusively would be a strong indication that penton base represents a functional link between the Ad capsid and the MT plus end motor.

We also further investigated the low pH-effect on the capsid protein hexon. We identified a subtle structural change upon low pH treatment which con be visualized by increased SDS sensitivity leading to hexon monomerization. The SDS sensitivity increase is relatively slow, occuring over several minutes at room temperature, and reversible, since pH neutralization reverses hexon into its SDS insensitive state. It would be interesting to see, if the here described effects are also possible for capsid associated hexon trimers or if the tightly packed arrangement in the capsid facets restricts possible structural changes. We assume, that a surface loop is responsible for the effect, which should also be exposed in capsid associated hexons. Furthermore, of the known low pH effects on hexon - increased hydrophobicity (Seth et al., 1985), increased dispase sensitivity (Varga et al., 1990), increased dynein binding (Bremner et al., 2009), increased SDS sensitivity to monomerization (this work) - we can now link two. Low pH dispase proteolysis inhibits SDS sensitivity to monomerization. It is possible that additional low pH effects are also linked to the same structural feature of the hexon trimer, the hypervariable region 1 (HVR1).

Besides determining the kinetics of hexon monomerization after shorter and shorter low pH treaments it would also be interesting to investigate low pH effects on hexon of additional Ad serotypes. Ad3, for instance, remains in the endo-lysosomal pathway for multilple hours, which might be explained by a decreased pH sensitivity of Ad3 hexon and therefore a more rigid capsid structure, preventing the exposure of protein VI into the endo-lysosomal lumen and ultimately endosomalysis. Other Ad40 and Ad41 enter their host organism through the gastrointestinal tract, being

exposed to a low pH environment before cell attachement. It would be interesting to see if Ad40 or Ad41 hexon exhibits a different pH sensitivity than Ad5 hexon. Furthermore, more and more viruses and additional pathogens have been reported to require a post-attachment low pH step for optimal infectivity. The work here implies that the rather vague requirement for low pH can be specified mechanistically to a small number of proteins or even an individual polypeptide. Identification of the crucial pH sensors in further pathogens and establishing ways to inhibit them might result in interesting therapeutic advances.

REFERENCES

Addinall, S.G., P.S. Mayr, S. Doyle, J.K. Sheehan, P.G. Woodman, and V.J. Allan. 2001. Phosphorylation by cdc2-CyclinB1 kinase releases cytoplasmic dynein from membranes. *J Biol Chem*. 276:15939-15944.

Akalu, A., H. Liebermann, U. Bauer, H. Granzow, and W. Seidel. 1999. The subgenus-specific C-terminal region of protein IX is located on the surface of the adenovirus capsid. *J Virol*. 73:6182-6187.

Albinsson, B., and A.H. Kidd. 1999. Adenovirus type 41 lacks an RGD alpha(v)-integrin binding motif on the penton base and undergoes delayed uptake in A549 cells. *Virus Res*. 64:125-136.

Allen, R.D., J. Metuzals, I. Tasaki, S.T. Brady, and S.P. Gilbert. 1982. Fast axonal transport in squid giant axon. *Science*. 218:1127-1129.

Alonso, C., J. Miskin, B. Hernaez, P. Fernandez-Zapatero, L. Soto, C. Canto, I. Rodriguez-Crespo, L. Dixon, and J.M. Escribano. 2001. African swine fever virus protein p54 interacts with the microtubular motor complex through direct binding to light-chain dynein. *J Virol*. 75:9819-9827.

Amieux, P.S., D.E. Cummings, K. Motamed, E.P. Brandon, L.A. Wailes, K. Le, R.L. Idzerda, and G.S. McKnight. 1997. Compensatory regulation of RIalpha protein levels in protein kinase A mutant mice. *J Biol Chem*. 272:3993-3998.

Andrews, N.W. 1995. Lysosome recruitment during host cell invasion by Trypanosoma cruzi. *Trends Cell Biol*. 5:133-137.

Arimoto, M., S.P. Koushika, B.C. Choudhary, C. Li, K. Matsumoto, and N. Hisamoto. 2011. The Caenorhabditis elegans JIP3 protein UNC-16 functions as an adaptor to link kinesin-1 with cytoplasmic dynein. *J Neurosci*. 31:2216-2224.

Bader, J.R., J.M. Kasuboski, M. Winding, P.S. Vaughan, E.H. Hinchcliffe, and K.T. Vaughan. 2011. Polo-like kinase1 is required for recruitment of dynein to kinetochores during mitosis. *J Biol Chem*. 286:20769-20777.

Bader, J.R., and K.T. Vaughan. 2010. Dynein at the kinetochore: Timing, Interactions and Functions. *Semin Cell Dev Biol*. 21:269-275.

Bagshaw, R.D., J.W. Callahan, and D.J. Mahuran. 2006. The Arf-family protein, Arl8b, is involved in the spatial distribution of lysosomes. *Biochem Biophys Res Commun*. 344:1186-1191.

Bailey, C.J., R.G. Crystal, and P.L. Leopold. 2003. Association of adenovirus with the microtubule organizing center. *J Virol*. 77:13275-13287.

Barbar, E. 2008. Dynein light chain LC8 is a dimerization hub essential in diverse protein networks. *Biochemistry*. 47:503-508.

Bello, L.J., and H.S. Ginsberg. 1967. Inhibition of host protein synthesis in type 5 adenovirus-infected cells. *J Virol*. 1:843-850.

Benson, S.D., J.K. Bamford, D.H. Bamford, and R.M. Burnett. 1999. Viral evolution revealed by bacteriophage PRD1 and human adenovirus coat protein structures. *Cell*. 98:825-833.

Bergelson, J.M., J.A. Cunningham, G. Droguett, E.A. Kurt-Jones, A. Krithivas, J.S. Hong, M.S. Horwitz, R.L. Crowell, and R.W. Finberg. 1997. Isolation of a common receptor for Coxsackie B viruses and adenoviruses 2 and 5. *Science*. 275:1320-1323.

Bielli, A., P.O. Thornqvist, A.G. Hendrick, R. Finn, K. Fitzgerald, and M.W. McCaffrey. 2001. The small GTPase Rab4A interacts with the central region of cytoplasmic dynein light intermediate chain-1. *Biochem Biophys Res Commun*. 281:1141-1153.

Boulanger, P.A., and F. Puvion. 1973. Large-scale preparation of soluble adenovirus hexon, penton and fiber antigens in highly purified form. *Eur J Biochem*. 39:37-42.

Bowman, A.B., R.S. Patel-King, S.E. Benashski, J.M. McCaffery, L.S. Goldstein, and S.M. King. 1999. Drosophila roadblock and Chlamydomonas LC7: a conserved family of dynein-associated proteins involved in axonal transport, flagellar motility, and mitosis. *J Cell Biol*. 146:165-180.

Brady, S.T. 1985. A novel brain ATPase with properties expected for the fast axonal transport motor. *Nature*. 317:73-75.

Brady, S.T., R.J. Lasek, and R.D. Allen. 1982. Fast axonal transport in extruded axoplasm from squid giant axon. *Science*. 218:1129-1131.

Bremner, K.H., J. Scherer, J. Yi, M. Vershinin, S.P. Gross, and R.B. Vallee. 2009. Adenovirus transport via direct interaction of cytoplasmic dynein with the viral capsid hexon subunit. *Cell Host Microbe*. 6:523-535.

Broker, T. 1984. Animal virus RNA processing. *In* Processing of RNA. D. Apirion, editor. CRC Press, Boca Raton, FL. 181-212.

Bucci, C., P. Thomsen, P. Nicoziani, J. McCarthy, and B. van Deurs. 2000. Rab7: a key to lysosome biogenesis. *Mol Biol Cell*. 11:467-480.

Burgess, S.A., M.L. Walker, H. Sakakibara, P.J. Knight, and K. Oiwa. 2003. Dynein structure and power stroke. *Nature*. 421:715-718.

Burkhardt, J.K., C.J. Echeverri, T. Nilsson, and R.B. Vallee. 1997. Overexpression of the dynamitin (p50) subunit of the dynactin complex disrupts dynein-dependent maintenance of membrane organelle distribution. *J Cell Biol*. 139:469-484.

Cai, Q., C. Gerwin, and Z.H. Sheng. 2005. Syntabulin-mediated anterograde transport of mitochondria along neuronal processes. *J Cell Biol*. 170:959-969.

Cai, Q., L. Lu, J.H. Tian, Y.B. Zhu, H. Qiao, and Z.H. Sheng. 2010. Snapin-regulated late endosomal transport is critical for efficient autophagy-lysosomal function in neurons. *Neuron*. 68:73-86.

Campbell, K.S., S. Cooper, M. Dessing, S. Yates, and A. Buder. 1998. Interaction of p59fyn kinase with the dynein light chain, Tctex-1, and colocalization during cytokinesis. *J Immunol*. 161:1728-1737.

Cantalupo, G., P. Alifano, V. Roberti, C.B. Bruni, and C. Bucci. 2001. Rab-interacting lysosomal protein (RILP): the Rab7 effector required for transport to lysosomes. *EMBO J*. 20:683-693.

Cardoso, C.M., L. Groth-Pedersen, M. Hoyer-Hansen, T. Kirkegaard, E. Corcelle, J.S. Andersen, M. Jaattela, and J. Nylandsted. 2009. Depletion of kinesin 5B affects lysosomal distribution and stability and induces peri-nuclear accumulation of autophagosomes in cancer cells. *PLoS One*. 4:e4424.

Carette, J.E., M. Raaben, A.C. Wong, A.S. Herbert, G. Obernosterer, N. Mulherkar, A.I. Kuehne, P.J. Kranzusch, A.M. Griffin, G. Ruthel, P. Dal Cin, J.M. Dye, S.P. Whelan, K. Chandran, and T.R. Brummelkamp. 2011. Ebola virus entry requires the cholesterol transporter Niemann-Pick C1. *Nature*. 477:340-343.

Carter, A.P., C. Cho, L. Jin, and R.D. Vale. 2011. Crystal structure of the dynein motor domain. *Science*. 331:1159-1165.

Carter, A.P., J.E. Garbarino, E.M. Wilson-Kubalek, W.E. Shipley, C. Cho, R.A. Milligan, R.D. Vale, and I.R. Gibbons. 2008. Structure and functional role of dynein's microtubule-binding domain. *Science*. 322:1691-1695.

Caviston, J.P., J.L. Ross, S.M. Antony, M. Tokito, and E.L. Holzbaur. 2007. Huntingtin facilitates dynein/dynactin-mediated vesicle transport. *Proc Natl Acad Sci U S A*. 104:10045-10050.

Caviston, J.P., A.L. Zajac, M. Tokito, and E.L. Holzbaur. 2011. Huntingtin coordinates the dynein-mediated dynamic positioning of endosomes and lysosomes. *Mol Biol Cell*. 22:478-492.

Chagas, C. 1909. Neue Trypanosomen. *Vorläufige Mitteilung Arch Schiff Tropenhygene*. 13:120-122.

Chardonnet, Y., and S. Dales. 1970. Early events in the interaction of adenoviruses with HeLa cells. I. Penetration of type 5 and intracellular release of the DNA genome. *Virology*. 40:462-477.

Chen, Y.M., C. Gerwin, and Z.H. Sheng. 2009. Dynein light chain LC8 regulates syntaphilin-mediated mitochondrial docking in axons. *J Neurosci*. 29:9429-9438.

Cho, K.I., Y. Cai, H. Yi, A. Yeh, A. Aslanukov, and P.A. Ferreira. 2007. Association of the kinesin-binding domain of RanBP2 to KIF5B and KIF5C determines mitochondria localization and function. *Traffic*. 8:1722-1735.

Conde, C., C. Arias, M. Robin, A. Li, M. Saito, J.Z. Chuang, A.C. Nairn, C.H. Sung, and A. Caceres. 2010. Evidence for the involvement of Lfc and Tctex-1 in axon formation. *J Neurosci*. 30:6793-6800.

Cote, M., J. Misasi, T. Ren, A. Bruchez, K. Lee, C.M. Filone, L. Hensley, Q. Li, D. Ory, K. Chandran, and J. Cunningham. 2011. Small molecule inhibitors reveal Niemann-Pick C1 is essential for Ebola virus infection. *Nature*. 477:344-348.

Cox, R.T., and A.C. Spradling. 2009. Clueless, a conserved Drosophila gene required for mitochondrial subcellular localization, interacts genetically with parkin. *Dis Model Mech*. 2:490-499.

Crepieux, P., H. Kwon, N. Leclerc, W. Spencer, S. Richard, R. Lin, and J. Hiscott. 1997. I kappaB alpha physically interacts with a cytoskeleton-associated protein through its signal response domain. *Mol Cell Biol*. 17:7375-7385.

Culver-Hanlon, T.L., S.A. Lex, A.D. Stephens, N.J. Quintyne, and S.J. King. 2006. A microtubule-binding domain in dynactin increases dynein processivity by skating along microtubules. *Nat Cell Biol*. 8:264-270.

D'Andrea, L.D., and L. Regan. 2003. TPR proteins: the versatile helix. *Trends Biochem Sci*. 28:655-662.

Dales, S. 1962. An Electron Microscope Study of Early Association between 2 Mammalian Viruses and Their Hosts. *Journal of Cell Biology*. 13:303-&.

de Jong, R.N., and P.C. van der Vliet. 1999. Mechanism of DNA replication in eukaryotic cells: cellular host factors stimulating adenovirus DNA replication. *Gene*. 236:1-12.

Deacon, S.W., A.S. Serpinskaya, P.S. Vaughan, M. Lopez Fanarraga, I. Vernos, K.T. Vaughan, and V.I. Gelfand. 2003. Dynactin is required for bidirectional organelle transport. *J Cell Biol*. 160:297-301.

Dell, K.R., C.W. Turck, and R.D. Vale. 2000. Mitotic phosphorylation of the dynein light intermediate chain is mediated by cdc2 kinase. *Traffic*. 1:38-44.

Dell'Acqua, M.L., and J.D. Scott. 1997. Protein kinase A anchoring. *J Biol Chem*. 272:12881-12884.

DeWitt, M.A., A.Y. Chang, P.A. Combs, and A. Yildiz. 2012. Cytoplasmic dynein moves through uncoordinated stepping of the AAA+ ring domains. *Science*. 335:221-225.

Dmitriev, I.P., E.A. Kashentseva, and D.T. Curiel. 2002. Engineering of adenovirus vectors containing heterologous peptide sequences in the C terminus of capsid protein IX. *J Virol*. 76:6893-6899.

Dodding, M.P., R. Mitter, A.C. Humphries, and M. Way. 2011. A kinesin-1 binding motif in vaccinia virus that is widespread throughout the human genome. *EMBO J*. 30:4523-4538.

Dodding, M.P., and M. Way. 2011. Coupling viruses to dynein and kinesin-1. *EMBO J*. 30:3527-3539.

Döhner, K., A. Wolfstein, U. Prank, C. Echeverri, D. Dujardin, R. Vallee, and B. Sodeik. 2002. Function of dynein and dynactin in herpes simplex virus capsid transport. *Mol Biol Cell*. 13:2795-2809.

Douglas, M.W., R.J. Diefenbach, F.L. Homa, M. Miranda-Saksena, F.J. Rixon, V. Vittone, K. Byth, and A.L. Cunningham. 2004. Herpes simplex virus type 1 capsid protein VP26 interacts with dynein light chains RP3 and Tctex1 and plays a role in retrograde cellular transport. *J Biol Chem*. 279:28522-28530.

Duguay, D., E. Belanger-Nelson, V. Mongrain, A. Beben, A. Khatchadourian, and N. Cermakian. 2011. Dynein light chain Tctex-type 1 modulates orexin signaling through its interaction with orexin 1 receptor. *PLoS One*. 6:e26430.

Dujardin, D.L., L.E. Barnhart, S.A. Stehman, E.R. Gomes, G.G. Gundersen, and R.B. Vallee. 2003. A role for cytoplasmic dynein and LIS1 in directed cell movement. *J Cell Biol*. 163:1205-1211.

Dumont, A., E. Boucrot, S. Drevensek, V. Daire, J.P. Gorvel, C. Pous, D.W. Holden, and S. Meresse. 2010. SKIP, the host target of the Salmonella virulence factor SifA, promotes kinesin-1-dependent vacuolar membrane exchanges. *Traffic*. 11:899-911.

Echeverri, C.J., B.M. Paschal, K.T. Vaughan, and R.B. Vallee. 1996. Molecular characterization of the 50-kD subunit of dynactin reveals function for the

complex in chromosome alignment and spindle organization during mitosis. *J Cell Biol*. 132:617-633.

Efimov, V.P., and N.R. Morris. 2000. The LIS1-related NUDF protein of Aspergillus nidulans interacts with the coiled-coil domain of the NUDE/RO11 protein. *J Cell Biol*. 150:681-688.

Endter, C., and T. Dobner. 2004. Cell transformation by human adenoviruses. *Curr Top Microbiol Immunol*. 273:163-214.

Engelke, M.F., C.J. Burckhardt, M.K. Morf, and U.F. Greber. 2011. The Dynactin Complex Enhances the Speed of Microtubule-Dependent Motions of Adenovirus Both Towards and Away from the Nucleus. *Viruses-Basel*. 3:233-253.

Enquist, L.W. 2012. Five questions about viral trafficking in neurons. *PLoS Pathog*. 8:e1002472.

Erzberger, J.P., and J.M. Berger. 2006. Evolutionary relationships and structural mechanisms of AAA+ proteins. *Annu Rev Biophys Biomol Struct*. 35:93-114.

Everitt, E., M.J. Persson, and C. Wohlfart. 1988. Ph-Dependent Exposure of Endoproteolytic Cleavage Sites of the Adenovirus-2 Hexon Protein. *Fems Microbiol Lett*. 49:229-233.

Fang, Y.D., X. Xu, Y.M. Dang, Y.M. Zhang, J.P. Zhang, J.Y. Hu, Q. Zhang, X. Dai, M. Teng, D.X. Zhang, and Y.S. Huang. 2011. MAP4 mechanism that stabilizes mitochondrial permeability transition in hypoxia: microtubule enhancement and DYNLT1 interaction with VDAC1. *PLoS One*. 6:e28052.

Faulkner, N.E., D.L. Dujardin, C.Y. Tai, K.T. Vaughan, C.B. O'Connell, Y. Wang, and R.B. Vallee. 2000. A role for the lissencephaly gene LIS1 in mitosis and cytoplasmic dynein function. *Nat Cell Biol*. 2:784-791.

Fejtova, A., D. Davydova, F. Bischof, V. Lazarevic, W.D. Altrock, S. Romorini, C. Schone, W. Zuschratter, M.R. Kreutz, C.C. Garner, N.E. Ziv, and E.D. Gundelfinger. 2009. Dynein light chain regulates axonal trafficking and synaptic levels of Bassoon. *J Cell Biol*. 185:341-355.

Fender, P., A. Boussaid, P. Mezin, and J. Chroboczek. 2005. Synthesis, cellular localization, and quantification of penton-dodecahedron in serotype 3 adenovirus-infected cells. *Virology*. 340:167-173.

Fender, P., R.W. Ruigrok, E. Gout, S. Buffet, and J. Chroboczek. 1997. Adenovirus dodecahedron, a new vector for human gene transfer. *Nat Biotechnol*. 15:52-56.

Fender, P., G. Schoehn, F. Perron-Sierra, G.C. Tucker, and H. Lortat-Jacob. 2008. Adenovirus dodecahedron cell attachment and entry are mediated by heparan sulfate and integrins and vary along the cell cycle. *Virology*. 371:155-164.

Fessler, S.P., F. Delgado-Lopez, and M.S. Horwitz. 2004. Mechanisms of E3 modulation of immune and inflammatory responses. *Curr Top Microbiol Immunol*. 273:113-135.

Fitzgerald, D.J.P., R. Padmanabhan, I. Pastan, and M.C. Willingham. 1983. Adenovirus-Induced Release of Epidermal Growth-Factor and Pseudomonas Toxin into the Cytosol of Kb-Cells during Receptor-Mediated Endocytosis. *Cell*. 32:607-617.

Fortsas, E., M. Petric, and M. Brown. 1994. Electrophoretic migration of adenovirus hexon under non-denaturing conditions. *Virus Res*. 31:57-65.

Franqueville, L., P. Henning, M. Magnusson, E. Vigne, G. Schoehn, M.E. Blair-Zajdel, N. Habib, L. Lindholm, G.E. Blair, S.S. Hong, and P. Boulanger. 2008. Protein crystals in Adenovirus type 5-infected cells: requirements for intranuclear crystallogenesis, structural and functional analysis. *PLoS One*. 3:e2894.

Fuschiotti, P., G. Schoehn, P. Fender, C.M. Fabry, E.A. Hewat, J. Chroboczek, R.W. Ruigrok, and J.F. Conway. 2006. Structure of the dodecahedral penton particle from human adenovirus type 3. *J Mol Biol*. 356:510-520.

Garg, S., M. Sharma, C. Ung, A. Tuli, D.C. Barral, D.L. Hava, N. Veerapen, G.S. Besra, N. Hacohen, and M.B. Brenner. 2011. Lysosomal trafficking, antigen presentation, and microbial killing are controlled by the Arf-like GTPase Arl8b. *Immunity*. 35:182-193.

Gastaldelli, M., N. Imelli, K. Boucke, B. Amstutz, O. Meier, and U.F. Greber. 2008. Infectious adenovirus type 2 transport through early but not late endosomes. *Traffic*. 9:2265-2278.

Gazzola, M., C.J. Burckhardt, B. Bayati, M. Engelke, B.S. Greber, and P. Koumoutsakos. 2009. A stochastic model for microtubule motors describes the in vivo cytoplasmic transport of human adenovirus. *PLoS Comput Biol*. 5:e1000623.

Gibbons, I.R., A. Lee-Eiford, G. Mocz, C.A. Phillipson, W.J. Tang, and B.H. Gibbons. 1987. Photosensitized cleavage of dynein heavy chains. Cleavage at the "V1 site" by irradiation at 365 nm in the presence of ATP and vanadate. *J Biol Chem*. 262:2780-2786.

Gibbons, I.R., and A.J. Rowe. 1965. Dynein: A Protein with Adenosine Triphosphatase Activity from Cilia. *Science*. 149:424-426.

Gill, S.R., T.A. Schroer, I. Szilak, E.R. Steuer, M.P. Sheetz, and D.W. Cleveland. 1991. Dynactin, a conserved, ubiquitously expressed component of an activator of vesicle motility mediated by cytoplasmic dynein. *J Cell Biol*. 115:1639-1650.

Ginsberg, H.S., and C.S. Young. 1976. Genetics of adenoviruses. *Adv Cancer Res*. 23:91-130.

Grabham, P.W., G.E. Seale, M. Bennecib, D.J. Goldberg, and R.B. Vallee. 2007. Cytoplasmic dynein and LIS1 are required for microtubule advance during growth cone remodeling and fast axonal outgrowth. *J Neurosci*. 27:5823-5834.

Greber, U.F., and M. Way. 2006. A superhighway to virus infection. *Cell*. 124:741-754.

Greber, U.F., P. Webster, J. Weber, and A. Helenius. 1996. The role of the adenovirus protease on virus entry into cells. *EMBO J*. 15:1766-1777.

Greber, U.F., M. Willetts, P. Webster, and A. Helenius. 1993. Stepwise dismantling of adenovirus 2 during entry into cells. *Cell*. 75:477-486.

Griffis, E.R., N. Stuurman, and R.D. Vale. 2007. Spindly, a novel protein essential for silencing the spindle assembly checkpoint, recruits dynein to the kinetochore. *J Cell Biol*. 177:1005-1015.

Gross, S.P., M.C. Tuma, S.W. Deacon, A.S. Serpinskaya, A.R. Reilein, and V.I. Gelfand. 2002. Interactions and regulation of molecular motors in Xenopus melanophores. *J Cell Biol*. 156:855-865.

Hall, J., Y. Song, P.A. Karplus, and E. Barbar. 2010. The crystal structure of dynein intermediate chain-light chain roadblock complex gives new insights into dynein assembly. *J Biol Chem*. 285:22566-22575.

Herman, B., and D.F. Albertini. 1983. Ligand-induced rapid redistribution of lysosomes is temporally distinct from endosome translocation. *Nature*. 304:738-740.

Heuser, J. 1989. Changes in lysosome shape and distribution correlated with changes in cytoplasmic pH. *J Cell Biol*. 108:855-864.

Hirokawa, N., Y. Noda, Y. Tanaka, and S. Niwa. 2009. Kinesin superfamily motor proteins and intracellular transport. *Nat Rev Mol Cell Biol*. 10:682-696.

Hirokawa, N., R. Sato-Yoshitake, N. Kobayashi, K.K. Pfister, G.S. Bloom, and S.T. Brady. 1991. Kinesin associates with anterogradely transported membranous organelles in vivo. *J Cell Biol*. 114:295-302.

Hofmann, I., and S. Munro. 2006. An N-terminally acetylated Arf-like GTPase is localised to lysosomes and affects their motility. *J Cell Sci*. 119:1494-1503.

Holzbaur, E.L., J.A. Hammarback, B.M. Paschal, N.G. Kravit, K.K. Pfister, and R.B. Vallee. 1991. Homology of a 150K cytoplasmic dynein-associated polypeptide with the Drosophila gene Glued. *Nature*. 351:579-583.

Hong, S.S., E. Szolajska, G. Schoehn, L. Franqueville, S. Myhre, L. Lindholm, R.W. Ruigrok, P. Boulanger, and J. Chroboczek. 2005. The 100K-chaperone protein from adenovirus serotype 2 (Subgroup C) assists in trimerization and nuclear localization of hexons from subgroups C and B adenoviruses. *J Mol Biol*. 352:125-138.

Hoogenraad, C.C., A. Akhmanova, S.A. Howell, B.R. Dortland, C.I. De Zeeuw, R. Willemsen, P. Visser, F. Grosveld, and N. Galjart. 2001. Mammalian Golgi-associated Bicaudal-D2 functions in the dynein-dynactin pathway by interacting with these complexes. *EMBO J*. 20:4041-4054.

Hook, P., and R. Vallee. 2012. Dynein dynamics. *Nat Struct Mol Biol*. 19:467-469.

Horgan, C.P., S.R. Hanscom, R.S. Jolly, C.E. Futter, and M.W. McCaffrey. 2010a. Rab11-FIP3 binds dynein light intermediate chain 2 and its overexpression fragments the Golgi complex. *Biochem Biophys Res Commun*. 394:387-392.

Horgan, C.P., S.R. Hanscom, R.S. Jolly, C.E. Futter, and M.W. McCaffrey. 2010b. Rab11-FIP3 links the Rab11 GTPase and cytoplasmic dynein to mediate transport to the endosomal-recycling compartment. *J Cell Sci*. 123:181-191.

Howe, A.K. 2011. Cross-talk between calcium and protein kinase A in the regulation of cell migration. *Curr Opin Cell Biol*. 23:554-561.

Huang, J., A.J. Roberts, A.E. Leschziner, and S.L. Reck-Peterson. 2012. Lis1 Acts as a "Clutch" between the ATPase and Microtubule-Binding Domains of the Dynein Motor. *Cell*. 150:975-986.

Jacob, Y., H. Badrane, P.E. Ceccaldi, and N. Tordo. 2000. Cytoplasmic dynein LC8 interacts with lyssavirus phosphoprotein. *J Virol*. 74:10217-10222.

Jaffrey, S.R., and S.H. Snyder. 1996. PIN: an associated protein inhibitor of neuronal nitric oxide synthase. *Science*. 274:774-777.

Jordens, I., M. Fernandez-Borja, M. Marsman, S. Dusseljee, L. Janssen, J. Calafat, H. Janssen, R. Wubbolts, and J. Neefjes. 2001. The Rab7 effector protein RILP controls lysosomal transport by inducing the recruitment of dynein-dynactin motors. *Curr Biol*. 11:1680-1685.

Kamal, A., A. Almenar-Queralt, J.F. LeBlanc, E.A. Roberts, and L.S. Goldstein. 2001. Kinesin-mediated axonal transport of a membrane compartment containing beta-secretase and presenilin-1 requires APP. *Nature*. 414:643-648.

Kamal, A., G.B. Stokin, Z. Yang, C.H. Xia, and L.S. Goldstein. 2000. Axonal transport of amyloid precursor protein is mediated by direct binding to the kinesin light chain subunit of kinesin-I. *Neuron*. 28:449-459.

Kanai, Y., Y. Okada, Y. Tanaka, A. Harada, S. Terada, and N. Hirokawa. 2000. KIF5C, a novel neuronal kinesin enriched in motor neurons. *J Neurosci*. 20:6374-6384.

Kardon, J.R., S.L. Reck-Peterson, and R.D. Vale. 2009. Regulation of the processivity and intracellular localization of Saccharomyces cerevisiae dynein by dynactin. *Proc Natl Acad Sci U S A*. 106:5669-5674.

Karki, S., and E.L. Holzbaur. 1995. Affinity chromatography demonstrates a direct binding between cytoplasmic dynein and the dynactin complex. *J Biol Chem*. 270:28806-28811.

Kelkar, S.A., K.K. Pfister, R.G. Crystal, and P.L. Leopold. 2004. Cytoplasmic dynein mediates adenovirus binding to microtubules. *J Virol*. 78:10122-10132.

Kim, H., S.C. Ling, G.C. Rogers, C. Kural, P.R. Selvin, S.L. Rogers, and V.I. Gelfand. 2007. Microtubule binding by dynactin is required for microtubule organization but not cargo transport. *J Cell Biol*. 176:641-651.

Kim, S., and H. Yu. 2011. Mutual regulation between the spindle checkpoint and APC/C. *Semin Cell Dev Biol*. 22:551-558.

King, S.J., M. Bonilla, M.E. Rodgers, and T.A. Schroer. 2002. Subunit organization in cytoplasmic dynein subcomplexes. *Protein Sci*. 11:1239-1250.

King, S.J., and T.A. Schroer. 2000. Dynactin increases the processivity of the cytoplasmic dynein motor. *Nat Cell Biol*. 2:20-24.

Kini, A.R., and C.A. Collins. 2001. Modulation of cytoplasmic dynein ATPase activity by the accessory subunits. *Cell Motil Cytoskeleton*. 48:52-60.

Kon, T., T. Oyama, R. Shimo-Kon, K. Imamula, T. Shima, K. Sutoh, and G. Kurisu. 2012. The 2.8 A crystal structure of the dynein motor domain. *Nature*. 484:345-350.

Krupovic, M., and D.H. Bamford. 2011. Double-stranded DNA viruses: 20 families and only five different architectural principles for virion assembly. *Curr Opin Virol*. 1:118-124.

Kubota, T., M. Matsuoka, T.H. Chang, M. Bray, S. Jones, M. Tashiro, A. Kato, and K. Ozato. 2009. Ebolavirus VP35 interacts with the cytoplasmic dynein light chain 8. *J Virol*. 83:6952-6956.

Lawrence, C.J., R.K. Dawe, K.R. Christie, D.W. Cleveland, S.C. Dawson, S.A. Endow, L.S. Goldstein, H.V. Goodson, N. Hirokawa, J. Howard, R.L. Malmberg, J.R. McIntosh, H. Miki, T.J. Mitchison, Y. Okada, A.S. Reddy, W.M. Saxton, M. Schliwa, J.M. Scholey, R.D. Vale, C.E. Walczak, and L. Wordeman. 2004. A standardized kinesin nomenclature. *J Cell Biol*. 167:19-22.

Lawrence, W.C., and H.S. Ginsberg. 1967. Intracellular uncoating of type 5 adenovirus deoxyribonucleic acid. *J Virol*. 1:851-867.

Lazarov, O., G.A. Morfini, E.B. Lee, M.H. Farah, A. Szodorai, S.R. DeBoer, V.E. Koliatsos, S. Kins, V.M. Lee, P.C. Wong, D.L. Price, S.T. Brady, and S.S. Sisodia. 2005. Axonal transport, amyloid precursor protein, kinesin-1, and the processing apparatus: revisited. *J Neurosci*. 25:2386-2395.

Leopold, P.L., G. Kreitzer, N. Miyazawa, S. Rempel, K.K. Pfister, E. Rodriguez-Boulan, and R.G. Crystal. 2000. Dynein- and microtubule-mediated translocation of adenovirus serotype 5 occurs after endosomal lysis. *Hum Gene Ther*. 11:151-165.

Li, E., D. Stupack, G.M. Bokoch, and G.R. Nemerow. 1998a. Adenovirus endocytosis requires actin cytoskeleton reorganization mediated by Rho family GTPases. *J Virol*. 72:8806-8812.

Li, E., D. Stupack, R. Klemke, D.A. Cheresh, and G.R. Nemerow. 1998b. Adenovirus endocytosis via alpha(v) integrins requires phosphoinositide-3-OH kinase. *J Virol*. 72:2055-2061.

Lichtenstein, D.L., K. Toth, K. Doronin, A.E. Tollefson, and W.S. Wold. 2004. Functions and mechanisms of action of the adenovirus E3 proteins. *Int Rev Immunol*. 23:75-111.

Ligon, L.A., S. Karki, M. Tokito, and E.L. Holzbaur. 2001. Dynein binds to beta-catenin and may tether microtubules at adherens junctions. *Nat Cell Biol*. 3:913-917.

Ligon, L.A., M. Tokito, J.M. Finklestein, F.E. Grossman, and E.L. Holzbaur. 2004. A direct interaction between cytoplasmic dynein and kinesin I may coordinate motor activity. *J Biol Chem*. 279:19201-19208.

Lin, S.X., and C.A. Collins. 1992. Immunolocalization of cytoplasmic dynein to lysosomes in cultured cells. *J Cell Sci*. 101 (Pt 1):125-137.

Lin, S.X., and C.A. Collins. 1993. Regulation of the intracellular distribution of cytoplasmic dynein by serum factors and calcium. *J Cell Sci*. 105 (Pt 2):579-588.

Lin, S.X., K.L. Ferro, and C.A. Collins. 1994. Cytoplasmic dynein undergoes intracellular redistribution concomitant with phosphorylation of the heavy chain in response to serum starvation and okadaic acid. *J Cell Biol*. 127:1009-1019.

Lindert, S., M. Silvestry, T.M. Mullen, G.R. Nemerow, and P.L. Stewart. 2009. Cryo-electron microscopy structure of an adenovirus-integrin complex indicates conformational changes in both penton base and integrin. *J Virol*. 83:11491-11501.

Liu, H., L. Jin, S.B. Koh, I. Atanasov, S. Schein, L. Wu, and Z.H. Zhou. 2010. Atomic structure of human adenovirus by cryo-EM reveals interactions among protein networks. *Science*. 329:1038-1043.

Luby-Phelps, K. 2000. Cytoarchitecture and physical properties of cytoplasm: volume, viscosity, diffusion, intracellular surface area. *Int Rev Cytol*. 192:189-221.

Luftig, R.B., and R.R. Weihing. 1975. Adenovirus binds to rat brain microtubules in vitro. *J Virol*. 16:696-706.

Lukashok, S.A., L. Tarassishin, Y. Li, and M.S. Horwitz. 2000. An adenovirus inhibitor of tumor necrosis factor alpha-induced apoptosis complexes with dynein and a small GTPase. *J Virol*. 74:4705-4709.

Luxton, G.W., J.I. Lee, S. Haverlock-Moyns, J.M. Schober, and G.A. Smith. 2006. The pseudorabies virus VP1/2 tegument protein is required for intracellular capsid transport. *J Virol*. 80:201-209.

Mabit, H., M.Y. Nakano, U. Prank, B. Saam, K. Dohner, B. Sodeik, and U.F. Greber. 2002. Intact microtubules support adenovirus and herpes simplex virus infections. *J Virol*. 76:9962-9971.

Maier, O., D.L. Galan, H. Wodrich, and C.M. Wiethoff. 2010. An N-terminal domain of adenovirus protein VI fragments membranes by inducing positive membrane curvature. *Virology*. 402:11-19.

Makokha, M., M. Hare, M. Li, T. Hays, and E. Barbar. 2002. Interactions of cytoplasmic dynein light chains Tctex-1 and LC8 with the intermediate chain IC74. *Biochemistry*. 41:4302-4311.

Mallery, D.L., W.A. McEwan, S.R. Bidgood, G.J. Towers, C.M. Johnson, and L.C. James. 2010. Antibodies mediate intracellular immunity through tripartite motif-containing 21 (TRIM21). *Proc Natl Acad Sci U S A*. 107:19985-19990.

Mallik, R., B.C. Carter, S.A. Lex, S.J. King, and S.P. Gross. 2004. Cytoplasmic dynein functions as a gear in response to load. *Nature*. 427:649-652.

Malone, C.J., L. Misner, N. Le Bot, M.C. Tsai, J.M. Campbell, J. Ahringer, and J.G. White. 2003. The C. elegans hook protein, ZYG-12, mediates the essential attachment between the centrosome and nucleus. *Cell*. 115:825-836.

Mangel, W.F., W.J. McGrath, D.L. Toledo, and C.W. Anderson. 1993. Viral DNA and a viral peptide can act as cofactors of adenovirus virion proteinase activity. *Nature*. 361:274-275.

Marks, M.S., and M.C. Seabra. 2001. The melanosome: membrane dynamics in black and white. *Nat Rev Mol Cell Biol*. 2:738-748.

Marsh, M., and A. Helenius. 2006. Virus entry: open sesame. *Cell*. 124:729-740.

Martin-Fernandez, M., S.V. Longshaw, I. Kirby, G. Santis, M.J. Tobin, D.T. Clarke, and G.R. Jones. 2004. Adenovirus type-5 entry and disassembly followed in living cells by FRET, fluorescence anisotropy, and FLIM. *Biophys J*. 87:1316-1327.

Martinez, N.W., X. Xue, R.G. Berro, G. Kreitzer, and M.D. Resh. 2008. Kinesin KIF4 regulates intracellular trafficking and stability of the human immunodeficiency virus type 1 Gag polyprotein. *J Virol*. 82:9937-9950.

Matthews, D.A., and W.C. Russell. 1994. Adenovirus protein-protein interactions: hexon and protein VI. *J Gen Virol*. 75 (Pt 12):3365-3374.

McKenney, R.J., M. Vershinin, A. Kunwar, R.B. Vallee, and S.P. Gross. 2010. LIS1 and NudE induce a persistent dynein force-producing state. *Cell*. 141:304-314.

McKenney, R.J., S.J. Weil, J. Scherer, and R.B. Vallee. 2011. Mutually exclusive cytoplasmic dynein regulation by NudE-Lis1 and dynactin. *J Biol Chem*. 286:39615-39622.

Medina-Kauwe, L.K. 2003. Endocytosis of adenovirus and adenovirus capsid proteins. *Adv Drug Deliv Rev*. 55:1485-1496.

Meulenbroek, R.A., K.L. Sargent, J. Lunde, B.J. Jasmin, and R.J. Parks. 2004. Use of adenovirus protein IX (pIX) to display large polypeptides on the virion--generation of fluorescent virus through the incorporation of pIX-GFP. *Mol Ther*. 9:617-624.

Mikami, A., B.M. Paschal, M. Mazumdar, and R.B. Vallee. 1993. Molecular cloning of the retrograde transport motor cytoplasmic dynein (MAP 1C). *Neuron*. 10:787-796.

Minke, P.F., I.H. Lee, J.H. Tinsley, K.S. Bruno, and M. Plamann. 1999. Neurospora crassa ro-10 and ro-11 genes encode novel proteins required for nuclear distribution. *Mol Microbiol*. 32:1065-1076.

Miyazawa, N., R.G. Crystal, and P.L. Leopold. 2001. Adenovirus serotype 7 retention in a late endosomal compartment prior to cytosol escape is modulated by fiber protein. *J Virol*. 75:1387-1400.

Mocz, G., and I.R. Gibbons. 2001. Model for the motor component of dynein heavy chain based on homology to the AAA family of oligomeric ATPases. *Structure*. 9:93-103.

Morgan, G.W., M. Hollinshead, B.J. Ferguson, B.J. Murphy, D.C.J. Carpentier, and G.L. Smith. 2010. Vaccinia Protein F12 Has Structural Similarity to Kinesin Light Chain and Contains a Motor Binding Motif Required for Virion Export. *Plos Pathog*. 6.

Morgan, J.L., Y. Song, and E. Barbar. 2011. Structural dynamics and multiregion interactions in dynein-dynactin recognition. *J Biol Chem*. 286:39349-39359.

Moss, B., and B.M. Ward. 2001. High-speed mass transit for poxviruses on microtubules. *Nat Cell Biol*. 3:E245-246.

Mou, T., J.R. Kraas, E.T. Fung, and S.L. Swope. 1998. Identification of a dynein molecular motor component in Torpedo electroplax; binding and phosphorylation of Tctex-1 by Fyn. *FEBS Lett*. 435:275-281.

Mueller, S., X. Cao, R. Welker, and E. Wimmer. 2002. Interaction of the poliovirus receptor CD155 with the dynein light chain Tctex-1 and its implication for poliovirus pathogenesis. *J Biol Chem*. 277:7897-7904.

Nagano, F., S. Orita, T. Sasaki, A. Naito, G. Sakaguchi, M. Maeda, T. Watanabe, E. Kominami, Y. Uchiyama, and Y. Takai. 1998. Interaction of Doc2 with tctex-1, a light chain of cytoplasmic dynein. Implication in dynein-dependent vesicle transport. *J Biol Chem*. 273:30065-30068.

Nakano, M.Y., K. Boucke, M. Suomalainen, R.P. Stidwill, and U.F. Greber. 2000. The first step of adenovirus type 2 disassembly occurs at the cell surface, independently of endocytosis and escape to the cytosol. *J Virol*. 74:7085-7095.

Nakata, T., and N. Hirokawa. 1995. Point mutation of adenosine triphosphate-binding motif generated rigor kinesin that selectively blocks anterograde lysosome membrane transport. *J Cell Biol*. 131:1039-1053.

Nemerow, G.R., and P.L. Stewart. 1999. Role of alpha(v) integrins in adenovirus cell entry and gene delivery. *Microbiol Mol Biol Rev*. 63:725-734.

Niclas, J., V.J. Allan, and R.D. Vale. 1996. Cell cycle regulation of dynein association with membranes modulates microtubule-based organelle transport. *J Cell Biol*. 133:585-593.

Nilsson, H., and M. Wallin. 1997. Evidence for several roles of dynein in pigment transport in melanophores. *Cell Motil Cytoskeleton*. 38:397-409.

Norrby, E., and P. Skaaret. 1967. The relationship between soluble antigens and the virion of adenovirus type 3. 3. Immunological identification of fiber antigen and isolated vertex capsomer antigen. *Virology*. 32:489-502.

Nyarko, A., Y. Song, and E. Barbar. 2012. Intrinsic Disorder in Dynein Intermediate Chain Modulates Its Interactions with NudE and Dynactin. *J Biol Chem*. 287:24884-24893.

Ohka, S., N. Matsuda, K. Tohyama, T. Oda, M. Morikawa, S. Kuge, and A. Nomoto. 2004. Receptor (CD155)-dependent endocytosis of poliovirus and retrograde axonal transport of the endosome. *J Virol*. 78:7186-7198.

Okada, Y., H. Yamazaki, Y. Sekine-Aizawa, and N. Hirokawa. 1995. The neuron-specific kinesin superfamily protein KIF1A is a unique monomeric motor for anterograde axonal transport of synaptic vesicle precursors. *Cell*. 81:769-780.

Ong, L.L., A.P. Lim, C.P. Er, S.A. Kuznetsov, and H. Yu. 2000. Kinectin-kinesin binding domains and their effects on organelle motility. *J Biol Chem*. 275:32854-32860.

Oosterom-Dragon, E.A., and H.S. Ginsberg. 1981. Characterization of two temperature-sensitive mutants of type 5 adenovirus with mutations in the 100,000-dalton protein gene. *J Virol*. 40:491-500.

Ori-McKenney, K.M., J. Xu, S.P. Gross, and R.B. Vallee. 2010. A cytoplasmic dynein tail mutation impairs motor processivity. *Nat Cell Biol*. 12:1228-1234.

Ostapchuk, P., and P. Hearing. 2005. Control of adenovirus packaging. *J Cell Biochem*. 96:25-35.

Palazzo, A.F., H.L. Joseph, Y.J. Chen, D.L. Dujardin, A.S. Alberts, K.K. Pfister, R.B. Vallee, and G.G. Gundersen. 2001. Cdc42, dynein, and dynactin regulate MTOC reorientation independent of Rho-regulated microtubule stabilization. *Curr Biol*. 11:1536-1541.

Palmer, K.J., H. Hughes, and D.J. Stephens. 2009. Specificity of cytoplasmic dynein subunits in discrete membrane-trafficking steps. *Mol Biol Cell*. 20:2885-2899.

Parks, R.J. 2005. Adenovirus protein IX: a new look at an old protein. *Mol Ther*. 11:19-25.

Paschal, B.M., H.S. Shpetner, and R.B. Vallee. 1987. MAP 1C is a microtubule-activated ATPase which translocates microtubules in vitro and has dynein-like properties. *J Cell Biol*. 105:1273-1282.

Paschal, B.M., and R.B. Vallee. 1987. Retrograde transport by the microtubule-associated protein MAP 1C. *Nature*. 330:181-183.

Patterson, S., and W.C. Russell. 1983. Ultrastructural and immunofluorescence studies of early events in adenovirus-HeLa cell interactions. *J Gen Virol*. 64:1091-1099.

Pavlos, N.J., T.S. Cheng, A. Qin, P.Y. Ng, H.T. Feng, E.S. Ang, A. Carrello, C.H. Sung, R. Jahn, M.H. Zheng, and J. Xu. 2011. Tctex-1, a novel interaction partner of Rab3D, is required for osteoclastic bone resorption. *Mol Cell Biol*. 31:1551-1564.

Pelka, P., J.N. Ablack, G.J. Fonseca, A.F. Yousef, and J.S. Mymryk. 2008. Intrinsic structural disorder in adenovirus E1A: a viral molecular hub linking multiple diverse processes. *J Virol*. 82:7252-7263.

Perez-Berna, A.J., R. Marabini, S.H. Scheres, R. Menendez-Conejero, I.P. Dmitriev, D.T. Curiel, W.F. Mangel, S.J. Flint, and C. San Martin. 2009. Structure and uncoating of immature adenovirus. *J Mol Biol*. 392:547-557.

Petit, C., M.L. Giron, J. Tobaly-Tapiero, P. Bittoun, E. Real, Y. Jacob, N. Tordo, H. De The, and A. Saib. 2003. Targeting of incoming retroviral Gag to the centrosome involves a direct interaction with the dynein light chain 8. *J Cell Sci*. 116:3433-3442.

Pfister, K.K., E.M. Fisher, I.R. Gibbons, T.S. Hays, E.L. Holzbaur, J.R. McIntosh, M.E. Porter, T.A. Schroer, K.T. Vaughan, G.B. Witman, S.M. King, and R.B. Vallee. 2005. Cytoplasmic dynein nomenclature. *J Cell Biol*. 171:411-413.

Pfister, K.K., M.C. Wagner, D.L. Stenoien, S.T. Brady, and G.S. Bloom. 1989. Monoclonal antibodies to kinesin heavy and light chains stain vesicle-like structures, but not microtubules, in cultured cells. *J Cell Biol*. 108:1453-1463.

Plitz, T., and K. Pfeffer. 2001. Intact lysosome transport and phagosome function despite kinectin deficiency. *Mol Cell Biol*. 21:6044-6055.

Purohit, A., S.H. Tynan, R. Vallee, and S.J. Doxsey. 1999. Direct interaction of pericentrin with cytoplasmic dynein light intermediate chain contributes to mitotic spindle organization. *J Cell Biol*. 147:481-492.

Qiu, W., N.D. Derr, B.S. Goodman, E. Villa, D. Wu, W. Shih, and S.L. Reck-Peterson. 2012. Dynein achieves processive motion using both stochastic and coordinated stepping. *Nat Struct Mol Biol*. 19:193-200.

Radtke, K., K. Dohner, and B. Sodeik. 2006. Viral interactions with the cytoskeleton: a hitchhiker's guide to the cell. *Cell Microbiol*. 8:387-400.

Radtke, K., D. Kieneke, A. Wolfstein, K. Michael, W. Steffen, T. Scholz, A. Karger, and B. Sodeik. 2010. Plus- and minus-end directed microtubule motors bind simultaneously to herpes simplex virus capsids using different inner tegument structures. *PLoS Pathog*. 6:e1000991.

Rapali, P., A. Szenes, L. Radnai, A. Bakos, G. Pal, and L. Nyitray. 2011. DYNLL/LC8: a light chain subunit of the dynein motor complex and beyond. *FEBS J*. 278:2980-2996.

Raposo, G., D. Tenza, D.M. Murphy, J.F. Berson, and M.S. Marks. 2001. Distinct protein sorting and localization to premelanosomes, melanosomes, and lysosomes in pigmented melanocytic cells. *Journal of Cell Biology*. 152:809-823.

Raux, H., A. Flamand, and D. Blondel. 2000. Interaction of the rabies virus P protein with the LC8 dynein light chain. *J Virol*. 74:10212-10216.

Reddy, A., E.V. Caler, and N.W. Andrews. 2001. Plasma membrane repair is mediated by Ca(2+)-regulated exocytosis of lysosomes. *Cell*. 106:157-169.

Reddy, V.S., S.K. Natchiar, P.L. Stewart, and G.R. Nemerow. 2010. Crystal structure of human adenovirus at 3.5 A resolution. *Science*. 329:1071-1075.

Reilein, A.R., I.S. Tint, N.I. Peunova, G.N. Enikolopov, and V.I. Gelfand. 1998. Regulation of organelle movement in melanophores by protein kinase A (PKA), protein kinase C (PKC), and protein phosphatase 2A (PP2A). *J Cell Biol*. 142:803-813.

Rentsendorj, A., J. Xie, M. MacVeigh, H. Agadjanian, S. Bass, D.H. Kim, J. Rossi, S.F. Hamm-Alvarez, and L.K. Medina-Kauwe. 2006. Typical and atypical trafficking pathways of Ad5 penton base recombinant protein: implications for gene transfer. *Gene Ther*. 13:821-836.

Rexroad, J., R.K. Evans, and C.R. Middaugh. 2006. Effect of pH and ionic strength on the physical stability of adenovirus type 5. *J Pharm Sci*. 95:237-247.

Rexroad, J., C.M. Wiethoff, A.P. Green, T.D. Kierstead, M.O. Scott, and C.R. Middaugh. 2003. Structural stability of adenovirus type 5. *J Pharm Sci*. 92:665-678.

Rice, S., A.W. Lin, D. Safer, C.L. Hart, N. Naber, B.O. Carragher, S.M. Cain, E. Pechatnikova, E.M. Wilson-Kubalek, M. Whittaker, E. Pate, R. Cooke, E.W. Taylor, R.A. Milligan, and R.D. Vale. 1999. A structural change in the kinesin motor protein that drives motility. *Nature*. 402:778-784.

Rietdorf, J., A. Ploubidou, I. Reckmann, A. Holmstrom, F. Frischknecht, M. Zettl, T. Zimmermann, and M. Way. 2001. Kinesin-dependent movement on microtubules precedes actin-based motility of vaccinia virus. *Nat Cell Biol*. 3:992-1000.

Roberts, A.J., B. Malkova, M.L. Walker, H. Sakakibara, N. Numata, T. Kon, R. Ohkura, T.A. Edwards, P.J. Knight, K. Sutoh, K. Oiwa, and S.A. Burgess. 2012. ATP-Driven Remodeling of the Linker Domain in the Dynein Motor. *Structure*.

Roberts, A.J., N. Numata, M.L. Walker, Y.S. Kato, B. Malkova, T. Kon, R. Ohkura, F. Arisaka, P.J. Knight, K. Sutoh, and S.A. Burgess. 2009. AAA+ Ring and linker swing mechanism in the dynein motor. *Cell*. 136:485-495.

Rodionov, V.I., A.J. Hope, T.M. Svitkina, and G.G. Borisy. 1998. Functional coordination of microtubule-based and actin-based motility in melanophores. *Curr Biol*. 8:165-168.

Rodriguez, A., I. Martinez, A. Chung, C.H. Berlot, and N.W. Andrews. 1999. cAMP regulates Ca2+-dependent exocytosis of lysosomes and lysosome-mediated cell invasion by trypanosomes. *J Biol Chem*. 274:16754-16759.

Rodriguez, A., E. Samoff, M.G. Rioult, A. Chung, and N.W. Andrews. 1996. Host cell invasion by trypanosomes requires lysosomes and microtubule/kinesin-mediated transport. *J Cell Biol*. 134:349-362.

Rodriguez, A., P. Webster, J. Ortego, and N.W. Andrews. 1997. Lysosomes behave as Ca2+-regulated exocytic vesicles in fibroblasts and epithelial cells. *J Cell Biol*. 137:93-104.

Rosa-Ferreira, C., and S. Munro. 2011. Arl8 and SKIP act together to link lysosomes to kinesin-1. *Dev Cell*. 21:1171-1178.

Rosse, C., K. Boeckeler, M. Linch, S. Radtke, D. Frith, K. Barnouin, A.S. Morsi, M. Hafezparast, M. Howell, and P.J. Parker. 2012. Binding of Dynein Intermediate Chain 2 to Paxillin controls Focal adhesion dynamics and migration. *J Cell Sci*.

Rowe, W.P., R.J. Huebner, L.K. Gilmore, R.H. Parrott, and T.G. Ward. 1953. Isolation of a cytopathogenic agent from human adenoids undergoing spontaneous degeneration in tissue culture. *Proc Soc Exp Biol Med*. 84:570-573.

Roy, D., D.R. Liston, V.J. Idone, A. Di, D.J. Nelson, C. Pujol, J.B. Bliska, S. Chakrabarti, and N.W. Andrews. 2004. A process for controlling intracellular bacterial infections induced by membrane injury. *Science*. 304:1515-1518.

Rux, J.J., and R.M. Burnett. 2000. Type-specific epitope locations revealed by X-ray crystallographic study of adenovirus type 5 hexon. *Mol Ther*. 1:18-30.

Rux, J.J., and R.M. Burnett. 2007. Large-scale purification and crystallization of adenovirus hexon. *Methods Mol Med*. 131:231-250.

Rux, J.J., P.R. Kuser, and R.M. Burnett. 2003. Structural and phylogenetic analysis of adenovirus hexons by use of high-resolution x-ray crystallographic, molecular modeling, and sequence-based methods. *J Virol*. 77:9553-9566.

Saftig, P., and J. Klumperman. 2009. Lysosome biogenesis and lysosomal membrane proteins: trafficking meets function. *Nat Rev Mol Cell Biol*. 10:623-635.

Saphire, A.C., T. Guan, E.C. Schirmer, G.R. Nemerow, and L. Gerace. 2000. Nuclear import of adenovirus DNA in vitro involves the nuclear protein import pathway and hsc70. *J Biol Chem*. 275:4298-4304.

Sargent, K.L., R.A. Meulenbroek, and R.J. Parks. 2004. Activation of adenoviral gene expression by protein IX is not required for efficient virus replication. *J Virol*. 78:5032-5037.

Sasaki, S., A. Shionoya, M. Ishida, M.J. Gambello, J. Yingling, A. Wynshaw-Boris, and S. Hirotsune. 2000. A LIS1/NUDEL/cytoplasmic dynein heavy chain complex in the developing and adult nervous system. *Neuron*. 28:681-696.

Sato-Yoshitake, R., H. Yorifuji, M. Inagaki, and N. Hirokawa. 1992. The phosphorylation of kinesin regulates its binding to synaptic vesicles. *J Biol Chem*. 267:23930-23936.

Scherer, J., and R.B. Vallee. 2011. Adenovirus recruits dynein by an evolutionary novel mechanism involving direct binding to pH-primed hexon. *Viruses*. 3:1417-1431.

Schiaffino, M.V. 2010. Signaling pathways in melanosome biogenesis and pathology. *Int J Biochem Cell Biol*. 42:1094-1104.

Schmidt, H., E.S. Gleave, and A.P. Carter. 2012. Insights into dynein motor domain function from a 3.3-A crystal structure. *Nat Struct Mol Biol*. 19:492-497, S491.

Schmoranzer, J., J.P. Fawcett, M. Segura, S. Tan, R.B. Vallee, T. Pawson, and G.G. Gundersen. 2009. Par3 and dynein associate to regulate local microtubule dynamics and centrosome orientation during migration. *Curr Biol*. 19:1065-1074.

Schneider, M.A., G.A. Spoden, L. Florin, and C. Lambert. 2011. Identification of the dynein light chains required for human papillomavirus infection. *Cell Microbiol*. 13:32-46.

Schnorrer, F., K. Bohmann, and C. Nusslein-Volhard. 2000. The molecular motor dynein is involved in targeting swallow and bicoid RNA to the anterior pole of Drosophila oocytes. *Nat Cell Biol*. 2:185-190.

Schwarzer, C., S. Barnikol-Watanabe, F.P. Thinnes, and N. Hilschmann. 2002. Voltage-dependent anion-selective channel (VDAC) interacts with the dynein light chain Tctex1 and the heat-shock protein PBP74. *Int J Biochem Cell Biol*. 34:1059-1070.

Sekine, Y., Y. Okada, Y. Noda, S. Kondo, H. Aizawa, R. Takemura, and N. Hirokawa. 1994. A novel microtubule-based motor protein (KIF4) for organelle transports, whose expression is regulated developmentally. *J Cell Biol*. 127:187-201.

Seksek, O., J. Biwersi, and A.S. Verkman. 1997. Translational diffusion of macromolecule-sized solutes in cytoplasm and nucleus. *J Cell Biol*. 138:131-142.

Seth, P., D. Fitzgerald, H. Ginsberg, M. Willingham, and I. Pastan. 1984. Evidence that the penton base of adenovirus is involved in potentiation of toxicity of Pseudomonas exotoxin conjugated to epidermal growth factor. *Mol Cell Biol*. 4:1528-1533.

Seth, P., M.C. Willingham, and I. Pastan. 1985. Binding of adenovirus and its external proteins to Triton X-114. Dependence on pH. *J Biol Chem*. 260:14431-14434.

Setou, M., T. Nakagawa, D.H. Seog, and N. Hirokawa. 2000. Kinesin superfamily motor protein KIF17 and mLin-10 in NMDA receptor-containing vesicle transport. *Science*. 288:1796-1802.

Sheetz, M.P., R. Vale, B. Schnapp, T. Schroer, and T. Reese. 1986. Vesicle movements and microtubule-based motors. *J Cell Sci Suppl*. 5:181-188.

Silvestry, M., S. Lindert, J.G. Smith, O. Maier, C.M. Wiethoff, G.R. Nemerow, and P.L. Stewart. 2009. Cryo-electron microscopy structure of adenovirus type 2 temperature-sensitive mutant 1 reveals insight into the cell entry defect. *J Virol*. 83:7375-7383.

Sivaram, M.V., T.L. Wadzinski, S.D. Redick, T. Manna, and S.J. Doxsey. 2009. Dynein light intermediate chain 1 is required for progress through the spindle assembly checkpoint. *EMBO J*. 28:902-914.

Smith, J.G., A. Cassany, L. Gerace, R. Ralston, and G.R. Nemerow. 2008. Neutralizing antibody blocks adenovirus infection by arresting microtubule-dependent cytoplasmic transport. *J Virol*. 82:6492-6500.

Smith, J.G., M. Silvestry, S. Lindert, W. Lu, G.R. Nemerow, and P.L. Stewart. 2010a. Insight into the mechanisms of adenovirus capsid disassembly from studies of defensin neutralization. *PLoS Pathog*. 6:e1000959.

Smith, J.G., C.M. Wiethoff, P.L. Stewart, and G.R. Nemerow. 2010b. Adenovirus. *Curr Top Microbiol Immunol*. 343:195-224.

Sodeik, B. 2000. Mechanisms of viral transport in the cytoplasm. *Trends Microbiol*. 8:465-472.

Song, J., R.C. Tyler, M.S. Lee, E.M. Tyler, and J.L. Markley. 2005. Solution structure of isoform 1 of Roadblock/LC7, a light chain in the dynein complex. *J Mol Biol*. 354:1043-1051.

Soppina, V., A.K. Rai, A.J. Ramaiya, P. Barak, and R. Mallik. 2009. Tug-of-war between dissimilar teams of microtubule motors regulates transport and fission of endosomes. *Proc Natl Acad Sci U S A*. 106:19381-19386.

Splinter, D., M.E. Tanenbaum, A. Lindqvist, D. Jaarsma, A. Flotho, K.L. Yu, I. Grigoriev, D. Engelsma, E.D. Haasdijk, N. Keijzer, J. Demmers, M. Fornerod, F. Melchior, C.C. Hoogenraad, R.H. Medema, and A. Akhmanova. 2010. Bicaudal D2, dynein, and kinesin-1 associate with nuclear pore complexes and regulate centrosome and nuclear positioning during mitotic entry. *PLoS Biol*. 8:e1000350.

Starr, D.A., B.C. Williams, T.S. Hays, and M.L. Goldberg. 1998. ZW10 helps recruit dynactin and dynein to the kinetochore. *J Cell Biol*. 142:763-774.

Stehman, S.A., Y. Chen, R.J. McKenney, and R.B. Vallee. 2007. NudE and NudEL are required for mitotic progression and are involved in dynein recruitment to kinetochores. *J Cell Biol*. 178:583-594.

Steuer, E.R., L. Wordeman, T.A. Schroer, and M.P. Sheetz. 1990. Localization of cytoplasmic dynein to mitotic spindles and kinetochores. *Nature*. 345:266-268.

Stewart, P.L., S.D. Fuller, and R.M. Burnett. 1993. Difference imaging of adenovirus: bridging the resolution gap between X-ray crystallography and electron microscopy. *EMBO J*. 12:2589-2599.

Strunze, S., M.F. Engelke, I.H. Wang, D. Puntener, K. Boucke, S. Schleich, M. Way, P. Schoenenberger, C.J. Burckhardt, and U.F. Greber. 2011. Kinesin-1-mediated capsid disassembly and disruption of the nuclear pore complex promote virus infection. *Cell Host Microbe*. 10:210-223.

Strunze, S., L.C. Trotman, K. Boucke, and U.F. Greber. 2005. Nuclear targeting of adenovirus type 2 requires CRM1-mediated nuclear export. *Mol Biol Cell*. 16:2999-3009.

Sugai, M., M. Saito, I. Sukegawa, Y. Katsushima, Y. Kinouchi, N. Nakahata, T. Shimosegawa, T. Yanagisawa, and J. Sukegawa. 2003. PTH/PTH-related protein receptor interacts directly with Tctex-1 through its COOH terminus. *Biochem Biophys Res Commun*. 311:24-31.

Suomalainen, M., M.Y. Nakano, K. Boucke, S. Keller, and U.F. Greber. 2001. Adenovirus-activated PKA and p38/MAPK pathways boost microtubule-mediated nuclear targeting of virus. *EMBO J*. 20:1310-1319.

Suomalainen, M., M.Y. Nakano, S. Keller, K. Boucke, R.P. Stidwill, and U.F. Greber. 1999. Microtubule-dependent plus- and minus end-directed motilities are competing processes for nuclear targeting of adenovirus. *J Cell Biol*. 144:657-672.

Svoboda, K., and S.M. Block. 1994. Force and velocity measured for single kinesin molecules. *Cell*. 77:773-784.

Svoboda, K., C.F. Schmidt, B.J. Schnapp, and S.M. Block. 1993. Direct observation of kinesin stepping by optical trapping interferometry. *Nature*. 365:721-727.

Tai, A.W., J.Z. Chuang, C. Bode, U. Wolfrum, and C.H. Sung. 1999. Rhodopsin's carboxy-terminal cytoplasmic tail acts as a membrane receptor for cytoplasmic dynein by binding to the dynein light chain Tctex-1. *Cell*. 97:877-887.

Tai, C.Y., D.L. Dujardin, N.E. Faulkner, and R.B. Vallee. 2002. Role of dynein, dynactin, and CLIP-170 interactions in LIS1 kinetochore function. *J Cell Biol*. 156:959-968.

Tan, S.C., J. Scherer, and R.B. Vallee. 2011. Recruitment of dynein to late endosomes and lysosomes through light intermediate chains. *Mol Biol Cell*. 22:467-477.

Tanaka, Y., Y. Kanai, Y. Okada, S. Nonaka, S. Takeda, A. Harada, and N. Hirokawa. 1998. Targeted disruption of mouse conventional kinesin heavy chain, kif5B, results in abnormal perinuclear clustering of mitochondria. *Cell*. 93:1147-1158.

Tang, W.J., and A.G. Gilman. 1992. Adenylyl cyclases. *Cell*. 70:869-872.

Tang, Y., U. Winkler, E.O. Freed, T.A. Torrey, W. Kim, H. Li, S.P. Goff, and H.C. Morse, 3rd. 1999. Cellular motor protein KIF-4 associates with retroviral Gag. *J Virol*. 73:10508-10513.

Tardieux, I., P. Webster, J. Ravesloot, W. Boron, J.A. Lunn, J.E. Heuser, and N.W. Andrews. 1992. Lysosome recruitment and fusion are early events required for trypanosome invasion of mammalian cells. *Cell*. 71:1117-1130.

Thiel, J.F., and K.O. Smith. 1967. Fluorescent focus assay of viruses on cell monolayers in plastic Petri plates. *Proc Soc Exp Biol Med*. 125:892-895.

Tollefson, A.E., A. Scaria, T.W. Hermiston, J.S. Ryerse, L.J. Wold, and W.S. Wold. 1996. The adenovirus death protein (E3-11.6K) is required at very late stages of infection for efficient cell lysis and release of adenovirus from infected cells. *J Virol*. 70:2296-2306.

Toprak, E., A. Yildiz, M.T. Hoffman, S.S. Rosenfeld, and P.R. Selvin. 2009. Why kinesin is so processive. *Proc Natl Acad Sci U S A*. 106:12717-12722.

Trotman, L.C., D.P. Achermann, S. Keller, M. Straub, and U.F. Greber. 2003. Non-classical export of an adenovirus structural protein. *Traffic*. 4:390-402.

Trotman, L.C., N. Mosberger, M. Fornerod, R.P. Stidwill, and U.F. Greber. 2001. Import of adenovirus DNA involves the nuclear pore complex receptor CAN/Nup214 and histone H1. *Nat Cell Biol*. 3:1092-1100.

Tsai, J.W., K.H. Bremner, and R.B. Vallee. 2007. Dual subcellular roles for LIS1 and dynein in radial neuronal migration in live brain tissue. *Nat Neurosci*. 10:970-979.

Tuma, M.C., and V.I. Gelfand. 1999. Molecular mechanisms of pigment transport in melanophores. *Pigment Cell Res*. 12:283-294.

Tynan, S.H., M.A. Gee, and R.B. Vallee. 2000a. Distinct but overlapping sites within the cytoplasmic dynein heavy chain for dimerization and for intermediate chain and light intermediate chain binding. *J Biol Chem*. 275:32769-32774.

Tynan, S.H., A. Purohit, S.J. Doxsey, and R.B. Vallee. 2000b. Light intermediate chain 1 defines a functional subfraction of cytoplasmic dynein which binds to pericentrin. *J Biol Chem*. 275:32763-32768.

Vale, R.D., T.S. Reese, and M.P. Sheetz. 1985. Identification of a novel force-generating protein, kinesin, involved in microtubule-based motility. *Cell*. 42:39-50.

Vallee, R.B., R.J. McKenney, and K.M. Ori-McKenney. 2012. Multiple modes of cytoplasmic dynein regulation. *Nat Cell Biol*. 14:224-230.

Vallee, R.B., G.E. Seale, and J.W. Tsai. 2009. Emerging roles for myosin II and cytoplasmic dynein in migrating neurons and growth cones. *Trends Cell Biol*. 19:347-355.

Varga, M.J., T. Bergman, and E. Everitt. 1990. Antibodies with specificities against a dispase-produced 15-kilodalton hexon fragment neutralize adenovirus type 2 infectivity. *J Virol*. 64:4217-4225.

Varma, D., A. Dawn, A. Ghosh-Roy, S.J. Weil, K.M. Ori-McKenney, Y. Zhao, J. Keen, R.B. Vallee, and J.C. Williams. 2010. Development and application of in vivo molecular traps reveals that dynein light chain occupancy differentially affects dynein-mediated processes. *Proc Natl Acad Sci U S A*. 107:3493-3498.

Vaughan, K.T., and R.B. Vallee. 1995. Cytoplasmic dynein binds dynactin through a direct interaction between the intermediate chains and p150Glued. *J Cell Biol*. 131:1507-1516.

Velicer, L.F., and H.S. Ginsberg. 1970. Synthesis, transport, and morphogenesis of type adenovirus capsid proteins. *J Virol*. 5:338-352.

Vellinga, J., S. Van der Heijdt, and R.C. Hoeben. 2005. The adenovirus capsid: major progress in minor proteins. *J Gen Virol*. 86:1581-1588.

Verhey, K.J., and J.W. Hammond. 2009. Traffic control: regulation of kinesin motors. *Nat Rev Mol Cell Biol*. 10:765-777.

Vlach, J., J. Lipov, M. Rumlova, V. Veverka, J. Lang, P. Srb, Z. Knejzlik, I. Pichova, E. Hunter, R. Hrabal, and T. Ruml. 2008. D-retrovirus morphogenetic switch driven by the targeting signal accessibility to Tctex-1 of dynein. *Proc Natl Acad Sci U S A*. 105:10565-10570.

Walters, R.W., P. Freimuth, T.O. Moninger, I. Ganske, J. Zabner, and M.J. Welsh. 2002. Adenovirus fiber disrupts CAR-mediated intercellular adhesion allowing virus escape. *Cell*. 110:789-799.

Wang, X., and T.L. Schwarz. 2009. The mechanism of Ca2+ -dependent regulation of kinesin-mediated mitochondrial motility. *Cell*. 136:163-174.

Wanschers, B., R. van de Vorstenbosch, M. Wijers, B. Wieringa, S.M. King, and J. Fransen. 2008. Rab6 family proteins interact with the dynein light chain protein DYNLRB1. *Cell Motil Cytoskeleton*. 65:183-196.

Ward, B.M., and B. Moss. 2004. Vaccinia virus A36R membrane protein provides a direct link between intracellular enveloped virions and the microtubule motor kinesin. *J Virol*. 78:2486-2493.

Waris, M., and P. Halonen. 1987. Purification of adenovirus hexon protein by high-performance liquid chromatography. *J Chromatogr*. 397:321-325.

Watanabe, Y., M. Ichikawa, T. Murayama, T. Kobayashi, T. Kitai, T. Takahagi, H. Sakakibara, K.H. Bui, T. Ishikawa, Y.Y. Toyoshima (2011). Submolecular structure of cytoplasmic dynein tail. Mol Biol Cell 22, 4705 (899).

Weatherbee, J.A., R.B. Luftig, and R.R. Weihing. 1977. Binding of adenovirus to microtubules. II. Depletion of high-molecular-weight microtubule-associated protein content reduces specificity of in vitro binding. *J Virol*. 21:732-742.

Weber, J.M. 1995. Adenovirus endopeptidase and its role in virus infection. *Curr Top Microbiol Immunol*. 199 (Pt 1):227-235.

Wen, W., J.L. Meinkoth, R.Y. Tsien, and S.S. Taylor. 1995. Identification of a signal for rapid export of proteins from the nucleus. *Cell*. 82:463-473.

Whyte, J., J.R. Bader, S.B. Tauhata, M. Raycroft, J. Hornick, K.K. Pfister, W.S. Lane, G.K. Chan, E.H. Hinchcliffe, P.S. Vaughan, and K.T. Vaughan. 2008. Phosphorylation regulates targeting of cytoplasmic dynein to kinetochores during mitosis. *J Cell Biol*. 183:819-834.

Wickham, T.J., P. Mathias, D.A. Cheresh, and G.R. Nemerow. 1993. Integrins alpha v beta 3 and alpha v beta 5 promote adenovirus internalization but not virus attachment. *Cell*. 73:309-319.

Wiethoff, C.M., H. Wodrich, L. Gerace, and G.R. Nemerow. 2005. Adenovirus protein VI mediates membrane disruption following capsid disassembly. *J Virol*. 79:1992-2000.

Williams, J.C., P.L. Roulhac, A.G. Roy, R.B. Vallee, M.C. Fitzgerald, and W.A. Hendrickson. 2007. Structural and thermodynamic characterization of a cytoplasmic dynein light chain-intermediate chain complex. *Proc Natl Acad Sci U S A*. 104:10028-10033.

Windheim, M., A. Hilgendorf, and H.G. Burgert. 2004. Immune evasion by adenovirus E3 proteins: exploitation of intracellular trafficking pathways. *Curr Top Microbiol Immunol*. 273:29-85.

Wodrich, H., T. Guan, G. Cingolani, D. Von Seggern, G. Nemerow, and L. Gerace. 2003. Switch from capsid protein import to adenovirus assembly by cleavage of nuclear transport signals. *EMBO J*. 22:6245-6255.

Wodrich, H., D. Henaff, B. Jammart, C. Segura-Morales, S. Seelmeir, O. Coux, Z. Ruzsics, C.M. Wiethoff, and E.J. Kremer. 2010. A capsid-encoded PPxY-motif facilitates adenovirus entry. *PLoS Pathog*. 6:e1000808.

Wohlfart, C. 1988. Neutralization of adenoviruses: kinetics, stoichiometry, and mechanisms. *J Virol*. 62:2321-2328.

Yamazaki, H., T. Nakata, Y. Okada, and N. Hirokawa. 1995. KIF3A/B: a heterodimeric kinesin superfamily protein that works as a microtubule plus end-directed motor for membrane organelle transport. *J Cell Biol*. 130:1387-1399.

Yano, H., F.S. Lee, H. Kong, J. Chuang, J. Arevalo, P. Perez, C. Sung, and M.V. Chao. 2001. Association of Trk neurotrophin receptors with components of the cytoplasmic dynein motor. *J Neurosci*. 21:RC125.

Ye, G.J., K.T. Vaughan, R.B. Vallee, and B. Roizman. 2000. The herpes simplex virus 1 U(L)34 protein interacts with a cytoplasmic dynein intermediate chain and targets nuclear membrane. *J Virol*. 74:1355-1363.

Yeh, T.Y., D. Peretti, J.Z. Chuang, E. Rodriguez-Boulan, and C.H. Sung. 2006. Regulatory dissociation of Tctex-1 light chain from dynein complex is essential for the apical delivery of rhodopsin. *Traffic*. 7:1495-1502.

Yi, J.Y., K.M. Ori-McKenney, R.J. McKenney, M. Vershinin, S.P. Gross, and R.B. Vallee. 2011. High-resolution imaging reveals indirect coordination of opposite motors and a role for LIS1 in high-load axonal transport. *J Cell Biol*. 195:193-201.

Yildiz, A., M. Tomishige, A. Gennerich, and R.D. Vale. 2008. Intramolecular strain coordinates kinesin stepping behavior along microtubules. *Cell*. 134:1030-1041.

Zhang, J., S. Li, S. Musa, H. Zhou, and X. Xiang. 2009. Dynein light intermediate chain in Aspergillus nidulans is essential for the interaction between heavy and intermediate chains. *J Biol Chem*. 284:34760-34768.

Zhang, W., and R. Arcos. 2005. Interaction of the adenovirus major core protein precursor, pVII, with the viral DNA packaging machinery. *Virology*. 334:194-202.

Zhang, W., and M.J. Imperiale. 2003. Requirement of the adenovirus IVa2 protein for virus assembly. *J Virol*. 77:3586-3594.

Zhu, H., H.Y. Lee, Y. Tong, B.S. Hong, K.P. Kim, Y. Shen, K.J. Lim, F. Mackenzie, W. Tempel, and H.W. Park. 2012. Crystal structures of the tetratricopeptide

repeat domains of kinesin light chains: insight into cargo recognition mechanisms. *PLoS One*. 7:e33943.

Zubieta, C., G. Schoehn, J. Chroboczek, and S. Cusack. 2005. The structure of the human adenovirus 2 penton. *Mol Cell*. 17:121-135.